DESIGN AND CONSTRUCTION OF A RAINFALL SIMULATOR FOR LARGE-SCALE TESTING OF EROSION CONTROL PRACTICES AND PRODUCTS

by

Matthew Allen Horne

A thesis submitted to the Graduate Faculty of
Auburn University
in partial fulfillment of the
requirements for the Degree of
Master of Science

Auburn, Alabama
May 6, 2017

Keywords: erosion, erosion control, rainfall, rainfall simulation, stormwater

Approved by

Wesley C. Zech, Chair, Professor of Civil Engineering
Xing Fang, Professor of Civil Engineering
Jose G. Vasconcelos, Associate Professor of Civil Engineering

ABSTRACT

Soil erosion and the resulting sediment deposition constitutes one of the greatest pollutants in our nation's waterways. Construction projects often generate large areas of exposed soil that remain disturbed throughout the duration of the project. Exposed soil, resulting from clearing, grubbing, and land grading activities, is more susceptible to erosion during a rain event due to lack of vegetative cover. Erosion control practices and products (i.e., vegetative cover, erosion control blankets, hydromulches, etc.) are an important aspect of any construction project due to their ability to limit the process of erosion. This study developed a testing apparatus capable of accurately and repeatedly simulating a 2-yr, 24-hr storm event in Auburn, Alabama with the goal of determining the performance and effectiveness of erosion control practices and products. The test protocols consisted of calibrating the rainfall simulator and validating the results through bare soil control tests. Data collection procedures consisted of recording rainfall depth in rain gauges, collecting and analyzing flour pellets for drop sizes, and suspended sediment concentration (SSC).

The optimum location for each sprinkler riser as well as the most accurate nozzle configurations were determined through the test procedures developed for this study. Through calibration testing, the simulator was found to produce rainfall intensities of 1.10, 1.78, and 3.76 in./hr. Uniformity of rainfall distribution ranged from 79-81%. The rainfall simulator's performance was also validated through three, 60 minute bare soil control tests. Results from these tests (i.e., erosion patterns, SSC) showed that consistent erosion patterns were achieved with maximum sediment concentrations ranging from approximately 55,000 – 82,000 mg/L.

ACKNOWLEDGEMENTS

The author would first like to thank Dr. Wesley C. Zech for his supervision and mentorship during the course of this research project and for encouraging a spirit of continued education throughout one's professional life. The author would also like to thank Dr. Wesley N. Donald, Dr. Michael A. Perez, Dr. Xing Fang, and Dr. Jose G. Vasconcelos for their support and assistance throughout this research project. The author would also like to thank the Alabama Department of Transportation (ALDOT) and the Highway Research Center (HRC) for their financial support; Mr. Guy Savage for assisting in the oversight of the construction and testing of the rainfall simulator test apparatus; and all undergraduate research assistants who assisted the author in construction and testing efforts for this project. Finally, the author would like to thank his parents, Ken and Donna Horne, for providing love, advice, and encouragement that helped the author accomplish his goals.

TABLE OF CONTENTS

LIST OF TABLES

LIST OF FIGURES

CHAPTER ONE:
INTRODUCTION

1.1 BACKGROUND

The U.S. construction industry is a lucrative and large sector of the nation's economy. In 2015, Congress allocated $325 billion for the construction and rehabilitation of highways in the U.S. (Congress 2015). Construction projects typically include land grading activities (i.e., clearing, grubbing, grading, and excavations) that require extensive earthwork, in which vegetation is removed, thereby resulting in the creation of vast amounts of exposed soil. A primary issue with exposed soil is its susceptibility to erosive forces introduced by a rainfall event. As much as 80 million tons (73 million metric tons) of sediment are eroded from United States construction sites each year (Novotny 2003). The discharge of stormwater runoff with high concentrations of sediment from construction sites has become a source of concern for government environmental agencies and general contractors alike.

Highly concentrated sediment-laden stormwater runoff can enter local waterways where suspended sediments settle out of suspension, resulting in deposition. This sedimentation process effectively degrades the existing ecosystem and overall water quality by increasing turbidity, making it difficult for aquatic wildlife to survive. These concerns led Congress to pass the National Pollutant Discharge Elimination System (NPDES) in 1990 under the Clean Water Act. Regulations under NPDES require that sediment pollution generated by construction activities be controlled onsite by the site operator. This is accomplished through the use of erosion and

sediment control (ESC) practices that include ground covers (i.e., vegetation, erosion control blankets, hydromulches), runoff control measures (i.e., inlet protection practices, ditch checks, turf reinforcement mats), and sediment controls (i.e., sediment basins and silt fences). With the increase in usage of such practices and products, it is important for researchers, practitioners, contractors, inspectors, and regulatory agencies to understand the in-field performance of various ESCs, along with suitable applications. Various standardized small-scale testing methods have been conducted in the past to accomplish these objectives. However, small-scale testing does not adequately represent conditions that various ESCs would experience in the field due to small plot size. To effectively replicate a field-like scenario, large-scale testing techniques have been developed to assess the performance of erosion control practices and products under controlled conditions. Since the 20th century, this has been accomplished with the help of rainfall simulators (Cullum 1997; Hirschi et al. 1990; Mutchler and Hermsmeier 1965; Paige et al. 2003).

1.2 RAINFALL SIMULATORS

Rainfall simulation has long been used to study the effects of rainfall on erosion (Birt et al. 2007; Bubenzer and Meyer 1965; Paige et al. 2003). The need for rainfall simulators arose when researchers determined that simulated rainfall provided more control over experiments in comparison to waiting for a natural rainfall event to occur to conduct experiments. The earliest rainfall simulators used drop-forming mechanisms such as hypodermic needles and string to generate drops (Mutchler and Hermsmeier 1965). With no pressure in the system, the raindrops had to be released at heights as high as 30 ft (9 m) to ensure that drops reached speeds near terminal velocity. Furthermore, these systems were highly susceptible to environmental conditions such as high winds. These constraints limited the use of drop-forming simulators primarily to indoor laboratory experiments. During the 1960's, pressurized rainfall simulation systems became more

popular as researchers desired to conduct larger scale, outdoor experiments (McLaughlin and Brown 2006; Moore et al. 1983; Paige et al. 2003; Sharpley and Kleinman 2003; Swanson 1965). Pressurized rainfall simulators differ from drop-forming simulators in that they rely on nozzles or sprinkler heads to produce rain-like drops. With a pressurized system, raindrops have the ability to reach terminal velocity quicker, thereby allowing for the design of shorter, more portable simulators. Furthermore, pressurized rainfall simulators provide some resistance to environmental conditions, allowing researchers to take their studies outdoors to test ESCs in similar conditions that practices and products would experience in the field. As technological advances have occurred through the 20th and 21st centuries, items such as solenoid valves, digital flowmeters, and software operated systems have increased the accuracy with which these simulators can simulate naturally occurring rain events (Blanquies et al. 2003; Elbasit et al. 2015; Miller 1987).

1.3 RESEARCH OBJECTIVES

The research contained in this thesis is part of a continuing effort by the Highway Research Center at Auburn University to study the performance and effectiveness of commonly used ESCs through large-scale testing techniques. The primary purpose of this research is to incorporate the use of a pressurized rainfall simulator in large-scale testing of erosion control practices and products on a 3H:1V (horizontal:vertical) slope. The study will be conducted at the Auburn University Erosion and Sediment Control Test Facility (AU-ESCTF) located in Opelika, Alabama. The research centered on the design and construction of a rainfall simulator capable of producing raindrop patterns similar to natural rainfall in a repeatable fashion, which was accomplished in two phases. Phase 1 focused on the design and construction of a large-scale rainfall simulator and test plot. Phase 2 focused on the calibration and validation of the rainfall simulator to ensure a system that has the ability to produce repeatable results, thereby minimizing experimental variability. For

the purposes of this study, calibration is defined as the process of determining the optimal location of the sprinkler risers and nozzle configurations to repeatedly and consistently simulate natural rainfall. Validation is defined as the process of conducting bare soil control tests to determine if the simulator is capable of consistently inducing erosion patterns similar to those experienced in the field.

The objectives of each phase are detailed below:

1. Design and construct a 40 ft (12 m) long, 8 ft (2.4 m) wide test plot on a 3H:1V slope test plot and apparatus for conducting erosion studies at the AU-ESCTF.
2. Design a rainfall simulator and electrical control system that will provide uniform coverage and produce consistent, repeatable rainfall on the test plot.
3. Develop testing protocols to ensure consistent, repeatable conditions for the test plot (i.e. plot preparation, soil type, compaction, moisture content).
4. Develop testing protocols to calibrate the rainfall simulator and ensure that the system is satisfying all criteria to produce uniform raindrop coverage that mimics natural rainfall.
5. Evaluate the performance of the rainfall simulator and its ability to simulate natural rainfall, while producing repeatable conditions through calibration of the rainfall simulator and validation of the test results.

To accomplish the abovementioned research objectives, the project was divided into the following tasks:

1. Identify, evaluate, and gain a thorough knowledge of relevant literature on the use of rainfall simulation to conduct erosion studies.

2. Design a rainfall simulator, based upon the findings of the literature review, which is capable of producing repeatable experimental results.
3. Construct the rainfall simulator, test plot, power supply, and test apparatus at the AU-ESCTF to satisfy the design requirements and maintain portability of the system.
4. Develop an applicable testing protocol based on existing standard test methodologies and procedures for rainfall simulator calibration.
5. Conduct large-scale experiments on bare earth plots to calibrate and validate the performance of the rainfall simulator system and test protocols to ensure repeatability of results.

Future research objectives not included in this study include: (1) determining a procedure to simulate various design storms, and (2) examining potential changes to the rainfall simulator to maximize the uniformity of rainfall distribution.

1.4 ORGANIZATION OF THESIS

This thesis is organized into six chapters to effectively communicate the steps taken to complete the research objectives listed above. Following this chapter, *Chapter Two: Literature Review*, examines existing literature pertaining to the design and construction of a multitude of rainfall simulator designs, as well as existing standards for the use of rainfall simulators in the testing and evaluation of erosion control practices and products. The testing procedures and experimental results from previous studies will be discussed. Furthermore, a comparison will be provided between the two primary types of rainfall simulators: drop-forming and pressurized. *Chapter Three: Rainfall Simulator Design and Construction*, provides a detailed description of the steps taken to design each component of the rainfall simulator and test plot constructed at the AU-ESCTF. *Chapter Four: Methods and Procedures*, details methods and procedures used for the

calibration of the rainfall simulator, as well as steps taken to test the erosive energy produced by the simulator. *Chapter Five: Results and Discussion*, provides a concise summary of the findings of the calibration of the rainfall simulator and testing of bare soil conditions and a variety of erosion control practices. *Chapter Six: Conclusions and Recommendations*, provides insight on the success of the design, construction, application, and use of the developed rainfall simulator for large-scale testing of various erosion control practices and products. Finally, recommendations are provided for future research that can be performed to further the body of knowledge in the use of rainfall simulation to test, evaluate, and understand the performance of erosion control products.

CHAPTER TWO:
LITERATURE REVIEW

2.1 BACKGROUND

Construction and earthwork activities (i.e., clearing, grubbing, and grading) increase the amount of exposed soil on construction sites by removing or weakening vegetation and its corresponding root mass, which typically stabilizes the soil surface (Perez 2014). This problem is often magnified by the conversion of previously permeable surfaces into impervious surfaces in the form of buildings, roadways, parking lots, or pedestrian paved paths. As a result, the ensuing decrease in infiltration rates leads to increases in surface runoff volumes and flow velocities (Clark and Pitt 1999). These factors create conditions where newly exposed soil is 100 times more likely to be eroded than on agricultural lands (Brady and Weil 1999). The increased susceptibility of soil to erosion on construction sites during the life cycle of the project has led to concerns over the amount of sediment reaching natural waterways either directly or indirectly via storm sewer systems and other means of conveyance. A primary concern is that the increased amount of suspended solids and corresponding turbidity has a negative impact on the aquatic ecosystem and water quality through the process of sedimentation (Perez 2014). Figure 2.1 provides an example of how drastically pollution from sediment-laden stormwater can affect a local ecosystem.

Figure 2.1 Sediment Pollution in the Black Warrior River, AL (Riverkeeper 2013).

To combat the proliferation of pollutants in the nation's water bodies, Phase I of the National Pollution Discharge Elimination System (NPDES) was established under the Clean Water Act in 1990 (Kinkade-Levario 2006). The goal of this legislation is to control "water pollution by regulating point sources that discharge pollutants into waters of the United States" (USEPA 2014). The NPDES achieves this goal by dictating strict guidelines on allowable runoff pollutant levels for medium to large municipal separate storm sewer systems (MS4s), construction sites disturbing five acres or more of land, and ten groups of industrial activities (USEPA 2005). In 1999, stricter regulations to stormwater were introduced in EPA's Phase II Final Rule. These regulations require NPDES permit coverage for stormwater runoff from small scale MS4s and construction activities disturbing 1 acre or more of land (USEPA 2005). To meet the permit requirements, temporary ESC practices (i.e., erosion control blankets, turf reinforcement mats, ditch checks, perimeter controls, and sediment basins) have been developed to reduce the amount of erosion occurring and

corresponding suspended sediment discharged from the site, thereby polluting nearby surface waters. The U.S. Environmental Protection Agency (USEPA) has stated that eroded sediment transported by stormwater runoff is far greater on construction sites with no ESCs versus sites that implement various ESCs (USEPA 2005). The use of ESCs on construction sites helps reduce erosion and control sediment transport via stormwater runoff, which in turn results in reduced negative impacts on nearby stream habitats and water reservoir capacities (USEPA 2005).

Cost effective and efficient deployment of various ESCs is of significant interest to both the construction industry and the environmental protection community. Rainfall simulators have been used extensively to test the performance of ESCs on both agricultural and disturbed soil (Birt et al. 2007) and to extend research studies of erosion (Bubenzer and Jones Jr. 1971). Rainfall simulators have also helped in studying the relationships between a multitude of factors associated with soil erosion (Elbasit et al. 2015). Natural rainfall can be difficult to use for conducting erosion focused research studies due to the unpredictability of natural rainfall. However, natural rainfall produces the most accurate real world conditions due to several factors: the natural rise and fall of the rainfall event, uniformity of rainfall distribution, and raindrops impacting at terminal velocity. While natural rainfall is most desirable for testing of these practices, simulated rainfall allows for expedited data collection and reproducible testing conditions (McLaughlin et al. 2001; Moore et al. 1983; Thomas and El Swaify 1989).

2.2 RAINFALL SIMULATORS CHARACTERISTICS

Rainfall simulators have been used since the 20th century to efficiently conduct erosion studies by mimicking natural rainfall conditions (Shoemaker 2009). These systems provide increased control over the experiment by allowing for the selection of attributes such as rainfall intensity, drop velocity, and test duration. However, a poorly designed and operated rainfall

simulator can lead to inaccurate rainfall conditions and affect the repeatability of erosion studies (Shoemaker 2009). As stated earlier, Rainfall simulators can be divided into two categories: drop forming and pressurized nozzle simulators. Simulators have been used for many years to study the effects of rainfall on a plot. Early simulators developed in the 1930's were used to study erosion and runoff, however, these experiments lacked knowledge on the drop characteristics produced by natural rainfall (Cabalka et al. 1998). To effectively simulate natural rainfall, the properties of raindrops would first have to be studied more in depth. One of the first reports on the properties of natural rainfall came from Laws (1941), where a relationship was found between raindrop size and drop velocity. It was later discovered that there was a relationship between drop size distribution and rainfall intensity (Laws and Parsons 1943).

2.2.1 Drop Forming Simulators

Drop forming simulators use either hanging yarn or hypodermic needles to produce drops (Mutchler and Hermsmeier 1965). Other simulators have used stainless steel tubing to form drops (Regmi and Thompson 2000). Drop forming simulators are used primarily on small plots in laboratory experiments studying infiltration, erosion, and soil splash (Moore et al. 1983). Early studies that use drop forming simulators had two major drawbacks: (1) the simulators produced large rainfall intensities of 5 to 14 in/hr. (13 to 36 cm/hr) and (2) the drops were formed at low heights, resulting in the failure of drops to reach terminal velocity upon impacting the surface (Epstein and Grant 1966). While drop forming simulators offer considerable control during an experiment, they also offer several challenges in operation, including: restricted flow performance due to frictional and capillary forces, difficulty in maintaining drop uniformity at low operating pressures, and requiring large heights, as much as 33 ft (10 m), to achieve terminal velocity (Birt

et al. 2007). The height required for these types of rainfall simulators to operate makes them unfeasible for use in field experiments (Blanquies et al. 2003).

2.2.2 Pressurized Nozzle Simulators

The alternative to drop forming simulators is pressurized nozzle simulators. These simulators are preferred for field-scale studies since they create greater rainfall intensities, are designed for portability, cover a large plot area effectively, and produce a more random drop size distribution similar to that of natural rainfall (Humphry et al. 2002). To accurately simulate natural rainfall, several design criteria must be considered and satisfied, which include: (1) drop size distribution and fall velocities similar to natural rainfall, (2) intensities similar to storms producing medium to high rates of runoff and erosion, (3) a study area large enough to accurately represent erosion conditions, (4) uniform drop distribution throughout the study area, (5) near-continuous rainfall application throughout the study area, (6) near vertical impact of most drops, (7) total kinetic energy similar to that of natural rainfall, (8) satisfactory performance in windy conditions, and (9) portability of the system (Meyer 1965).

2.3 DROP SIZE DISTRIBUTION

Simulated rainfall has become a useful tool for researchers studying infiltration and erosion due to the fact that their simulators produce rainfall events that can be replicated at chosen times and locations (Bubenzer et al. 1985). However, as previously mentioned, it is important that the drop size distribution of the simulated rainfall closely mimic natural rainfall conditions (Meyer 1965). Raindrop size can vary from mist droplets to drops of 0.24 to 0.28 in. (6 to 7 mm) in diameter, with the median diameter varying depending upon the storm intensity (Hudson 1993). The distribution of drop sizes was found to be correlated to the intensity of the storm event (Laws and Parsons 1943). A diagram showing the relationship between the two variables, drop size and

intensity, is shown in Figure 2.2. By selecting a theoretical rainfall intensity (in./hr), the median drop diameter (mm) can be determined by drawing a straight line from the selected intensity to the median drop diameter line (designated by a "50"). From there, a horizontal line can be drawn to connect to the y-axis, which in this case designates median drop diameter. For example, by selecting a rainfall intensity of 0.185 in./hr (0.470 cm/hr) on the x axis, drawing a straight line to the median diameter line, and connecting to the y-axis, it can be estimated that the median drop size for that respective rainfall intensity is 0.06 in. (1.6 mm). The value for drop diameter found in the chart can also be compared to the value calculated using Equation 2.1 (Ekern 1950):

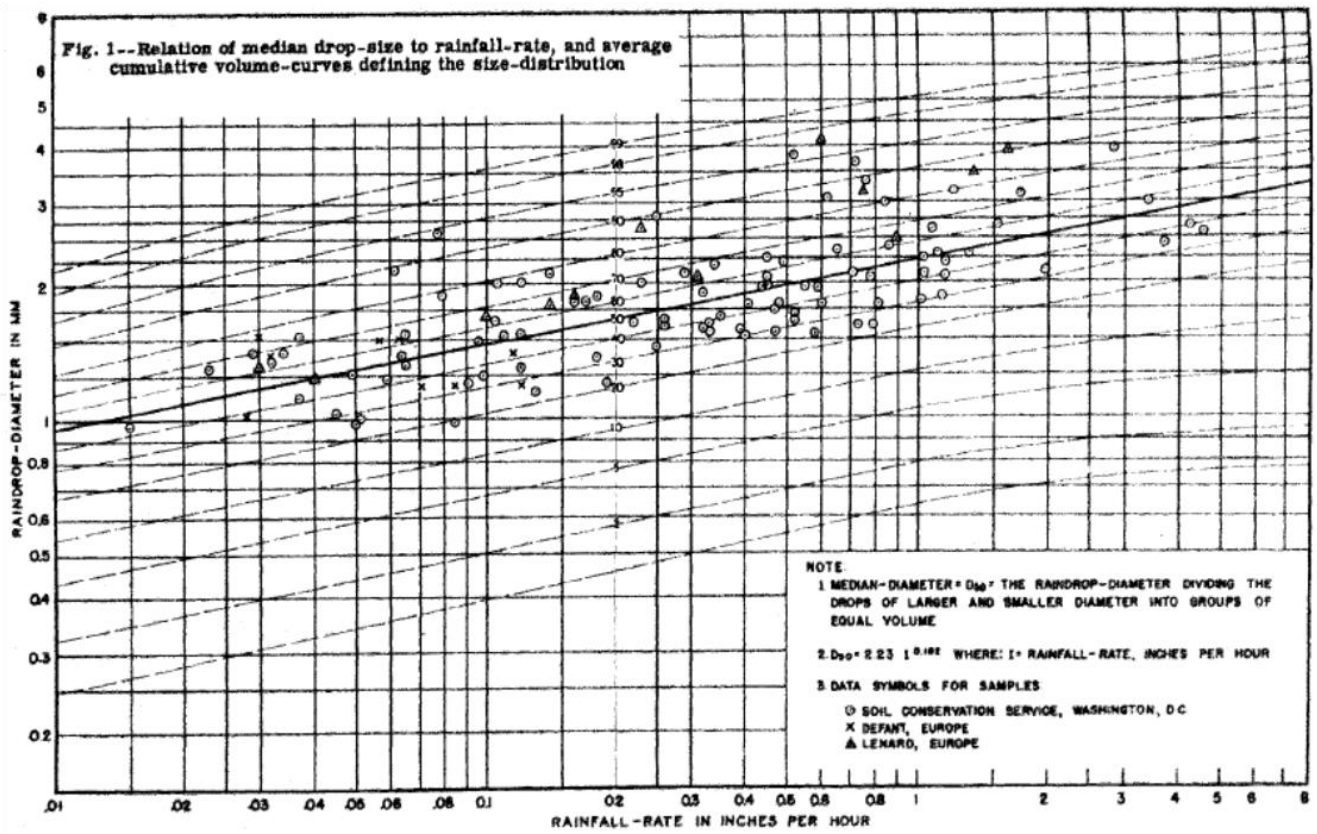

Figure 2.2 Relationship of Drop Size to Intensity (Laws and Parsons 1943).

$$D_m = 2.23I^{0.182} \quad \text{(EQ. 2.1)}$$

where,

D_m = Median Drop Diameter, (mm)
I = Intensity of Precipitation, (in./hr)

To calculate D_m, a value for I must be selected. For a 2-yr, 24-hr storm in the state of Alabama, I is approximately 0.185 in./hr. (Perez et al. 2015). Using this value, the median drop diameter is calculated to be approximately 0.065 in. (1.64 mm). This median drop diameter is comparable to the values reported by Laws (1943) in Figure 2.2. The desire to determine the drop size distribution of simulated rainfall first arose from early attempts to measure the susceptibility to erosion and infiltration capacity of small plots (Laws and Parsons 1943). Techniques used to measure the distribution include the stain method, flour method, momentum method, photographic method, immersion method, and oil method (Eigel and Moore 1983), which are described here forth.

2.3.1 The Stain Method

The stain method works on the idea that when a rain drop impacts a uniform absorbent surface, the ensuing stain produced is proportional to the diameter of the drop (Hall 1970). Absorbent surfaces appropriate for this test include filter paper, blotting paper, blueprint paper, paper toweling, photographic paper, adding machine tape, and glazed paper (Eigel and Moore 1983). This method is hampered by the fact that large drops can splash on impact, thereby introducing error into the results of the test method (Eigel and Moore 1983).

2.3.2 The Flour Method

The flour method was first used by Bentley (1904) and has seen widespread use since. This method, as described by Eigel and Moore (1983), is performed by dropping water-drops of a known mass into trays containing a 25 mm thick layer of flour. The pellets formed by the drops

hitting the flour are then oven dried and weighed to determine the mass ratio. The process is repeated to obtain multiple mass ratios to create a calibration curve. Flour trays are then exposed to simulated rainfall and drop size is determined using the calibration curves. This method is inconsistent in that calibration curves can vary from bag to bag of flour and the method has difficulty determining calibration curves for smaller drop sizes (Laws 1941).

This method is yet to be an accepted, standardized test method in the industry. It is currently undergoing review within ASTM to become a standard test method. For each target intensity, three, 9 in. (23 cm) diameter cake pans are filled to 1 in. (2.5 cm) in depth with all-purpose flour. The covered cake pans are then placed and evenly spaced along the test plot. Each pan is mounted 12 in. (30.5 cm) off the ground. When the target intensity is reached, the cake pans are uncovered for 2 to 4 seconds, depending on how quickly the flour is covered with raindrops. Once the pans are covered, the pellets are allowed to air dry for 12 hours. The contents of the pan are then screened through a #70 sieve to remove excess flour. Any double pellets are removed during this process. The pellets are then transferred to an evaporating dish and placed in an oven at 110 °F (43 °C) for 6 hours. Next, the hardened pellets are sorted using a sieve stack comprised of a #4, #8, #10, #14, #20, #30 sieves and the pan. The pellets are sieved for 2 minutes and the total weight and pellet count for each sieve is recorded. The average drop diameter can be calculated from the flour pellet weight using Equation 2.2.

$$D_r = \sqrt[3]{\left(\frac{6}{\pi}\right) W} \qquad \text{(EQ. 2.2)}$$

where,

D_r = Raindrop diameter, (mm)
W = Average pellet weight, (mg)

2.3.3 Photographic Method

The photographic method allows for a direct measurement of the size and shapes of a water drop. While this method might seem the most accurate, it is not efficient in determining drop size distributions and the equipment used is not well suited for use in a field-scale experiments (Eigel and Moore 1983).

2.3.4 Momentum Method

In this method, pressure transducers and piezoelectric sensors are used to measure a raindrop's size. This method is not commonly used for determining the drop size distribution for a rainfall simulator since the equipment is expensive and not effective at determining the size distribution where multiple size drops are used (Eigel and Moore 1983).

2.3.5 Immersion Method

The immersion method is performed by collecting raindrops in oil. Due to the low density of the oil, the raindrop is enveloped and preserved by the liquid, allowing for measurement of the drop diameter with a microscope (Eigel and Moore 1983). This method is not suitable for use in field-scale simulator experiments due to several problems: large drops disintegrating upon impact with the oil, evaporation of drops not immersed in the oil, and the failure of the oil to immerse small drops (McCool 1982).

2.3.6 Oil Method

The method recommended by Eigel and Moore (1983) is the oil method. This method is based on the similar premise as the immersion method, that raindrops will be immersed in a less dense, more viscous fluid, preserving the shape of the drop. The oil used is a 2:1 mix of STP® oil

treatment and heavy mineral oil. The mixture is then placed next to a scale and exposed to rainfall. A photograph is quickly taken thereafter so the drop diameters can be determined.

2.4 TERMINAL VELOCITY

For simulated rainfall to mimic natural rainfall, raindrops must achieve terminal velocity before impacting the surface (Meyer 1965). Terminal velocity is achieved when the downward gravitational forces acting on the raindrop are cancelled out by the drag acting on the drop (Hall 2015). Laws (1941) found that raindrops approach terminal velocity as they fall through the air and that the terminal velocity varies with drop size. Figure 2.3 displays the relationship between drop size and terminal velocity.

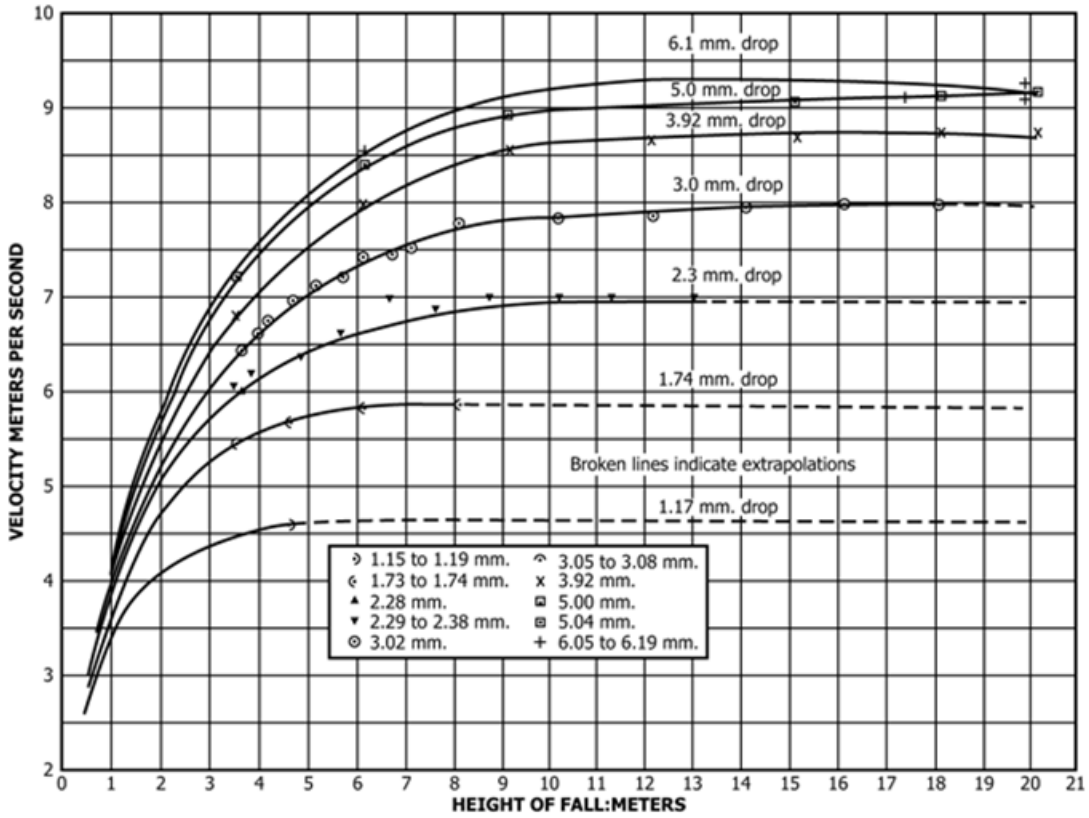

Figure 2.3 Fall Velocity vs. Fall Height (ASTM 2015).

With pressurized nozzle simulators, drops are formed with an initial velocity, allowing for shorter fall heights as compared to drop forming simulators (Mutchler and Hermsmeier 1965). In

the literature, simulated rainfall achieved terminal velocity using nozzle heights of 6.5 ft to 9.8 ft (2.0 m to 3.0 m) (Bubenzer et al. 1985; Humphry et al. 2002; Moore et al. 1983). Pressurized nozzle simulators are superior to drop forming simulators in this aspect, since drop forming simulators can require 33 ft (10 m) or more of fall height to reach terminal velocity (Regmi and Thompson 2000). Since the effect a raindrop has on erosion is correlated with the energy of the raindrop (Ekern 1950), it is crucial that a researcher's rainfall simulator produce rainfall near terminal velocity to achieve accurate results in the erosion study.

2.5 RAINFALL INTENSITY

Laws and Parsons (1943) found that the drop size distribution of rainfall was directly correlated to the intensity. Therefore, to accurately reproduce the drop size distribution of the desired storm, researchers must also ensure their simulator is producing similar intensities to the storms they are trying to simulate. When designing a rainfall simulator, it is important to decide what intensity storm(s) to simulate. In the construction industry, ESC practices are generally designed for a 2-yr, 24 hr storm event (USEPA 2012). A 2-yr, 24 hr storm has a 50% probability of occurring in any given year. Figure 2.4 and Table 2.1 summarize Atlas 14 point precipitation estimates for the state of Alabama obtained from the National Oceanic and Atmospheric Administration (NOAA 2014) in graphical and tabular form, respectively.

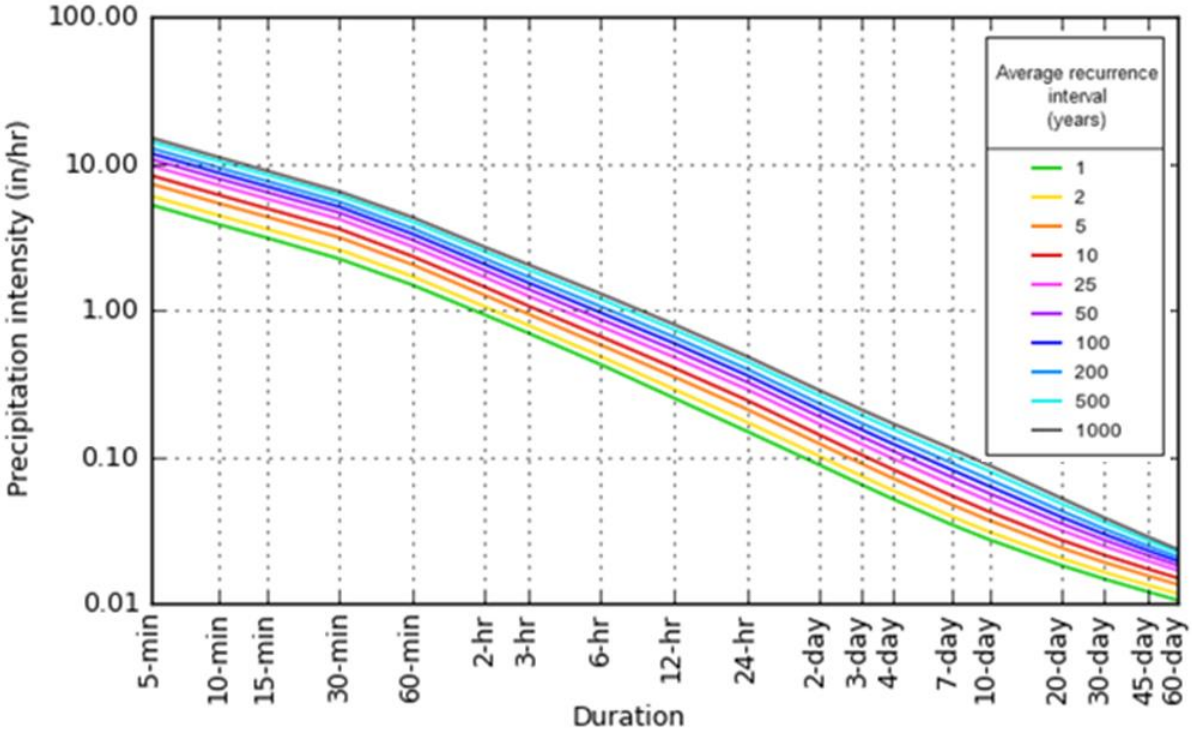

Figure 2.4 Precipitation Frequency Estimates for Alabama (NOAA 2014).

Table 2.1 Precipitation Estimates for Alabama (NOAA 2014)

Duration	Average Recurrence Interval (Years)									
	1	2	5	10	25	50	100	200	500	1000
5-min	5.23	6.01	7.27	8.30	9.68	10.7	11.7	12.7	14.0	15.0
10-min	3.83	4.40	5.33	6.08	7.09	7.84	8.59	9.32	10.3	11.0
15-min	3.12	3.58	4.33	4.94	5.76	6.38	6.98	7.58	8.35	8.92
30-min	2.24	2.58	3.13	3.58	4.17	4.62	5.05	5.48	6.03	6.43
60-min	1.49	1.70	2.04	2.33	2.72	3.02	3.31	3.61	4.00	4.29
2-hr	0.928	1.05	1.26	1.44	1.68	1.86	2.05	2.24	2.49	2.68
3-hr	0.700	0.792	0.944	1.07	1.25	1.40	1.54	1.69	1.89	2.05
6-hr	0.426	0.484	0.579	0.661	0.777	0.868	0.962	1.06	1.19	1.29
12-hr	0.253	0.290	0.353	0.406	0.480	0.538	0.597	0.657	0.739	0.802
24-hr	0.150	0.173	0.212	0.244	0.290	0.325	0.361	0.398	0.447	0.485
2-day	0.088	0.101	0.123	0.141	0.167	0.188	0.209	0.231	0.261	0.284
3-day	0.064	0.074	0.089	0.103	0.122	0.137	0.153	0.169	0.191	0.209
4-day	0.052	0.059	0.072	0.083	0.098	0.110	0.123	0.136	0.155	0.169
7-day	0.035	0.039	0.047	0.055	0.065	0.073	0.082	0.091	0.104	0.114
10-day	0.027	0.031	0.037	0.042	0.050	0.057	0.063	0.070	0.080	0.088
20-day	0.018	0.020	0.024	0.027	0.032	0.035	0.039	0.043	0.048	0.052
30-day	0.015	0.016	0.019	0.021	0.025	0.027	0.030	0.032	0.036	0.038
45-day	0.012	0.013	0.016	0.017	0.020	0.021	0.023	0.025	0.027	0.029
60-day	0.011	0.012	0.014	0.015	0.017	0.018	0.020	0.021	0.022	0.023

From Table 2.1, the 2-yr, 24 hr storm will generate 0.173 in/hr of rainfall. However, most state transportation departments use the rainfall contour curves from Technical Paper No. 40 (Hershfield 1961). Perez et al. (2015) inserted the rainfall contour curves for a 2-yr, 24 hr storm into ArcGIS™ to generate rainfall intensity contours, as shown in Figure 2.5, and calculated the average rainfall depth of 4.43 in. for the State of Alabama. This value provides a total amount of rainfall for a 2-yr, 24 hr storm and can be used when making design decisions for the rainfall simulator, which will be applicable to the State of Alabama.

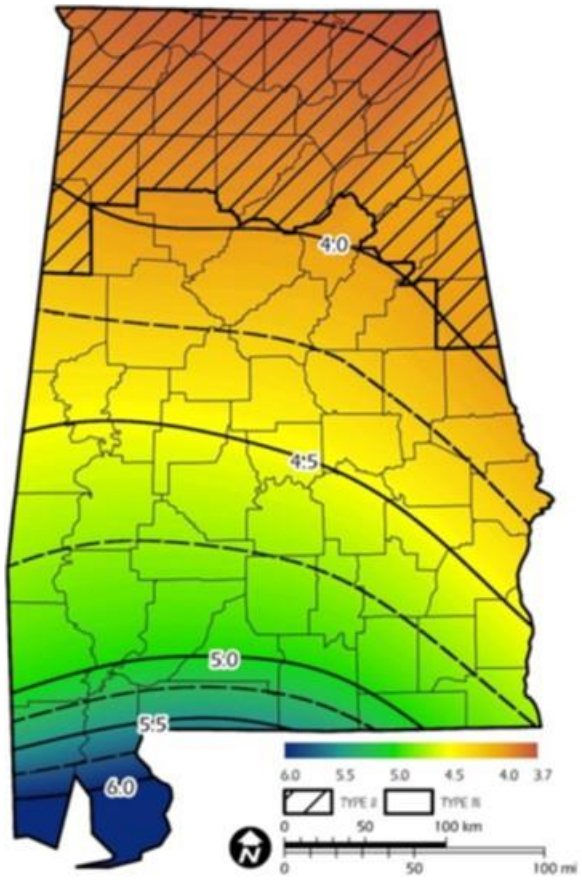

Figure 2.5 2-yr, 24 hr Rainfall Distribution, in. (Perez et al. 2015).

2.6 KINETIC ENERGY OF NATURAL RAINFALL

Soil erosion is a mechanical process that is initiated by the energy delivered from raindrops upon impact (Wischmeier and Smith 1958). In America's corn belt, an average storm can generate 100 tons of deadweight loss on one acre of soil just from rainfall (Wischmeier and Smith 1958). An accurate representation of the relationship between erosion caused by natural and simulated rainfall has not been established for field studies (Barnett and Dooley 1972). Therefore, it is necessary to ensure that the kinetic energy of simulated rainfall is similar to natural rainfall since this property is the single measure that can relate the two (Blanquies et al. 2003). The kinetic energy of natural rainfall can be calculated using Equation 2.3 (Wischmeier and Smith 1958).

$$KE = 916 + 331 \log_{10} I \quad \text{(EQ. 2.3)}$$

where,

KE = Kinetic energy, (ft-tons/acre-in.)
I = Rainfall Intensity, (in./hr)

Using the value for total rainfall listed in the previous section (Perez et al. 2015) of 4.43 in. (11.25 cm), or 0.185 in/hr (0.470 cm/hr), the kinetic energy for a 2-yr, 24-hr storm is calculated to be approximately 673 foot-tons/acre-in (20 J/L). In a comparison between natural and simulated rainfall, Barnett and Dooley (1972) found that the amount of soil loss per unit of *EI* (kinetic energy and intensity) was less for simulated rainfall than natural rainfall. However, after performing regression on the rainfall data, it was found that there was no statistically significant difference in soil loss between the two types of rainfall (Barnett and Dooley 1972). Kinetic energy can also be measured from the physical properties of simulated rainfall: raindrop size, fall velocity, and drop size distribution (Eigel and Moore 1983). Therefore, if a simulator is designed to ensure these properties are similar to natural rainfall, it can be assumed that the simulated rainfall will have a total kinetic energy similar to natural rainfall.

2.7 UNIFORM RAINFALL DROP DISTRIBUTION

For a rainfall simulator to effectively simulate natural rainfall, it must cover the entire plot area in a uniform fashion and create a random drop distribution (Meyer 1965). Uniform drop distribution can be difficult to achieve since pressurized nozzle simulators sacrifice uniformity to produce higher intensities (Humphry et al. 2002). With these simulators, the uniformity of the drop distribution is dependent upon nozzle pressure, spacing, and oscillation (Paige et al. 2003). The drop distribution is not uniform over the area covered by the nozzle spray, with more concentrated spray occurring directly under the nozzle. To resolve this, nozzles are spaced so that areas of less coverage from the nozzles are overlapped (Paige et al. 2003). Researchers can verify

that their simulator is creating uniform spray coverage using Christensen's coefficient of uniformity (Christiansen 1942):

$$C_U = 100\left[1.0 - \left(\frac{\sum\left(\left|D_i - D_{avg}\right|\right)}{n * D_{avg}}\right)\right] \quad \text{(EQ. 2.4)}$$

where,

C_U = Uniformity of spray, (%)
D_i = Depth of water in rain gauge, (cm)
D_{avg} = Average depth in rain gauge, (cm)
n = Number of observations

Testing of the uniformity of drop distribution should be conducted during the initial calibration period and at the beginning of each testing season (ASTM 2015). A few methods of acquiring data to calculate the coefficient of uniformity were identified in review of the literature. Humphry et al. (2002) installed 221, 3.9 in. (100 mm) diameter cups placed 5 in. (0.125 m) apart on the test plot. Rainfall was collected in the cups over a period of 30 minutes of continuous flow from the simulator. The cups were then weighed to determine the volume in each individual cup. Moore et al. (1983) used a similar method in which they placed rain gauges 12 in. (300 mm) apart throughout the test plot to measure spray uniformity. Using one nozzle, Humphry et al. (2002) reported a CU of 93% using one nozzle. Moore et al. (1983) reported an average CU of 82%. The decrease in uniformity can be attributed to the much larger simulator used by Moore. Adding additional nozzles allows for large-scale testing but sacrifices the uniformity of drop distribution due to the potential for unequal overlap of the simulated rainfall (Shoemaker 2009). In this study, a minimum value for Christensen's coefficient of uniformity was selected to be 80%.

2.8 CHARACTERISTICS OF VARIOUS PRESSURIZED RAINFALL SIMULATORS

Researchers have found various methods to satisfy the criteria required to accurately simulate natural rainfall. Differences in design exist between each study, leading to differences in

values for drop size distribution, uniformity, terminal velocity, etc. Table 2.2 summarizes several studies that used pressurized nozzle rainfall simulators (Humphry et al. 2002; Moore et al. 1983; Paige et al. 2003; Shelton et al. 1985).

Table 2.2 Summary of Pressurized Rainfall Simulator Designs

Study	Median Drop Size (mm)	Height of Rainfall Simulator (ft)	Rainfall Intensity (in./hr)	Coefficient of Uniformity (%)	Plot Size (ft^2)
Paige et al. (2003)	N/A	8	0.51-5.12	92.7	131
Paige et al. (2003)	N/A	8	5.51-7.87	91.6	131
Moore et al. (1983)	N/A	9.8	0.14-7.28	82.0	1065
Shelton et al. (1985)	1.8-2.2	7.9-9.8	5.08	72.0	387
Humphry et al. (2002)	1.9	9.8	2.8	93.0	32

As discussed in Section 2.4, by pressurizing the simulated rainfall, researches are able to decrease the height of their simulators from 30 ft (9.1 m), to 8 to 10 ft (2.4 to 3.05 m). The values for rainfall intensity, coefficient of uniformity and plot size, shown in Table 2.2 also confirm that as intensities and plot sizes are increased, uniformity of rainfall distribution decreases.

2.8.1 Erosion Studies Using Simulated Rainfall

Various methods are employed in the testing of erosion control practices. Through the literature review, many studies were identified that employed simulated rainfall to generate splash erosion and runoff for their tests (Benik et al. 2003; Foltz and Dooley 2003; Kim et al. 2001; King and Bjorneberg 2011; McLaughlin and Brown 2006; Ming-Han et al. 2003; Shoemaker et al. 2012; Xiao et al. 2010). While each of these studies simulated rainfall to conduct their experiments, the means by which they designed their experiment and rainfall simulator vary from study to study.

Shoemaker et al. (2012) developed a laboratory scale rainfall simulator to conduct studies on the effectiveness of anionic polyacrylamide (PAM) as an erosion control measure. The simulator was installed at a height of 10 ft (3.05 m) and used a pressure regulator and solenoid valve to control flow. Two plots, each with a surface area of 8 ft^2 (0.72 m^2), were constructed and

placed under the simulator at a 3:1 (H:V) slope. Using Christiansen's coefficient of uniformity, Shoemaker et al. (2012) calculated that the simulator was capable of producing uniformity coefficients ranging from 83% to 87% over the two plots. Shoemaker's rainfall simulator is shown in Figure 2.6.

Figure 2.6 Laboratory Scale Rainfall Simulator (Shoemaker et al. 2012).

The simulator designed by Shoemaker et al. (2012) produced a rainfall intensity of 4.4 in./hr (11.2 cm/hr). Tests consisted of four, 15 minute rainfall events separated by 15 minutes of no rainfall. Each rainfall period was capable of producing 1.1 in. (28 mm) of rainfall.

Kim et al. (2001) conducted a study examining the effectiveness of PAM treatments on steep vegetable fields in South Korea. Six test plots were constructed on slopes ranging from 29% to 30%. Each test plot was constructed to have a surface area of 26 ft^2 (8 m^2). Kim's rainfall simulator was constructed with steel angles and sprinklers set at a height of 8 ft (2.4 m). The simulator was capable of generating rainfall intensities from 2.8 in./hr to 3.3 in./hr (70 mm/hr to

85 mm/hr). Individual tests were separated into 30 minute dry runs, a 30 minute pause for data collection, and a 30 minute wet run.

Benik et al. (2003) conducted a rainfall simulation study investigating the effect of erosion control products in the establishment of vegetation on highway embankments using a rotating-boom rainfall simulator based on Swanson's (1965) design. The test plot was constructed on a sediment basin slope located in a highway project in Minneapolis, Minnesota. The plots were located on a 2.8H:1V side slope. Each test plot was tilled to a depth of 6 in. (15 cm). This study examined five treatments: bare treatment, straw mulch, Soil Guard bonded-fiber matrix (Mat, Inc.), CFS072R straw/coconut blanket (Greenfix of America Company), and Curlex III wood-fiber blanket (American Excelsior Company). Each plot had a length of 32 ft (9.75 m). The width of each plot was determined by the product being tested. Plots covered in blanket treatments had widths of 8 ft (2.4 m) while bare plots, plots covered in straw-mulch or bonded-fiber matrix had widths of 4 ft (1.2 m). The plot widths were designed to all fit within the radius of spray produced by the simulator. The rotating-boom simulator was capable of producing a uniform, circular spray pattern over a diameter of 50 ft (15.2 m). Pressure regulators were installed at each nozzle to maintain a constant pressure and rainfall intensity of 8 psi (55 kPa) and 2.4 in./hr (60 mm/hr), respectively. Simulations were conducted under two vegetative conditions: no/little vegetation and good vegetative growth. Each test consisted of a dry and wet run to assess the effect initial moisture content had on various treatment methods. Tests lasted 90 minutes and 60 minutes after runoff from the plot was observed for dry runs and wet runs, respectively.

Foltz and Dooley (2003) conducted a study to compare the effectiveness of wood strands to straw as erosion control practices. Test plots were housed in steel frames 13 ft (4 m) long and 4 ft (1.24 m) wide. Each frame was set on a single slope of 30%. The rainfall simulator used in

this studied was based on the Purdue simulator developed by Foster et al. (1982). VeeJet 80150 nozzles produced a constant rainfall intensity of 2 in./hr (50 mm/hr). Four soil conditions were tested in this experiment: bare soil, straw treatment, wide wood strand treatment, and narrow wood strand treatment. Tests were divided into three segments totaling 25 minutes. First, a rain and inflow sequence was produced by the simulated rainfall. Over the second and third segments, the inflow was increased to reach the critical shear and twice the critical shear, respectively. Figure 2.7 provides a detailed sketch of the plot layout.

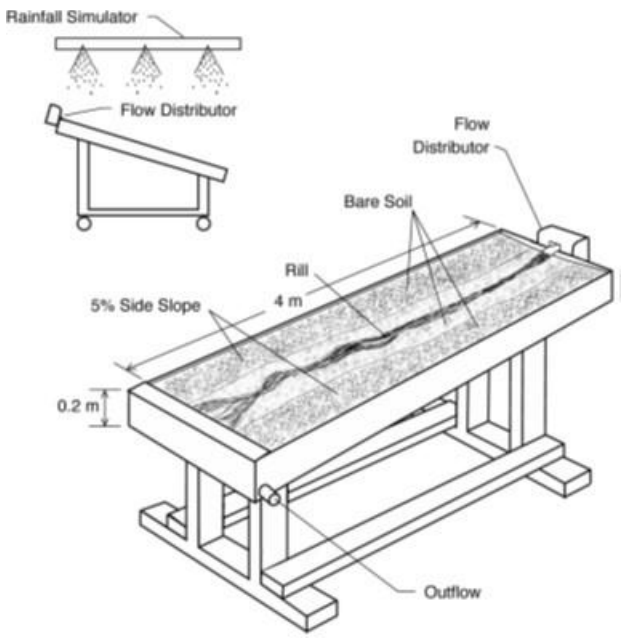

Figure 2.7 Plot Layout Design (Foltz and Dooley 2003).

Ming-Han et al. (2003) investigated the performance of five rolled erosion control products (RECPs) and one hydraulically applied product using field scale rainfall simulation. The six treatments applied in this study include: turf reinforcement mats (TRMs) constructed out of polypropylene fibers (Synthetic Industries), open weave textile (OWT) constructed out of polypropylene fibers (Synthetic Industries), erosion control blankets (ECBs) constructed out of wheat straw and jute netting (Synthetic Industries), ECBs constructed out of straw fibers bound by

polypropylene netting (North American Green), ECB constructed out of aspen curled wood bound by degradable netting (American Excelsior Company), and a bonded fiber matrix (BFM) constructed out of softwood fibers bonded by adhesive (Canfor). Each treatment was tested on a 2H:1V slope and a 3H:1V slope. Test plots on the 2H:1V slope were 20 ft (6 m) wide and 50 ft (15 m) long. Test plots on the 3H:1V slope were 20 ft (6 m) wide and 70 ft (21 m) long. Treatments were installed according to manufacturers' specifications. Hydroseed was mixed following Texas Department of Transportation (TxDOT) guidelines and applied during installation of each treatment. The rainfall simulator was mounted 18 in. (0.46 m) above the test plot and designed to apply rainfall intensities of 1.19 in./hr (30.2 mm/hr), 5.73 in./hr (145.5 mm/hr), and 7.23 in./hr (183.6 mm/hr). Each treatment was subjected to six tests. Treatments were tested in two iterations, 10 minutes in length, for each storm intensity.

McLaughlin and Brown (2006) conducted a rainfall simulation study with the objective of determining if the application of PAM to different mulches provided any improvement in the practice as an erosion control. For this study, 3.3 ft (1 m) wide by 6.6 ft (2 m) long test plots were constructed. Each plot was set on a slope of either 10% or 20%. A rainfall simulator based on a similar design to that of Miller's (1987) was constructed for this experiment. A 1/2HH-SS50WSQ Fulljet nozzle was installed 13 ft (4 m) above the test plots to produce rain drops. The nozzle was set at a pressure of 5 psi (34 kPa) and produced droplet sizes similar to natural rainfall. During tests, the simulator produced a constant rainfall intensity of 2.6 in./hr (68 mm/hr). The intensity was reduced to a rate of 1.3 in./hr (34 mm/hr) by programming a solenoid valve to cycle off and on in 10 second intervals. Tests were run until 5 minutes after runoff was observed from the test plots. The rainfall simulator constructed for this experiment is shown in Figure 2.8.

Figure 2.8 Pressurized Nozzle Simulator (McLaughlin and Brown 2006).

Xiao et al. (2010) used a rainfall simulator based on Humphry's (2002) simulator design to test the effectiveness of using compost as an erosion control on roadside embankments. The rainfall simulator had an average rainfall intensity of 2.5 in./hr (64 mm/hr) and a nozzle height of 9.8 ft (3 m). A test plot with an area of 432 $in.^2$ (2730 cm^2) was constructed underneath the simulator on a 3H:1V slope. Figure 2.9 displays the rainfall simulator and test plot configuration.

Figure 2.9 Pressurized Rainfall Simulator (Xiao et al. 2010).

The base soil was initially tested for erodibility by compacting it to a dry density of 1.50 g/cm^3 and exposing the soil to 1 hr of simulated rainfall. Two compost configurations were selected for single event testing: (1) unpelletized compost and (2) unpelletized compost with pelletized "cut short" compost. The long term effectiveness of the compost was tested by subjecting the test plot to multiple rainfall events, each 1 hr in duration, for each test. Six repeated rainfall events were simulated with three day intervals between tests to allow adequate time for the dry.

Robeson (2014) conducted a study where data from bare-soil rainfall simulation tests were compiled from large-scale laboratories around the country. Data collected from these labs was then used to create an equation whereby erosion predictions could be made to fulfill USEPA stabilization requirements. The laboratories from which data was collected for this study included: (1) ErosionLab® in Wisconsin, (2) San Diego State University, (3) Texas Transportation Institute, (4) Texas Research International, and (5) Utah State University. Robeson (2014) found that the prediction equation was a function of several characteristics related to simulated rainfall and test

slope conditions: (1) rainfall intensity, (2) test plot area, (3), duration of test, (4), gradient of the slope, (5) median raindrop diameter, (6) kinetic energy of rainfall, (7) percent clay in soil, and (8) percent compaction of soil.

The research studies discussed above show that there are multiple designs for rainfall simulators and multiple test procedures implemented to test various practices. With each study possessing contrasting test procedures, comparison of results could prove to be limited. Table 2.3 summarizes the rainfall simulator design and test protocols from each study previously discussed.

Table 2.3 Summary of Previous Research Studies

	Nozzle Height, ft (m)	Plot Area, ft^2 (m^2)	Coefficient of Uniformity	Simulated Rainfall Intensity, in./hr (cm/hr)	Test Duration, min
Shoemaker et al.	10 (3.05)	8 (0.72)	83-87%	4.4 (11.2)	60
Kim et al.	8 (2.4)	26 (8)	--	2.8-3.3 (7-8.5)	30
Benik et al.	9 (2.7)	256, 128 (24, 12)	--	2.4 (6)	90, 60
Foltz and Dooley	8 (2.4)	52 (5)	--	2 (5)	25
Ming-Han et al.	1.5 (0.46)	1000, 1400 (93, 130)	--	1.19, 5.73, 7.23 (3.02, 14.55, 18.36)	10
McLaughlin and Brown	13 (4)	22 (2)	--	1.3-2.6 (3.4-6.8)	5 min. After Runoff
Xiao et al.	9.8 (3)	3 (0.28)	--	2.8 (7)	60

2.9 CURRENT STANDARD TEST METHODOLOGIES

In order to ensure that a study's results can be replicated, standard test methods should be followed whenever they are applicable. Designing test procedures around standard methodologies allows the research to compare results with previous and concurrent studies. Furthermore, it allows the results from the study to be more readily replicated.

2.9.1 ASTM D6459

Large-scale testing of rolled erosion control practices (RECPs) and products (i.e., erosion control blankets, turf reinforcement mats, etc.) should be conducted in accordance with ASTM D6459-15. This standard test method is used for testing RECPs performance using simulated

rainfall induced erosion (ASTM 2015). A RECP is defined as "a temporary degradable or long term non-degradable material manufactured or fabricated into rolls designed to reduce soil erosion and assist in the growth, establishment, and protection of vegetation" (ASTM 2015). A rainfall simulator used to conduct this test must have sprinkler heads, sprinkler risers, pressure gauges, and valves. Raindrop size should be 0.04 to 0.25 in. (1 to 6 mm). Furthermore, the risers should be constructed to create a fall height of 14 ft (4.3 m). This design is shown in Figure 2.10.

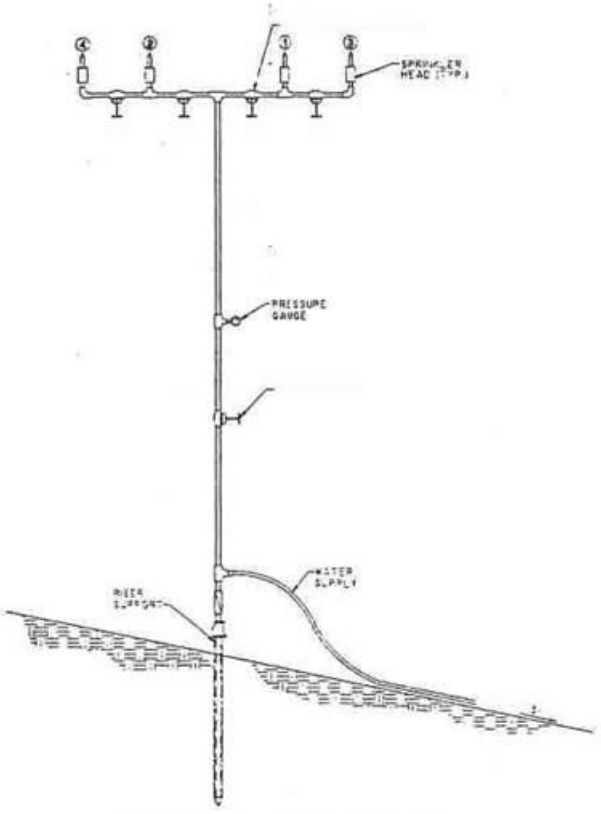

Figure 2.10 Typical Rainfall Simulator (ASTM 2015).

To accurately test a RECP, the test plot must be properly prepared and the simulator calibrated. The steps for test plot preparation and simulator calibration, as described by the ASTM standard (2015), are summarized below.

2.9.1.1 Test Plot Preparation

A geotechnical stable test plot must be constructed on a 3H:1V slope with a length of 40 ft (12 m). Either loam, clay, or sand should be placed on the test plot at a thickness of at least 11.8 in. (30 cm). The recommended grain sizes and plasticity indices are listed in Table 2.4.

Table 2.4 Test Plot Soil Characteristics (ASTM 2015)

Grain Size (mm)	SAND	LOAM	CLAY
D_{100}	$D_{100} < 40$	$D_{100} < 25$	$D_{100} < 10$
D_{85}	$1.0 < D_{85} < 10.0$	$0.5 < D_{85} < 5.0$	$0.01 < D_{85} < 1.0$
D_{50}	$0.08 < D_{50} < 2.0$	$0.01 < D_{50} < 1.0$	$0.001 < D_{50} < 0.1$
D_{15}	$0.001 < D_{15}$	$0.05 < D_{15}$	$D_{15} < 0.0015$
Plasticity Index	Nonplastic	$1 < PI < 8$	$14 < PI$

The veneer should then be placed in 6 in. (15 cm) lifts and compacted to 90 ± 3% standard proctor density as defined by ASTM D698. Test plots, with dimensions of 8 ft by 40 ft (2.4 m by 12 m), should be located on the embankment. Soil should be loosened to a depth of 4 in. (10 cm) using a metal rake or other capable equipment. The soil should then be smoothed with a metal rake and lightly compacted.

2.9.1.2 Simulator Calibration

To calibrate a rainfall simulator, the values for rainfall intensity, uniformity of drop distribution, and drop size distributions for each intensity must be calculated. To ensure accuracy in the uniformity test, calibration should not be conducted when wind speeds reach higher than 5 mph (8 km/hr). The first step in the calibration process is to install the sprinkler manifolds around the perimeter of the test plot. Testing should then be done to determine the spacing between risers that results in the highest uniformity of spray. The recommended method for collecting data to calculate the uniformity coefficient is to place rain gauges throughout the plot to collect rainfall during the 15 minute calibration test.

The drop size distribution is measured using a flour method similar to the one described in Section 2.3.2. Three pie pans will be filled with sifted flour and struck off to a level surface. The pans are then placed on 7.9 in. (20 cm) high supports along the centerline of the plot at the horizontal quarter points. At the intensity to be tested, the covers of the pie pans should be removed for only a few seconds. Once the flour pellets have dried for 12 hours, the contents can then be sorted through a 70-mesh sieve. Remaining pellets are to be transferred to evaporating dishes and heated at 110°F (43°C) for 6 hours. The total weight of the pellets should then be recorded. The pellets should then be sieved by shaking for 2 min. The total weight and pellet count for each sieve can then be recorded. These measurements are then be used to determine the median drop diameter (mm) produced at a specific rainfall intensity using Equation 2. The fall height of the raindrops can be determined by holding a surveyor's rod into the spray of a single riser and measuring the wetted height.

2.9.2 ASTM D3977

In a research study conducted by Guo (2006), three different methods of determining the amount of solids in storm water runoff were compared: (1) USEPA total suspended solids (TSS) method, (2) Standard (TSS) method, and (3) ASTM's suspended sediment concentration (SSC). Guo stated that "the measured SSC was very close to the true concentration of solids." The test procedures for determining SSC are published in ASTM D3977 (1997). As summarized by ASTM D3977, SSC is calculated by allowing the sediment to settle and then siphoning off all excess water. Next, the volume of the remaining water and sediment is measured and the sediment is dried and weighed.

After collecting grab samples to determine SSC, the samples should be grouped in accordance with chronological order of collection (ASTM 1997). ASTM D3977 specifies that in

order to determine the SSC, first allow the sediment in the sample container to settle in a refrigerator for two days. The supernatant, or excess water, is then vacuumed away. The supernatant should be stored for determining a dissolved-solids correction factor later. Next, the exact volume of the sample is determined by placing the sample on a level surface and marking the water level on the sample bottle. Water is then used to rinse the sediment and supernatant from the sample bottle into an evaporating dish. The sample bottle is then refilled with water to the mark with a graduated cylinder. The volume of water poured from the cylinder to reach the mark on the sample bottle should be recorded. Following determination of the sample, the evaporating dish is placed in an oven with the temperature set just below the boiling point for water. The sample should remain in the oven until all discernible traces of water have evaporated. Once this is accomplished, the temperature in the oven should be raised at held at a temperature of 221°F (105°C) for two hours. The evaporating dish should then be transferred to a desiccator to allow the sediment to cool to room temperature to prevent a misreading to occur due to thermal expansion from the heated pan. A desiccator is a device that prevents sediment samples from absorbing moisture in the surrounding air (ASTM 1997). Once the samples have reached room temperature, the dishes should be quickly weighed to the nearest 0.0001 gram to minimize the absorption of air-borne moisture by the sample. A dissolved-solids correction factor is calculated by transferring a known amount of supernatant to an evaporating dish using a volumetric pipet. A similar process to drying the samples is used to dry the supernatant and determine the weight of its contents to the nearest 0.0001 gram.

2.10 SUMMARY

This section provides an overview of the issues related to erosion and the corresponding sediment pollution, its association with construction activities, and the requirements established

by regulatory agencies in an effort to mitigate the problem of sediment pollution. The use of rainfall simulators in testing ESC practices and products is discussed and an overview of the two types of simulators used: drop-forming and pressurized simulators are discussed. Through a review of available literature, performance characteristics of each type of simulator were identified. Table 2.5 provides a comparison of the two types of simulators.

Table 2.5 Comparison of Rainfall Simulators

Category	Drop-Forming	Pressurized
Portability	Stationary	Portable
Drop Size Distribution	More Control	Less Control
Uniformity	90-95%	80-85%
Terminal Velocity	30 ft.	14 ft.
Rainfall Intensity	Lower Intensities	Higher Intensities
Resistance to Environmental Conditions	Poor Performance	Resistant to Wind

After a review of available literature, the overall designs of drop-forming and pressurized simulators were compared and contrasted. The analysis focused on the design criteria as described by Moore et al. (1983): (1) drop size distribution and fall velocities similar to natural rainfall, (2) intensities similar to storms producing medium to high rates of runoff and erosion, (3) uniform drop distribution throughout the study area, (4) near-continuous rainfall application throughout the study area, (5) near vertical impact of most drops, and (6) total kinetic energy similar to that of natural rainfall. Based upon the results displayed in Table 2.5, it was decided to focus research efforts on pressurized simulators. Through a review of available literature, it was determined that limitations intrinsic to the design of drop-forming simulators would hinder its effectiveness in a field application. Finally, existing standards related to the use of rainfall simulation in ESC testing were identified and discussed.

CHAPTER THREE:
RAINFALL SIMULATOR DESIGN AND CONSTRUCTION

3.1 INTRODUCTION

At the AU-ESCTF, a rainfall simulator was designed and constructed for the purpose of testing the effectiveness of various erosion and sediment control (ESC) practices using large-scale testing techniques and better understanding their performance. The design and construction of the rainfall simulator testing apparatus consisted of the following components: a test plot constructed on a fill slope, a catchment basin, retaining wall, sprinkler risers, water delivery system, and power supply. Target flow rates were based on calculations to accurately simulate the peak 60 minutes of a Type III, 2-yr, 24 hr storm in Alabama.

3.2 RAINFALL EVENT DESIGN AND CALCULATION OF FLOW RATES

After a review of available literature, a Type III 2-yr, 24-hr storm event in Alabama was chosen for use in the rainfall simulation. This design storm comes from TR-55, which provides procedures for estimating storm characteristics (e.g., runoff and peak discharges) for small watersheds (NRCS 1986). To account for the variability of rainfall intensity based on geographic region, the NRCS developed synthetic rainfall distributions, described as Type I, IA, II, and III storms, which are plotted in Figure 3.1.

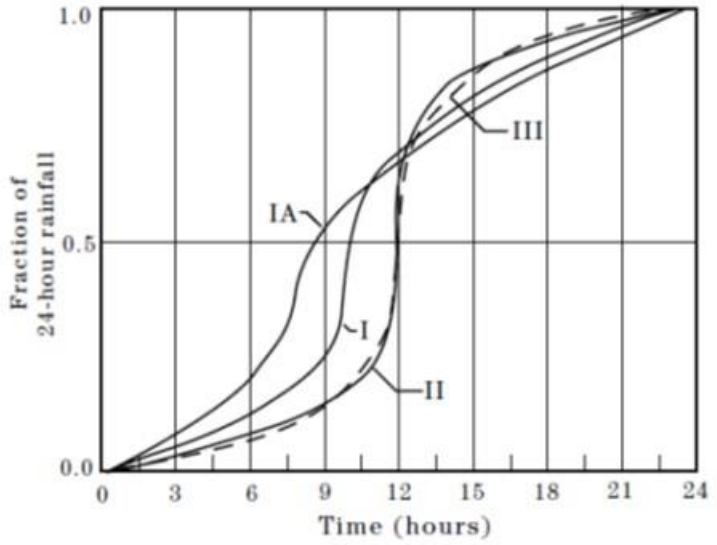

Figure 3.1 SCS 24-hr Rainfall Distributions (NRCS 1986).

Types I and IA correspond to the Pacific regions. Type III storms describe storms in the Gulf of Mexico and Atlantic coast regions. Type II storms represent the rest of the country (NRCS 1986). Figure 3.2 presents a geospatial view of the synthetic rainfall distributions as well as the location of the study area.

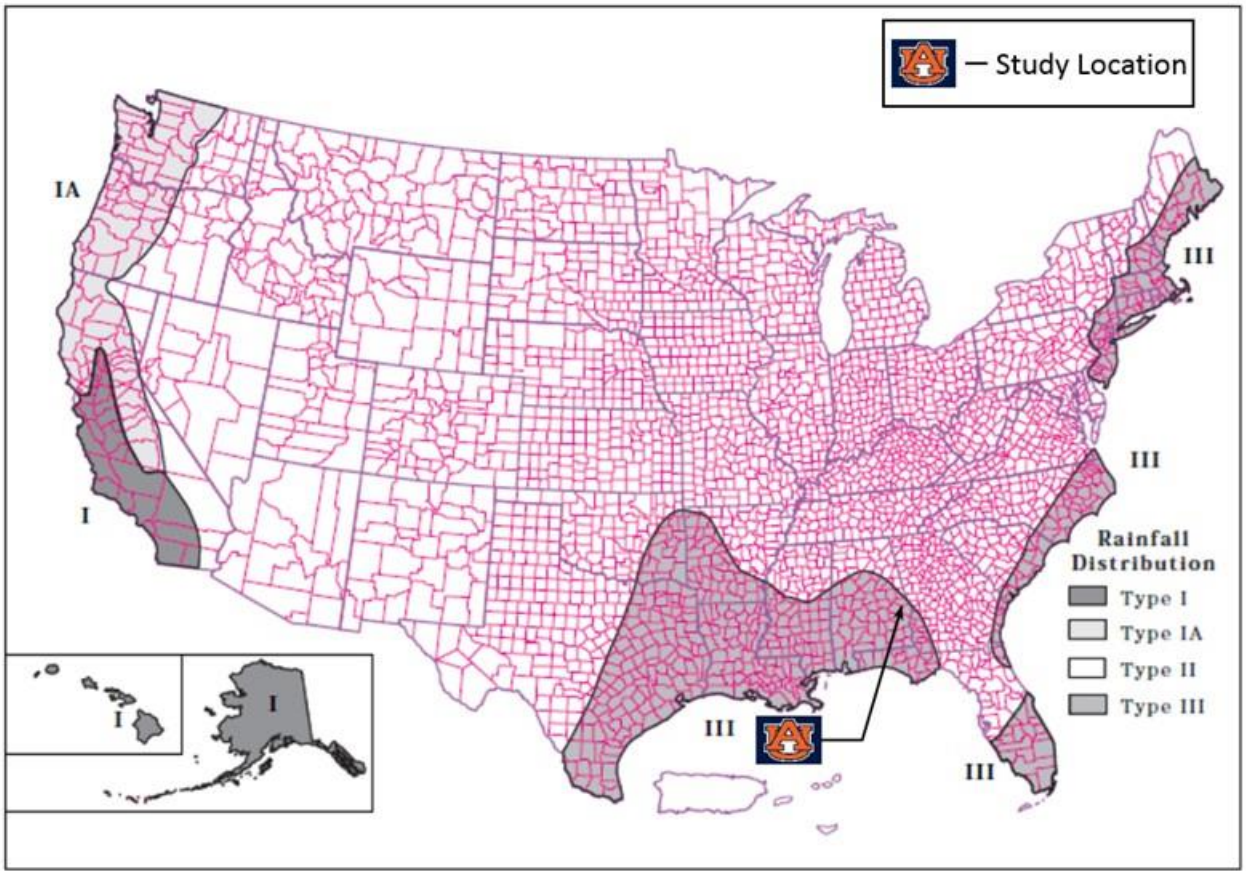

Figure 3.2 Geographic Boundaries for SCS Rainfall Distributions (NRCS 1986).

To determine the flow rates required to accurately simulate such a storm, a rainfall intensity hyetograph was developed using Bentley's Pondpack software. The hyetograph was then trimmed to clearly display the peak 60 minutes of the storm event. Intensities were then selected from the peak 60 minutes of the hyetograph at 10 minute intervals to accurately simulate the rise and fall of the rainfall event. Intensities were selected from the peak 60 minutes to simulate a worst case scenario test for the erosion control practices under consideration. By using variable intensities instead of a single intensity to simulate a rain event, the amount of water applied to the test plot for each test interval would more accurately represent conditions experienced in the field. Figure 3.3 displays the peak 60-minutes of the 2-yr, 24-hr rainfall event with selected 10 minute rainfall intensities displayed accordingly.

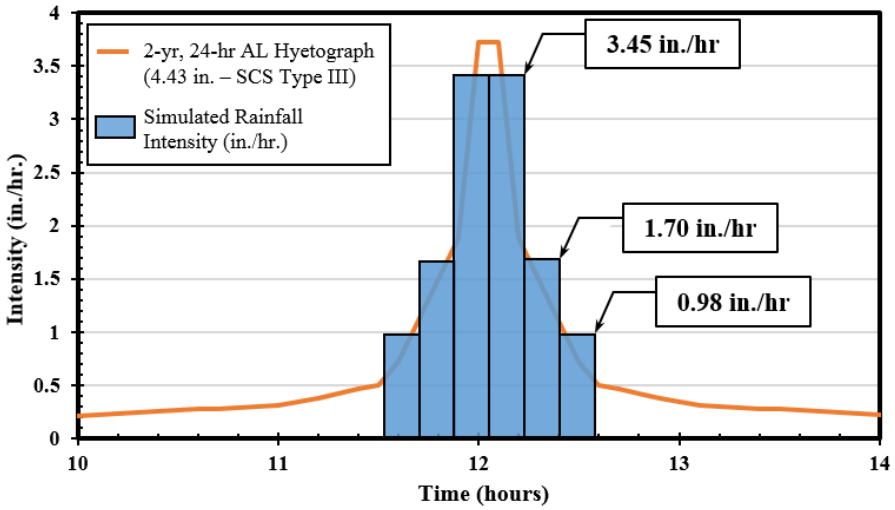

Figure 3.3 Peak 60 Minute Intensities for Type III 2-yr, 24 hr Storm in Alabama.

The selected intensities were then converted to units of gallons per minute to determine the volume of water required for each test interval and for the overall experiment. This was accomplished by converting the intensities to units of feet per minute and multiplying by the plot area of 320 ft^2 (30 m^2). These values were then converted to units of gallons per minute, the typical standard units used when discussing flow rates of sprinkler systems in the United States. Each flow rate was then multiplied by the test interval of 10 minutes to calculate a total volume of flow. Finally, the target median drop sizes were calculated using the theoretical intensities and Equation 2-1, previously discussed in the literature review. Table 3.1 displays the selected intensities and corresponding flow rates and volumes.

Table 3.1 Rainfall Data for a 2-yr, 24-hr SCS Type III Storm Event

Test Interval	TIME (min)	Target Intensity (in./hr)	Theoretical Median Drop Size (mm)	Flow Rate (gpm)	Total Volume (gal)
1	0 – 10	0.98	2.2	3.24	32.4
2	10-20	1.70	2.5	5.64	56.4
3	20-30	3.45	2.8	11.46	114.6
4	30 – 40	3.45	2.8	11.46	114.6
5	40 – 50	1.70	2.5	5.64	56.4
6	50 – 60	0.98	2.2	3.24	32.4
Cumulative	60				406.8

3.3 RAINFALL SIMULATOR DESIGN

The rainfall simulator was designed with the criteria discussed in the literature review in mind and is comprised of the following components: sprinkler heads, sprinkler canopy, risers, water delivery system, and a power supply. Sprinkler heads were selected based on an ability to uniformly distribute drops and produce drop sizes similar to natural rainfall. The sprinkler canopy was designed to allow for the simulation of variable intensities. The risers were designed to provide a stable means of conveying water while simultaneously providing enough height for the simulated rainfall to reach near terminal velocity. The water delivery system was designed to provide adequate flow to the risers while maintaining a suitable operating pressure. Finally, a power supply was designed to control the solenoid valves on each riser and provide complete control over the rainfall intensities produced by the simulator.

3.3.1 Sprinkler Heads

The method with which water is applied to the test plot is one of the most important aspects to any rainfall simulator. Drop forming simulators typically rely on hypodermic needles or string to form drops. Their application is generally limited to laboratory settings due to their extreme vulnerability to environmental conditions such as high wind speeds. Pressurized sprinkler systems are more resilient in outdoor environments and provide better coverage on field-scale plots. Based on a review of pertinent literature and a comparison of each type of simulator shown in Table 2.5, it was decided to pursue a simulator design that used pressurized sprinkler nozzles to apply water to the test plot.

After reviewing several commercially available pressurized sprinkler heads, the Nelson Irrigation PC-S3000 sprinkler head was selected due to its ability to operate at pressures as low as 10 psi, apply water in a 190° arc, and variety of available nozzles. The PC-S3000 uses nozzles to

control the flow rate through each sprinkler head. At any given pressure, the nozzles will allow a specific flow rate through the sprinkler. Furthermore, the sprinkler heads can be equipped with pressure regulators to ensure a constant pressure and thereby a constant flow rate is maintained. Figure 3.4 displays an exploded and constructed view of the sprinkler head assembly. The nozzles installed in the sprinkler head were selected based on the target flow rates displayed in Table 3.1 as well as the number of sprinkler heads installed in the rainfall simulator. Table 3.2 displays the flow rate for each selected nozzle type.

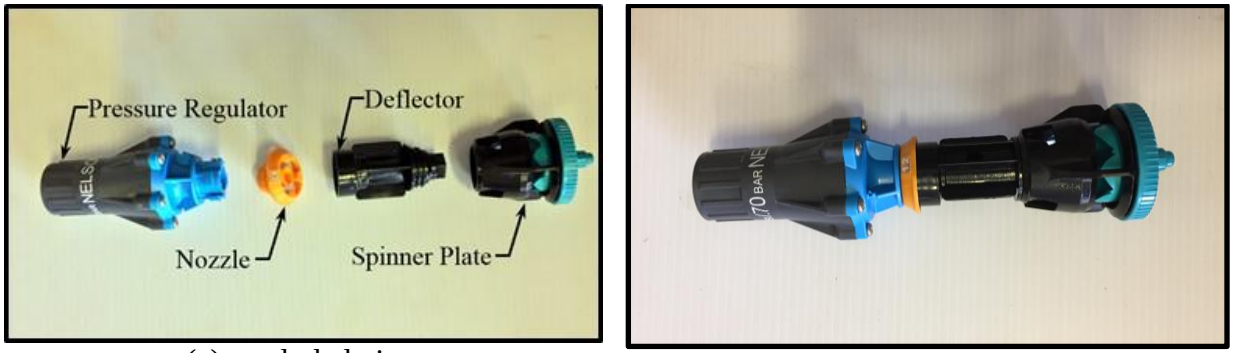

(a) exploded view (b) constructed view

Figure 3.4 Sprinkler Head Assembly.

Table 3.2 Nozzle Sizes and Flow Rates

# - Color Stripe	Flow Rate @ 10 PSI (gpm)
#12 – Beige Gold	0.79
#13 – Gold Lime	0.92
#21 – Turquoise Yellow	2.38

The above nozzles were selected so that the flow rates for each interval would approximate those listed in Table 3.1. Several combinations of the selected nozzles were used to achieve the desired flow rates. These combinations are displayed in Table 3.3. During calibration extensive overspray of simulated rainfall was witnessed. The radius of spray produced by the sprinkler heads was larger than the dimensions of the test plot. The overspray resulted in much higher flow rates required to achieve the target intensities compared to the theoretically required flow rate.

Table 3.3 Nozzle Combinations per Test Interval

Test Interval	Nozzles Used	Total Flow (gpm)	Theoretically Required Flow (gpm)	Percent Difference (%)
1 & 6	12 - #12	9.48	3.24	98.1
2 & 5	12 – #12 6 - #13	15.00	5.64	90.7
3 & 4	12 - #12 6 - #13 6 - #21	29.28	11.46	87.5

3.3.2 Sprinkler Canopy

To effectively distribute water over the test plot, a rain canopy with four sprinkler heads was designed for each riser. The canopy was designed to allow for each sprinkler head to be individually operated to achieve the flow rates discussed in Section 3.3.1. The canopy was designed out of galvanized steel to provide structural stability as well as resistance to corrosive forces. The canopy connected to the supporting riser through a ¾ in. (19 mm) galvanized steel tee in the center of the canopy. Since the installed sprinkler heads applied water in 190° arc, an inline canopy design was used to maximize water application to the test plot. Solenoid valves were installed in between each sprinkler head to allow for individual operation of each sprinkler head. The canopy was designed to be symmetrical, with 12 in. (30 cm) between each sprinkler head to allow for adequate spacing. Six inch (15 cm) galvanized steel nipples were used to support the canopy and deliver flow to each sprinkler head. The middle two sprinkler heads housed the #12, beige-gold nozzles. The sprinkler head on the far right and left housed the #13, gold-lime nozzle and the #21 turquoise-yellow nozzle, respectively. Drawings displaying the detail and dimensions of the sprinkler canopy are provided in Figure 3.5.

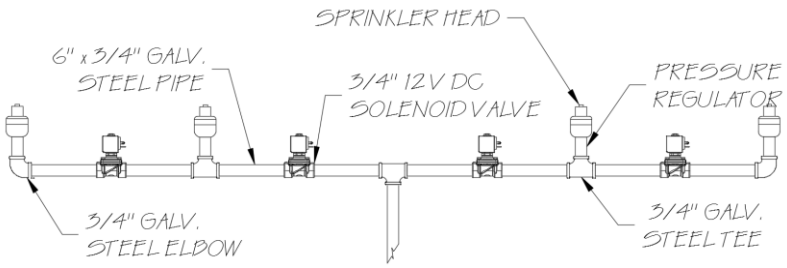

Figure 3.5 Rain Canopy Detail.

3.3.3 Sprinkler Riser

A riser was designed out of ¾ in. (19 mm) galvanized steel pipe to support the sprinkler canopy as well as deliver water to the sprinkler heads. The riser was broken into three sections: two 24 in. (61 cm) sections and a 120 in. (3 m) section. A ¾ in. (19 mm) gate valve was installed on the riser to regulate flow. Furthermore, a ¾ in. (19 mm) reducer tee was installed to allow for the attachment of a 0 to 100 psi (0 to 690 kPa) pressure gauge. Figure 3.6 shows the riser in detail.

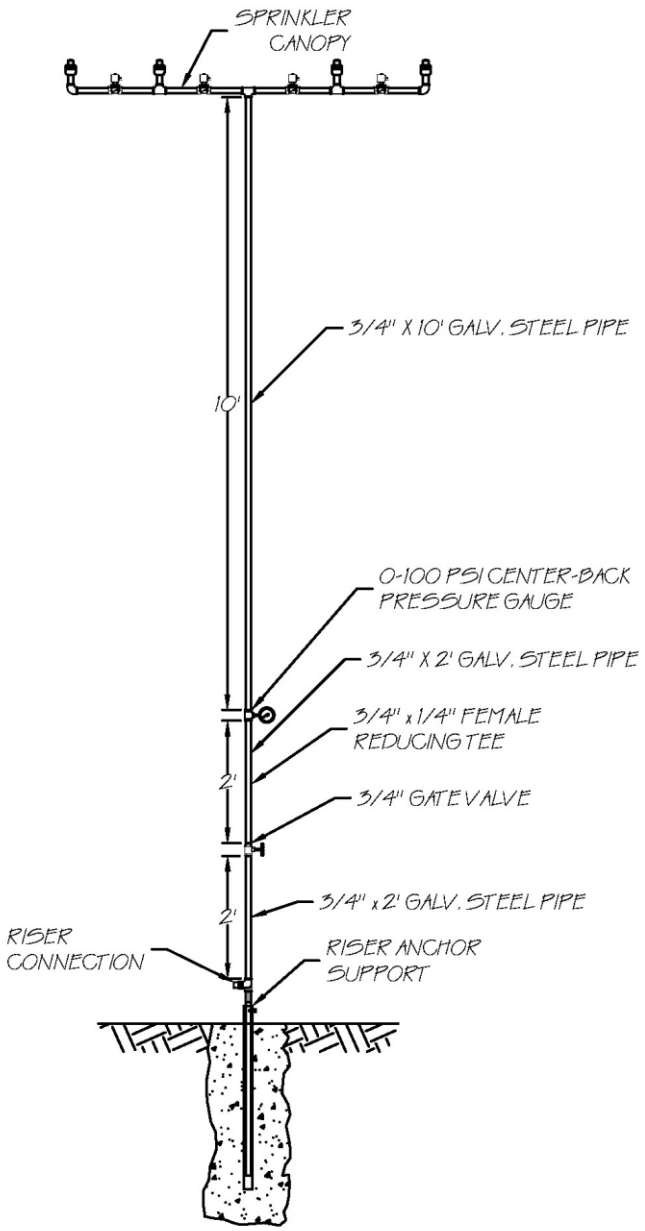

Figure 3.6 Sprinkler Riser Detail.

3.3.4 Riser Anchor

The sprinkler anchors were designed to provide a stable base for the sprinkler riser and canopy as well as ensure the entire system was plumb. The anchor consisted of a 24 in. (61 cm) long, ¾ in. (19 mm) diameter galvanized steel support pipe and a 4 in. by 4 in. by 12 ft (10 cm by 10 cm by 3.7 m) lumber post. The support pipe was attached to the riser with a ¾ in. (19 mm)

galvanized steel tee. The support pipe and tee were sealed with epoxy sealant to prevent flow from entering the support structure. A ¾ in. (19 mm) male cam and groove plug with threaded male national pipe thread (NPT) pipe connections was attached to the tee for water delivery purposes. The bottom 9 ft (2.7 m) of the riser were attached to the support post with metal brackets to support the riser against its own weight and hold the riser plumb and level. Drawings for the anchor are provided in Figure 3.7.

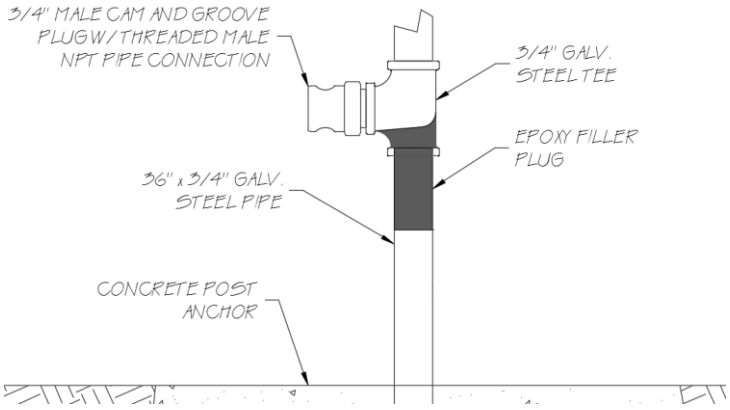

Figure 3.7 Riser Anchor Detail.

3.3.5 Water Supply Design

To achieve a uniform drop distribution on the 320 ft^2 (30 m^2) test plot, six sprinkler risers were spaced around the test plot. The spacing of the risers was determined during calibration by adjusting the position of each riser until uniformity of drop distribution was maximized and satisfied the minimum Christensen uniformity coefficient of 80%. The spacing of the risers allowed the rainfall simulator to produce intensities of approximately 1 to 4 in./hr (2.5 to 10 cm/hr) in a uniform fashion. A 3 in. (7.6 cm) diameter lay-flat hose was used to convey flow from the pump to each riser location. A North Star high pressure water pump was used to supply and pressurize water to the rainfall simulator. The pump curve, displaying the relationship between pump head (ft) and flow rate (gpm), was obtained from the manufacturer. An analysis was

conducted of the pipe network to determine the head losses due to fittings, pipe friction, and elevation change. These values were plotted in a system curve and superimposed over the pump curve to ensure that the pump head would satisfy the requirements of the rainfall simulator. The point where the pump and system curves intersect represents the typical operating point for the pump in terms of pump head and flow rate. Values for the loss coefficients (K) were obtained from Vano Engineering (Engineering 2012). Values for pipe roughness (k_s), kinematic viscosity (ν), and specific weight (γ), were obtained from an engineering fluid mechanics textbook (Crowe 2005). Table 3.4 displays the coefficients and constants used in the analysis of the pipe network. Known values for friction coefficients (K) of gate valves when ¼ to ¾ closed were plotted to determine K values when fully closed. These values were then fitted with an exponential trendline to plot the K values associated with the gate valve at various percentages of closure. The loss coefficient plot for gate valves is shown in Figure 3.8. The pump and system curves are shown in Figure 3.9.

Table 3.4 Coefficients and Constants for Pipe Network Analysis

Pipe Network Element	**Loss Coefficients (K)**
Pipe Entrance	0.04
Tee	2.0
Gate Valve (Closed)	138
Pipe Network Element	**Pipe Roughness (k_s)**
Rubber Pipe (ft)	8.33E-05
Other Constants	
Kinematic Viscosity, ν (ft^2/s)	1.06E-05
Diameter of Pipe (ft)	0.25
Area of Pipe (ft^2)	0.049
Length of Pipe (ft)	115
Specific Weight, γ (lb/ft^3)	62.3
Target Pressure (lb/ft^2)	8640

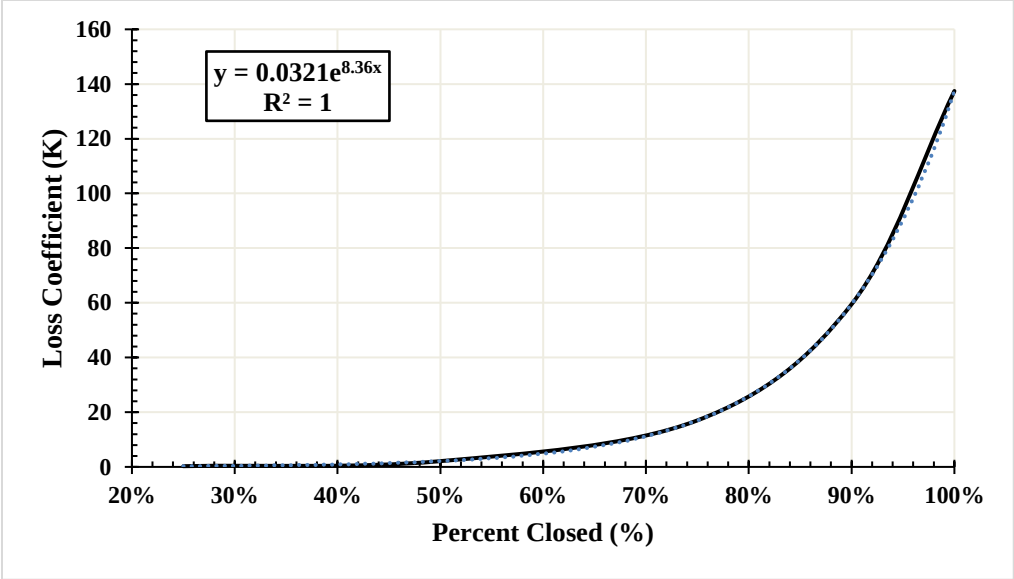

Figure 3.8 Gate Valve Frictional Coefficients.

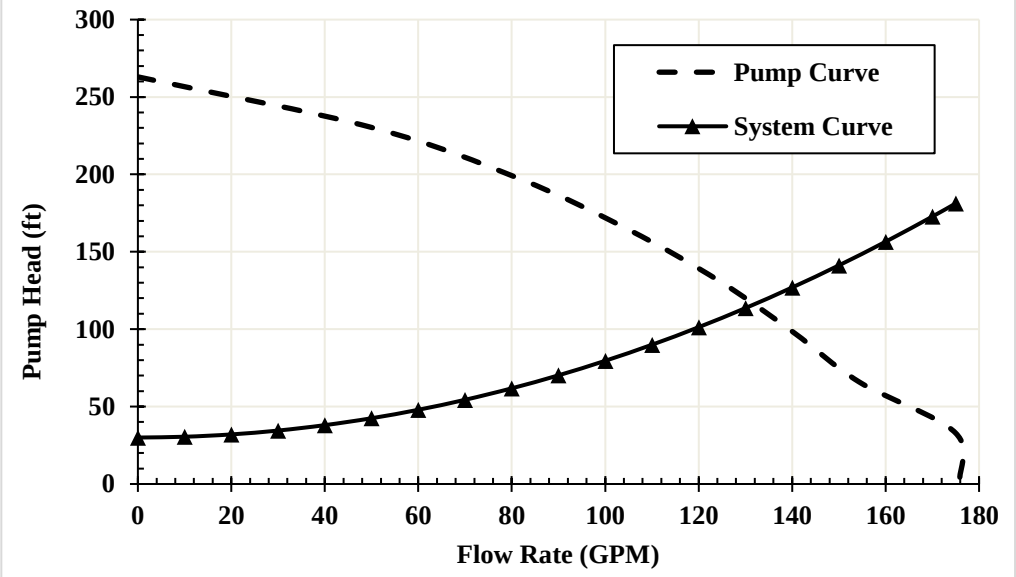

Figure 3.9 Pump vs. System Curve.

Rigid hose was selected for its availability, durability, ease of use, and minimal storage requirements. At each riser location, a female reducing tee was used to reduce the hose diameter from 3 in. (7.6 cm) to ¾ in. (2 cm). A ¾ in. (2 cm) hose was then used to deliver flow from the tee to the riser. At the riser, a ¾ in. (2 cm) cam and groove hose coupling was installed to connect

the hose to the base of the riser. A depiction of the riser locations and hose network is provided in Figure 3.10.

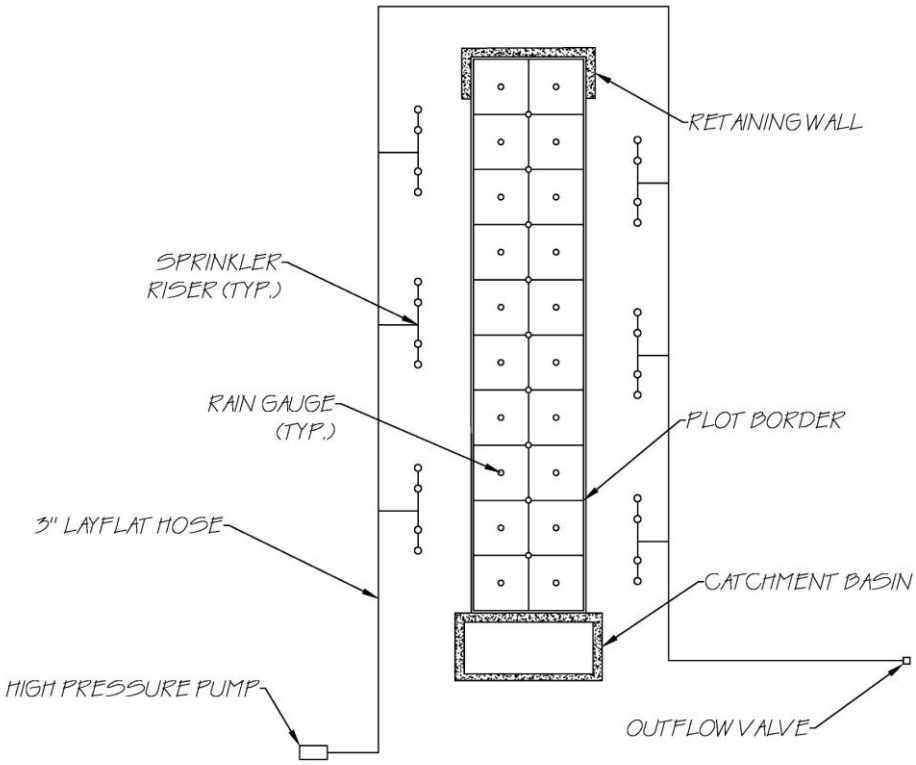

Figure 3.10 Test Plot Layout and Hose Network.

3.3.6 Wind Screen Design

In initial testing of a single sprinkler riser, the cross winds acting on the test plot were found to have a substantial impact on the rain drop distribution produced by the sprinkler nozzles. To minimize the impact of cross winds on rainfall simulation experiments, a series of wind screens, suspension cables, and support posts were designed with the goal of reducing wind speeds on the plot to at most 1 mi/hr (1.6 km/hr). The support system was compromised of six, 6 in. by 6 in., 20 ft (12 cm by 12 cm, 6 m) lumber posts, ¼ in. (6.4 mm) suspension cable, ¼ in. (6.4 mm) thimbles, ¼ in. (6.4 mm) clips, and 1/2 in. by 10 in. (12.7 mm by 25.4 cm) eye bolts. The windscreens were custom designed and fitted with grommets by Willacooche Industrial Fabrics (WINFAB). The

grommets woven into the fabric allowed for the screen to be deployed up and down on the support wires similarly to a curtain. The design for the structural support for the screens is shown in Figure 3.11.

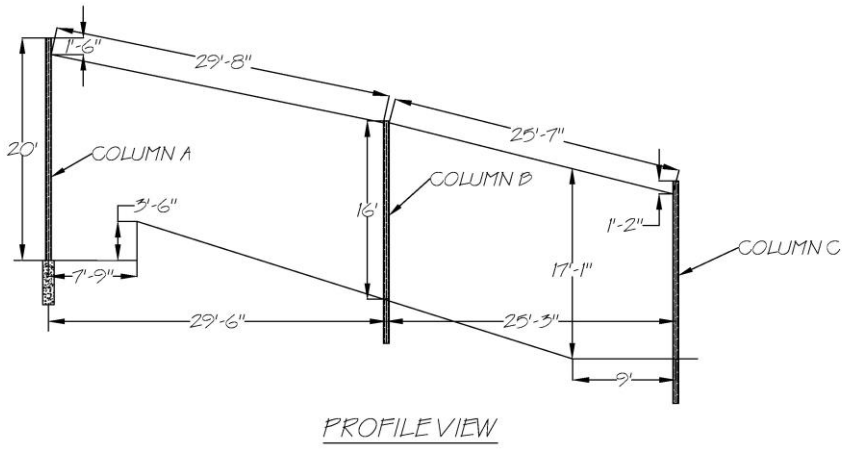

Figure 3.11 Windscreen Support Detail.

3.4 TEST PLOT CONSTRUCTION

To conduct tests according to ASTM D6459-15, several modifications had to be made to the site. Construction of a retaining wall and catchment basin, as well as grading of the slope, was conducted by a group of undergraduate students from the McWhorter School of Building Science at Auburn University as part of their semester project. Originally, the slope was measured to be approximately 4H:1V using a total station. To raise the grade and support the soil that would be added to grade the slope, a reinforced, cast in place concrete wall was poured. A 12 in. (30 cm) thick footing was poured below the wall to provide adequate base support. The detail for the retaining wall is shown in Figure 3.12.

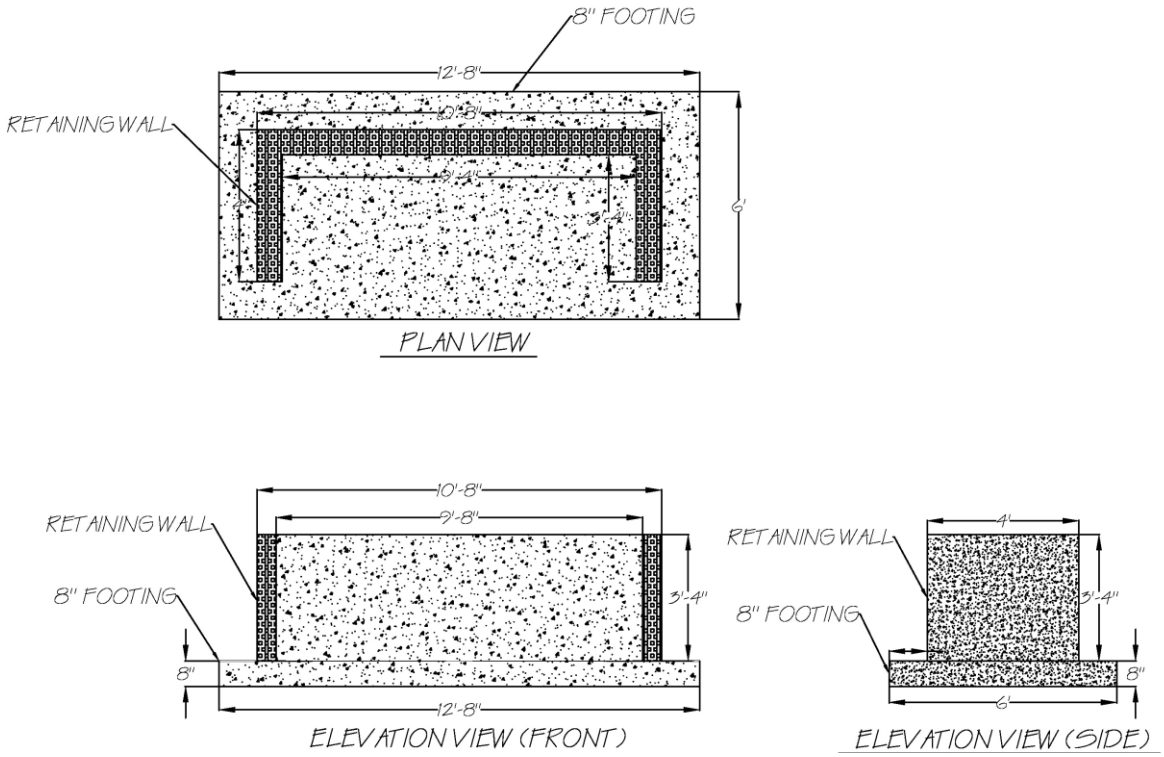

Figure 3.12 Retaining Wall Detail.

A catchment basin was designed and constructed to contain all runoff generated throughout the duration of a test. The dimensions of the catchment basin were selected based on the estimated volume of runoff that would be generated during a test. The total volume of flow listed in Table 3.1, approximately 782 gallons (2960 L), was increased by 10% so that the selected basin dimensions would provide insurance against overflow. The basin was constructed out of reinforced, cast in place concrete. An 8 in. (20 cm) thick footing was poured below the basin to provide adequate support for the basin. Drawings detailing the catchment basin are provided in Figure 3.13. Photos depicting the construction process are provided in Figure 3.14.

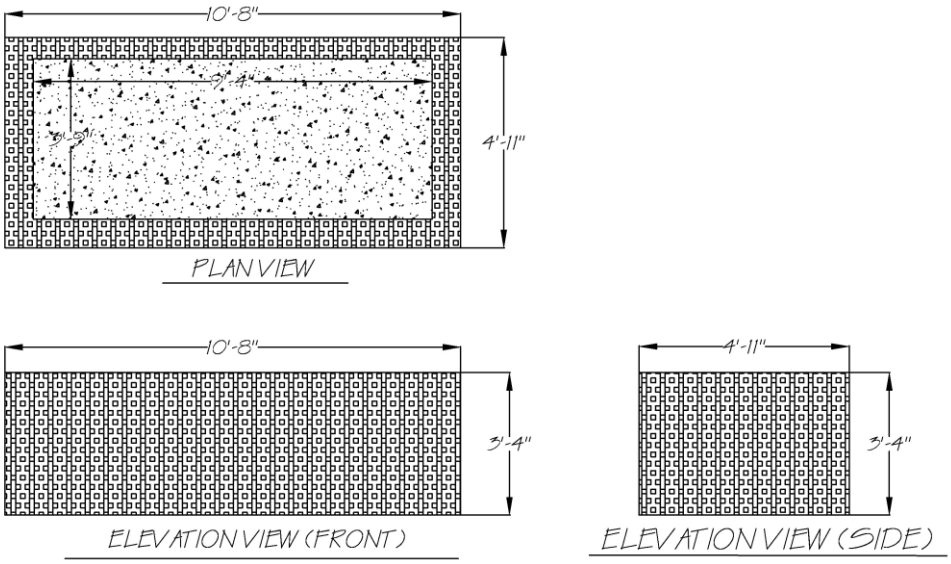

Figure 3.13 Catchment Basin Detail.

(a) test area (pre-construction)

(b) steel reinforcement for basin

(c) pouring retaining wall footing

(d) formwork for retaining wall

Figure 3.14 Construction of Basin and Retaining Wall.

After the retaining wall and catchment basin were constructed, earthwork began to grade the slope from 4H:1V to 3H:1V. The soil added to the slope was brought from a stockpile on site. To ensure that the soil was graded into a 3:1 slope, string lines were pulled from the top of the retaining wall to the top, front face of the catchment basin. As soil was added to the slope, a trench compactor was used to adequately compact the soil and construct a structurally stable slope.

Finally, once the retaining wall, catch basin, and slope were constructed, a test plot border was installed. The border was constructed out of 2 in. by 8 in. (5 cm by 20 cm) pressure treated lumber. The individual boards were connected using brackets. The border was designed to rest on top of the existing slope. Figure 3.15 shows the completed plot border. Once the border was installed, stakes were installed along both edges of the border to prevent movement and minimize warping in the boards.

Figure 3.15 Test Plot Border Construction.

The next step was to excavate 12 in. (30 cm) of soil from inside the plot. This proved to be a difficult task due to the compaction of the slope with a trench compactor during the initial construction phase. At the time of this process, an excavator was not available. In its place, a dual tine tiller was used to loosen the soil by running the equipment up and down the plot. The loose soil was then shoveled out of the plot and used to build up the side slopes. In areas where the tiller

could not reach (i.e. along the plot borders), a pick axe was used to loosen the soil to the same depth as the tiller. Figure 3.16(a) and (b) show the excavated plot as well as the tiller used to loosen the soil. During this phase, the joints in the border were sealed with a caulk gun to ensure that the border would be water tight during future tests. Figure 3.16(c) provides an example of the sealed joints. Next, 5 in. (13 cm) lawn edging was installed in 20 ft (6 m) lengths. The edging was attached 1 in. (2.5 cm) down onto the border to provide for a flexible border that can prevent runoff from flowing off the sides of the border. Figure 3.16(d) and (e) show the lawn edging installed on the plot border.

(a) excavation of test plot

(b) excavation of test plot

(c) border joints sealed with caulk

(d) plot border with lawn edging

Figure 3.16 Test Plot Border Construction, Phase 2.

Once a depth of 12 in. (30 cm) had been reached, backfilling of the test plot with the 12 in. (30 cm) soil veneer began. This process consisted of several steps: screening soil from the stockpile on site, transporting the screened soil to the test plot, raking the soil out into a smooth grade, rolling the soil into a smooth surface, and compacting the backfill in 6 in. (15 cm) lifts. Foreign objects (i.e. rocks, clods, roots, debris, etc.) were removed from the soil stockpile using a ¼" (6.4 mm) screen. Soil would be placed on the screen using a skid steer. Using shovels, the soil was then spread across the screen until all the soil had been cleaned. Figure 3.17(a), (b), and (c) provide examples of this process. Once a substantial amount of the screened soil had accumulated, the soil was then transported to the test plot using a skid steer. Soil was added to the top, middle, and bottom portions of the test plot and spread out in a uniform fashion from each area using metal rakes and shovels as shown in Figure 3.17(d) and (e). Between each stockpile loaded into the test plot, an 18 in. by 24 in., 270 lb (46 cm by 60 cm, 122 kg) turf roller was used to flatten and slightly compact the soil. String lines were pulled at the 6 in. (15 cm) and 12 in. (30 cm) mark along the border to designate when a lift had been completed. Once enough soil had been added to reach a string line at all points of the test plot, a plate compactor was used to compact the soil to the specified density of 90% ± 3%. Photos of the compaction of the test plot are shown in Figure 3.17(f) and (g).

(a) portion of soil stockpile

(b) screening the soil stockpile

(c) screened soil stockpile

(d) backfilling test plot with screened soil

(e) spreading soil with shovels

(f) compacting soil with a turf roller

(g) compacting slope with a plate compactor

Figure 3.17 Backfilling the Test Plot with 12 in. (30 cm) Soil Veneer.

Once the test plot had been filled, the side slopes were built up to the same grade as the test plot to ensure that both the risers and the middle two support posts would be on the same elevation. The side slopes were built up in 6 in. (15 cm) lifts. Between each lift, the slopes were compacted with a plate compactor and a compaction rammer to ensure adequate compaction and slope stability. Upon reaching the final grade for the side slopes, stabilization measures (i.e. TRMs, temporary/permanent seeding) were deployed to minimize erosion. Pictures summarizing this process are provided in Figure 3.18.

(a) terracing of side slopes for compaction (b) compaction of slope with a rammer

(c) compaction of slope with a plate compactor (d) compaction of slope with a bobcat

Figure 3.18 Construction of the Side Slopes.

Once the side slopes were compacted, the location for each of the six, 20 ft (6 m) support posts for the windscreen were located. A 12 in. (30 cm) diameter, 3 ft (0.9 m) long auger was rented to drill each of the holes. A 2 ft (0.6 m) extension was also used to achieve post hole depths up to 5 ft (1.5 m). The anchor bolts for the top two support posts were set into position by

determining the height required of the anchor bolt to secure the anchor bracket. A nut and washer were then installed to maintain the correct height. The anchor bolts were then placed in the post hole and secured into place using a board. Next, ½ in. by 10 in. (1.3 cm by 25 cm) eye bolts were installed into each post to provide connection points for the guy wires suspended between posts. This process is displayed in Figure 3.19.

(a) drilling holes with an auger

(b) mount for anchor bolt

(c) cutting rebar for footings

(d) installing eye bolts into support posts

Figure 3.19 Construction of Support Posts.

Next, four of the posts were placed inside the middle and lower post hole locations at a depth of 4 ft. Each post was set plumb and braced using 2 in. by 4 in. (5 cm by 10 cm) boards attached to stakes. Concrete was delivered by a truck and cast-in-place. For the two footings, three, 4 ft (1.2 m) long #3 reinforcement bars were placed as the concrete was poured. Once the concrete had set, the braces were removed from each post and anchor brackets were installed on each footing. For the top two support posts, a mini excavator was used to lift the lumber in place.

The base of each post was set inside an anchor bracket by hand. Large nails were then driven through openings in the bracket into the base of the post to create a pivot point. Each post was then lashed to the bucket of the mini excavator and raised into position. With the bucket carrying most of the weight, the post was held plumb and braced against a nearby shed and against stakes driven into the ground. The installation process is shown in Figure 3.20.

(a) setting 20 ft support post

(b) pouring concrete footings

(c) placing concrete in post holes

(d) post set in poured concrete

(e) installing top two support posts

Figure 3.20 Installation of Support Posts.

3.5 POWER SUPPLY AND AUTOMATION

To simulate variable intensity rainfall, solenoid valves were installed on each riser to allow for individual control of each sprinkler head. The valves on each riser were connected to a single power grid by direct-burial irrigation cable wired to junction boxes at each riser. A control box with four switches provided complete control over which valves were active during testing. Two 12V car batteries were wired in parallel to the control box to power the entire system. A schematic of the power supply system is displayed in Figure 3.21.

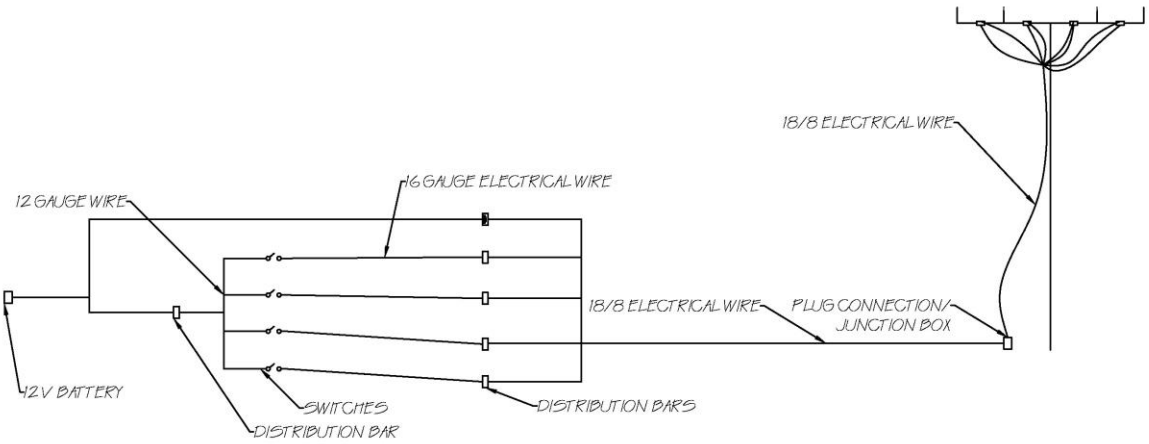

Figure 3.21 Power Supply Schematic

Junction boxes were installed at each sprinkler riser to power the solenoid valves and maintain a degree of portability for the rainfall simulator. The box was mounted to a stake constructed out of 2 in. by 6 in. (5 cm by 15 cm) lumber. At each box, a female, 10 pole MIL-Spec connector was soldered to each cable. The plug was installed inside a gang box that mounted to the front of the junction box. A male, 10 pole MIL Spec connector was soldered to the cable attached to the valves on each riser. This male connector plugged into the female connector in the gang box. Creating this system of plugs allowed the simulators to be easily disconnected and moved if necessary. PVC electrical conduit was attached to each junction box to provide a secure,

weather proof means for running the copper cable underground to the control box. The buried conduit was trenched in on both sides of the test plot. Figure 3.22 provides several images detailing this process.

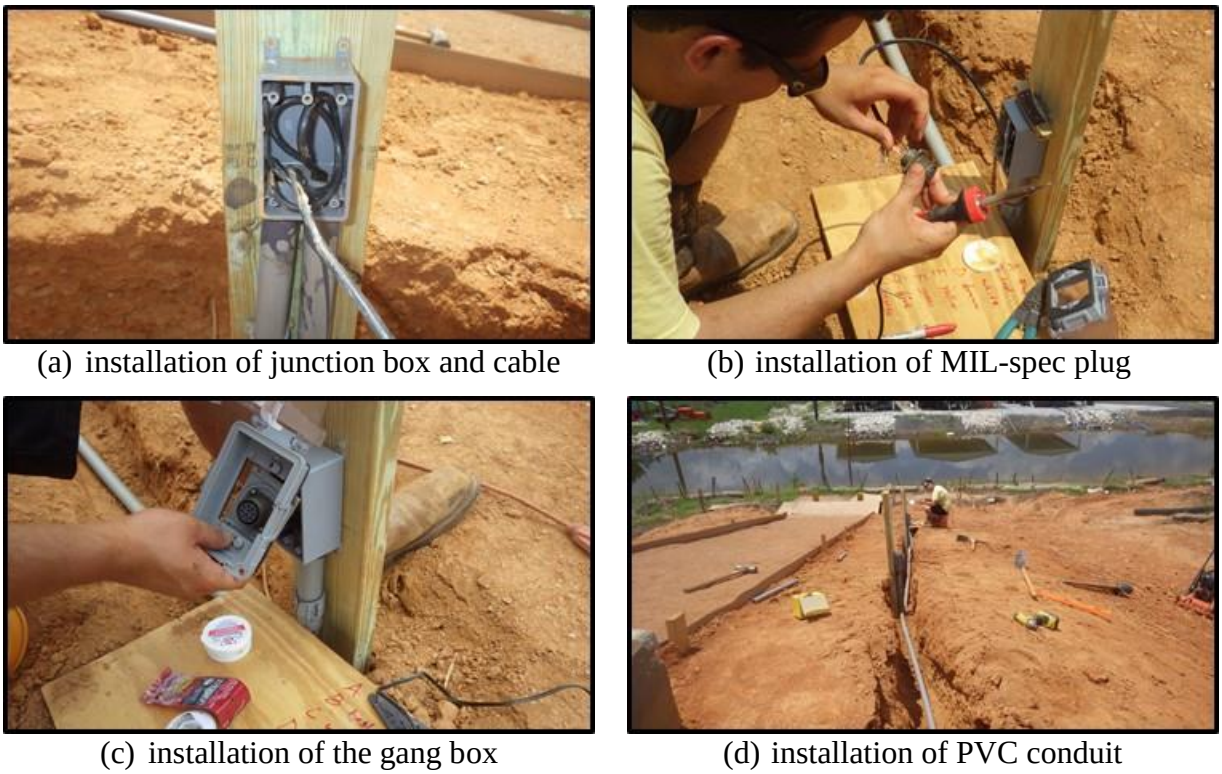

(a) installation of junction box and cable (b) installation of MIL-spec plug

(c) installation of the gang box (d) installation of PVC conduit

Figure 3.22 Installation of Junction Boxes and Conduit.

A control box was constructed to provide power to each riser as well as maintain control over which valves were active during testing. Six female MIL Spec connectors were mounted to the bottom of the box to provide individual connections to each riser. A male MIL Spec connector was wired to each irrigation cable and attached to the female connectors on the bottom face of the box. Four wires from each cable were selected to serve as ground connections: white, blue, yellow, and black. The remaining four wires: brown, green, orange, and red, were selected to serve as positive connections. The wires were secured using terminal block distribution bars. The grounding terminal block was wired to the negative wire running to the power source. The four

positive terminal blocks were wired to four switches, one for each block. The four switches controlled current flow to each terminal block and dictated which valves were active. Each switch was then connected to a single terminal block that was wired to the positive wire from the power source. Pictures displaying the control box are shown in Figure 3.23.

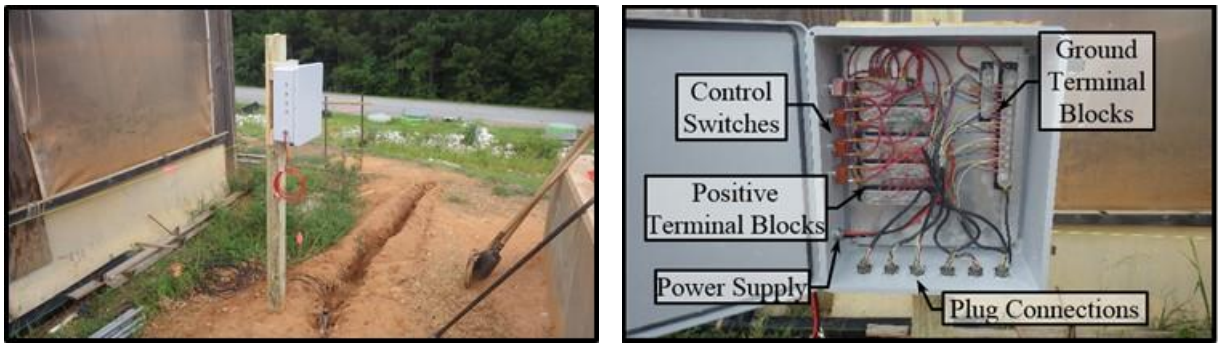

(a) valve switches on control box (b) wiring layout of control box

Figure 3.23 Electrical Control Box.

3.6 COST ANALYSIS

A majority of the rainfall simulator was constructed from components readily available in the local Auburn, AL area. Parts that were not available locally were ordered from vendors such as McMaster-Carr, Grainger, and Ferguson. A significant amount of money was able to be saved on this project due to the availability of equipment and resources at the AU-ESCTF. Major expenses for the project included electrical features such as solenoid valves and control, concrete for the catchment basin and retaining wall, sprinkler heads, and the galvanized steel pipe and fittings. Table 3.5 provides a general cost breakdown for the construction of the rainfall simulator. The cost estimate takes into account only material costs. Labor costs were minimized by using undergraduate research assistants and other undergraduate volunteers. The sprinkler head estimate includes the nozzles, sprinkler heads, and pressure regulators. Plumbing includes all galvanized pipe and fittings for the risers. The measurement devices category represents expenditures on pressure gauges and rain gauges. Finally, all costs for the construction of the test plot including

hose network, catchment basin and retaining wall, and plot layout are included in the test plot category.

Table 3.5 Cost Breakdown of Rainfall Simulator

Component	Cost
Water Delivery	$1,760
Sprinkler Risers	$3,050
Measurement Devices	$350
Test Plot Construction	$3,560
Electrical	$2,630
Miscellaneous	$510
Total Cost	**$11,860**

3.7 SUMMARY

Design and construction of the rainfall simulator, water delivery system, and test plot required thorough research into previous designs and means for automation of the system. The project was also designed to provide an economical system by which natural rainfall could be accurately and repeatedly simulated to test rolled erosion control products. A majority of the simulator design was based on the design provided in ASTM D6459 (REF). However, several innovative changes were made to the standard design. Solenoid valves were installed in place of ball valves to provide instantaneous changes in rainfall intensity. Also, Nelson Irrigation PC-S3000 sprinkler heads were used in place of Veejet nozzles. These sprinkler heads provide the capability to simulate various storm events by simply changing out the nozzle in the sprinkler assembly. Finally, the riser height was increased from 10 ft (3 m) to 14 ft (4.3 m). The sprinkler risers and canopy were constructed from galvanized iron pipe to provide stability, a means of flow conveyance, and resistance to corrosive elements. Water was supplied to the simulator from a storage pond on site. The flow was pressurized using a high pressure pump. Figure 3.24 displays an aerial view of the completed rainfall simulator apparatus.

Figure 3.24 Completed Rainfall Simulator Test Slope.

CHAPTER FOUR:
METHODS AND PROCEDURES

4.1 INTRODUCTION

This section describes the experimental procedures developed for calibration and validation of the rainfall simulator system, as well as, for field-scale testing of erosion control practices and products. The test methodologies and installation procedures are based upon current standards from ASTM and the Erosion Control Technology Council (ECTC). The experimental procedures were designed to ensure each calibration and product test were conducted in a consistent manner to minimize variability between tests.

The primary research objective for this project was to construct a large-scale rainfall simulator capable of producing simulated rainfall for field-scale testing of erosion control practices and products. Initially, calibration tests were performed to determine the characteristics of the rainfall simulator (i.e. measured rainfall intensity, drop distribution, and drop size) as well as the optimal location for each of the six sprinkler risers. Using rainfall depth data collected from the rain gauges installed on the test plot, the measured rainfall intensities were compared to the theoretical rainfall intensities listed in Table 3.1.Using the flour pan method, the drop size distribution for the rainfall simulator was determined. Once the performance of the simulator was validated, bare soil tests were conducted to determine the repeatability of results produced by the rainfall simulator system. The repeatability of results was quantified by collecting grab samples during tests and calculating suspended sediment concentration (SSC) as well as determining bulk erosion from the test plot. Each of these elements are discussed in more detail in the following sections.

4.2 PRELIMINARY TESTING OF THE RAINFALL SIMULATOR

During the early stages of the project, a single riser was constructed at the Harbert Engineering Center on Auburn University's campus. The design of the riser followed the specifications listed in Section 3.3.3, except that riser was constructed to be 10 ft tall to fit inside the loading bay. Furthermore, ball valves were installed in place of solenoid valves so that extensive wiring would not have to be done. The primary objective of this initial study was to determine if the rainfall simulator as designed would be capable of simulating natural rainfall before materials for all six risers were purchased. To support the riser, a 1.25 in. (3.18 cm) galvanized steel pipe was set inside a 5 gallon (19 L) bucket. The pipe was held plumb while concrete was placed in the bucket to maintain permanent support for the pipe. Once the concrete had set, the riser was slid into the support pipe. Wood shims were placed in the gap between the riser and support pipe to hold the riser plumb and prevent rotation. Water for calibration testing was provided by connecting a ¾ in. (2 cm) hose to the riser and a water spigot in the loading bay.

Initial testing focused on collecting data on rainfall volume to calculate the uniformity of the rainfall distribution. To collect rainfall samples, 200, 1 quart (0.95 L) cups were placed in a grid consistent of 1 ft (0.3 m) spacing on-center, horizontally and vertically as shown in Figure 4.1.

Figure 4.1 Grid Layout.

Each test was conducted for a duration of 10 minutes. After each test, the volume of rainfall in each cup was measured in mL using a graduated cylinder. Each value was recorded on a data sheet and transferred to an Excel spreadsheet to calculate the coefficient of uniformity for further analysis. Christiansen's coefficient of uniformity is calculated using Equation 4.1.

$$C_U = 100\left[1.0 - \left(\frac{\sum\left(\left|D_i - D_{avg}\right|\right)}{n * D_{avg}}\right)\right] \quad \text{(EQ. 4.1)}$$

where,

C_U = Uniformity of spray, (%)
D_i = Depth of water in rain gauge, (cm)
D_{avg} = Average depth in rain gauge, (cm)
n = Number of observations

4.3 TESTING FACILITY

The rainfall simulator and test plot was constructed at the Auburn University Erosion and Sediment Control Facility (AU-ESCTF) located at the National Center for Asphalt Technology (NCAT) test track in Opelika, Alabama. The AU-ESCTF has three primary objectives: (1) research and development, (2) product evaluation, and (3) training. The test facility is a joint operation between Auburn University's Department of Civil Engineering and Alabama Department of Transportation (ALDOT). As such, the majority of the research efforts at the facility are geared towards conducting large-scale, performance based testing of ALDOT's standard ESC practices to better understand their performance in field installations. The knowledge gained in this process allows for recommendations to be for improvements to the standard ALDOT ESC designs and practices, in order to improve performance and stormwater quality throughout the state. The facility also acts as an independent, third party evaluator of a variety of manufactured products. These products are subjected to the same large-scale, performance-based tests as the standard ALDOT ESC practices. The results from these tests

provide useful information on the integrity of the manufactured products and allow for comparisons to be made between standard practices and manufactured products. The knowledge gained from the first two missions of the AU-ESCTF is transferred to industry professionals through training events hosted at the facility. Field days and tours are held throughout the year to educate owners, contractors, designers, regulators, and inspectors on how to properly install, inspect, and maintain ESCs that are commonly employed in the field.

The test facility currently has the capability to conduct intermediate and field-scale rainfall simulations on erosion control practices, large-scale testing of ditch checks and inlet protection practices (IPPs) using channelized flow, large-scale testing of various sediment basin configurations, and large-scale testing of sediment barrier practices using sheet flow. Water for field scale rainfall simulation and other large scale test apparatus' is supplied by a 28,000 ft^3 (793 m^3) upper storage pond. During drought conditions, the upper retention pond can be replenished from a lower storage pond on site. An aerial view of the AU-ESCTF showing the various testing apparatus' and training stations is provided in Figure 4.2. Research apparatus' are designated by orange circles while demonstration and training areas are designated by blue circles.

Figure 4.2 Aerial View of the AU-ESCTF.

4.4 CALIBRATION PROCEDURES

Initially, the rainfall simulator apparatus was calibrated to determine experimental values for rainfall intensity as well as to optimize the location of each sprinkler riser to maximize the uniformity of the rainfall distribution. The calibration process was critical in proving that the rainfall simulator accurately and repeatedly simulated conditions similar to natural rainfall (i.e. uniformity, drop size, terminal velocity).

To measure rainfall intensity and rainfall distribution, 29 rain gauges were installed throughout the test plot. The layout for the rain gauges is shown in Figure 4.3.

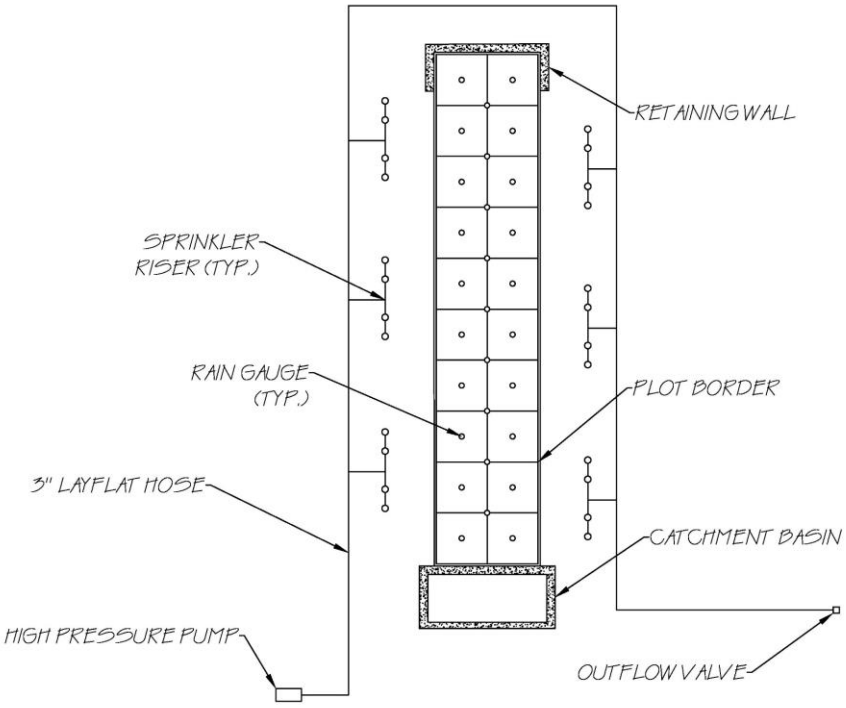

Figure 4.3 Rain Gauge Layout.

For each target intensity, a calibration test was run for a duration of 15 minutes. At the end of the test, the rainfall depth in each rain gauge was measured and recorded in centimeters. The data was then transposed to an excel spreadsheet to calculate the Christiansen uniformity coefficient (Equation 4.1), average rainfall intensity (Equation 4.2), and conduct statistical

analyses on the data. Furthermore, the data was converted to a .csv file and imported into ArcMap to generate a raster surface of the rainfall depth for each calibration test. Each raster surface provided an effective visualization of the rainfall distribution uniformity generated by the rainfall simulator. To quantify experimental rainfall intensity, the values for rainfall depth measured from each rain gauge were recorded. Using Equation 4.2, values for experimental rainfall intensity were computed and compared to the targeted rainfall intensities by converting the experimental values from units of cm/hr into in./hr. Based upon the results of each test, the locations of each sprinkler riser were altered as necessary to achieve maximum uniformity of rainfall. Furthermore, nozzles were interchanged to minimize the difference between theoretical and experimental values for rainfall intensity. Pictures depicting the calibration process are provided in Figure 4.4.

(a) rain gauge locations

(b) measuring depth in rain gauge

(c) calibration test for test interval 1 of 6

Figure 4.4 Rainfall Simulator Calibration Process.

$$i = 60\left[\sum_{j=1}^{J}\frac{D_j}{Jt}\right] \quad \text{(EQ. 4.2)}$$

where,

i = Rainfall intensity, (cm/hr)
D_j = Depth of rainfall, (cm)
J = Number of rain gauges
t = Test duration, (min)

Once the Christiansen's coefficient of uniformity was at least 80% for each target intensity, the raindrop size distribution for each intensity was measured. For each intensity, three 9 in. (23 cm) cake pans were filled with sifted, all-purpose flour to a depth of 1 in. (25.4 mm). Next, the pans were labeled, covered, and placed in the middle of the test plot at 10 ft (3 m), 20 ft (6 m), and 30 ft (9 m). Each pan was set 12 in. (30 cm) above the surface of the test plot. The covers were then removed to allow the flour to be exposed to rainfall for 2 to 4 seconds with the exact time of exposure being recorded. Once all samples were collected, the flour was allowed to air dry for at least 12 hours. Once the flour had air dried, the contents of one pan was screened by hand using a #50 sieve. The contents of the sieve were then transferred into an evaporating dish. This process was repeated until all nine samples had been screened. Each evaporating dish was then placed inside an oven for 6 hours at 110°F (43°C). The dried pellets from each evaporating dish were then transferred into a sieve stack consisting of #4, #8, #10, #14, #20, #30 sieve, and the pan. The pellets were hand sieved for 2 minutes. Foreign matter and double pellets were removed from each sieve. The contents of each individual sieve were then counted and weighed using an analytical balance with a precision of 0.001 g. Using Equation 4.3, the raindrop diameter (mm) for each evaporating dish was calculated using recorded data for average weight (mg).

$$D_r = \sqrt[3]{\left(\frac{6}{\pi}\right) W} \qquad \text{(EQ. 4.3)}$$

where,

D_r = Raindrop diameter, (mm)
W = Average pellet weight, (mg)

The values for the raindrop diameter and number of pellets were used to plot the raindrop size distribution for each intensity. This process was repeated three times for each test intensity. This process is depicted in Figure 4.5.

(a) sifted flour in 9 in. (23 cm) pan

(b) collection of flour pellets

(c) sieving flour from pellets

(d) separating pellets in a sieve stack

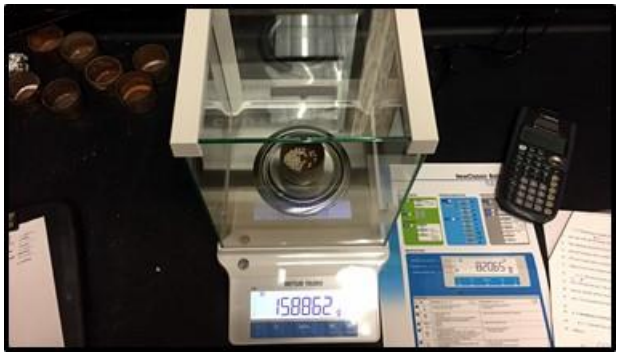

(e) weighing flour pellets

Figure 4.5 Drop Size Distribution Testing.

Following the calculation of the raindrop size distribution, the kinetic energy generated at each rainfall intensity was calculated. First, the raindrop fall height was determined by holding a surveyor's rod vertically in front of the center of a single sprinkler riser while the riser was operational. The wetted height was then measured and recorded as the average fall height for the raindrops. Next, using the average raindrop diameters computed from the previous step, the average volume of the raindrops was calculated using Equation 4.4:

$$V_{avg} = \frac{4}{3}\pi\left(\frac{d_{avg}}{2}\right)^3 \quad \text{(EQ. 4.4)}$$

where,

V_{avg} = Average volume of raindrop, (mm^3)
d_{avg} = Average diameter of raindrop, (mm)

Using the values for average volume (mm^3) and density of water (1 mg/mm^3), the average mass of the raindrops at each intensity were computed using Equation 4.5:

$$m_{avg} = \rho v \quad \text{(EQ. 4.5)}$$

where,

m_{avg} = Average mass of raindrop, (mg)
ρ = Density of water, (mg/mm^3)
v = Average volume of water, (mm^3)

The average mass of the raindrops was first converted into units of kilograms. Next, the velocity of the raindrops was determined using Figure 4.6. The experimental values for kinetic energy were calculated using Equation 4.7.

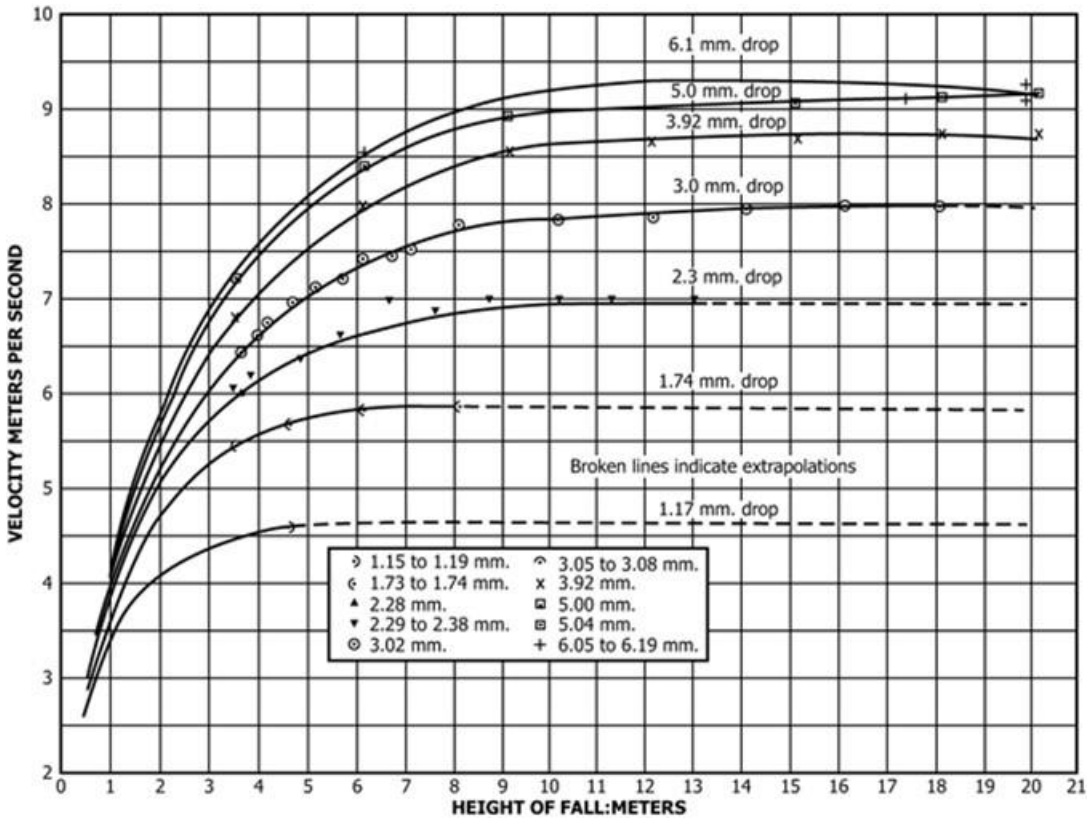

Figure 4.6 Fall velocity of Rain Drops. (ASTM 2015)

$$KE = 0.5mv^2 \quad \text{(EQ. 4.6)}$$

where,

KE = Kinetic energy, (J)
m = Average mass of raindrop, (kg)
v = Velocity of raindrop, (m/s)

The final step of the calibration process was to calculate the erosion index (EI). The erosion index was first developed by Wischmeier and Smith (1958) as part of the Universal Soil Loss Equation (USLE). EI is used to quantify the erosive energy of rainfall and is calculated using Equation 4.8.

$$EI = I * 1099 * \left[1 - 0.72e^{(-1.27I)}\right] \quad \text{(EQ. 4.7)}$$

where,

EI = Erosion index
I = Rainfall intensity, (in./hr)

4.5 VALIDATION PROCEDURES

Once the rainfall simulator had been properly calibrated to ensure rainfall patterns were similar to a Type III 2-yr, 24 hr storm event, erosion tests were conducted on a bare soil slope to guarantee that the data collected throughout the duration of a test was repeatable. By validating the results generated by rainfall induced erosion, the research process could then move towards performance testing.

4.5.1 Slope Preparation

The initial step for each validation test was to prepare the slope in a consistent and repeatable manner. To remove any rill erosion from the previous test, the soil veneer was tilled to a depth of 4 in. (10 cm) using a dual tine tiller. The tiller was set in the forward tine gear when going up the slope and the reverse tine gear when going down the slope. This process is depicted in Figure 4.7.

(a) test slope before preparation (b) tilling slope in forward tine gear

(c) tilling slope in reverse tine gear (d) test slope post tilling

Figure 4.7 Slope Preparation Using Tiller.

The slope was then smoothed using metal rakes and an 8 ft (2.4 m) level. A level was used to screed the slope to ensure that the soil was prepared in an even, level fashion. This prevented runoff from collecting on one side of the test plot and producing unnatural erosion patterns. Screened, sandy soil was added as needed to replace soil from previous tests. Foreign objects in the soil (i.e., rocks, roots, dirt clods) were removed at this time. Finally, water was added to the plot if necessary using a garden hose and nozzle to achieve the target moisture content of the soil (15 $\pm$ 5%). Figure 4.8 provides a depiction of this process.

(a) leveling soil on slope

(b) test plot after leveling soil

(c) adding water to reach optimum moisture content

Figure 4.8 Preparing soil in test plot.

The soil was then compacted to a density of 86 ± 6% using a turf roller. A winch was installed at the top of the slope on the retaining wall and connected to the turf roller to ensure that the soil compaction was performed in a uniform and consistent manner between tests. Soil compaction was checked in accordance with ASTM D2937. The locations for sampling were

selected by creating a 2 ft by 2 ft (0.6 m by 0.6 m) grid on the slope and using the random number generator on a TI-36X Pro calculator to select the locations for soil sampling. The grid is displayed in Figure 4.9.

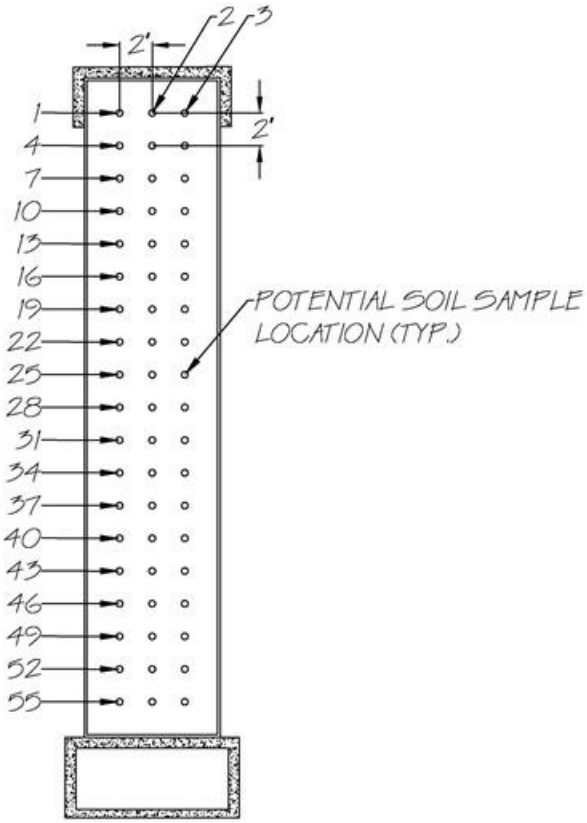

Figure 4.9 Soil Sampling Grid.

Once three locations were selected, the in-situ density was determined using ASTM D2937 (ASTM 2010). A standard cylinder and drive apparatus were used to collect density samples. The cylinder was driven into the slope by dropping the hammer on the drive apparatus until the cylinder was approximately ½ in. (13 mm) below the surface. Using a shovel, the soil surrounding the cylinder was excavated. The cylinder was then removed. Any soil clinging to the surface of the cylinder was removed and the edges of the cylinder were struck flush with a straight edge. The

mass of the cylinder and soil sample was then recorded to the nearest 1 gram. Photos depicting this process are shown in Figure 4.10.

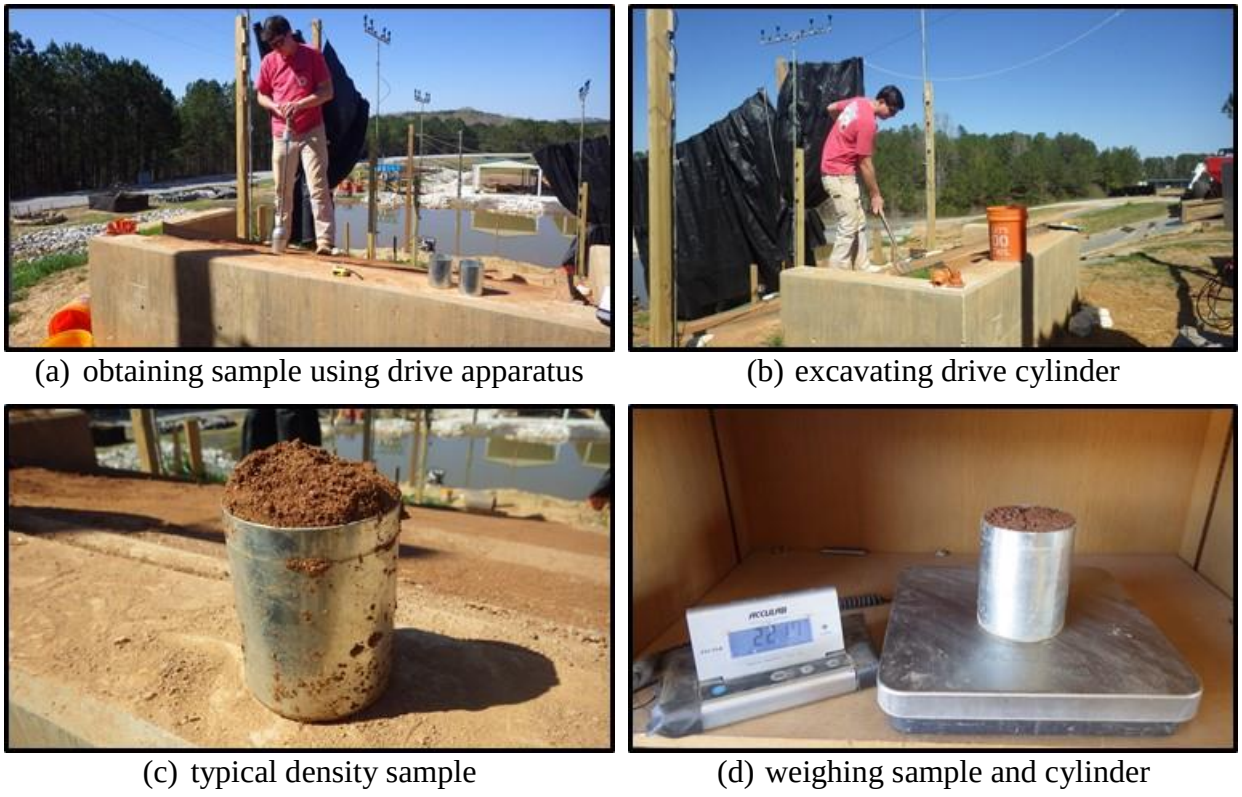

(a) obtaining sample using drive apparatus (b) excavating drive cylinder

(c) typical density sample (d) weighing sample and cylinder

Figure 4.10 Soil Sampling Process.

Once the soil was removed from the cylinder, a representative sample was removed to calculate the water content according to ASTM D4643 (ASTM 2008). To begin, the mass of a clean, dry, microwave-safe container was measured and recorded to the nearest 0.1 grams. The representative soil sample was then placed in the container and immediately weighed. The mass was recorded to the nearest 0.1 grams. The sample was then heated in the microwave oven for 3 minutes. Once the drying time had elapsed, the weight of the specimen and container was immediately recorded. A glass rod was then used to mix the soil. The soil and container is shown in Figure 4.11.

Figure 4.11 Drying Soil Using the Microwave Method.

The container was returned to the oven and heated for another minute. This process was repeated until the change in mass between two consecutive heating cycles was less than or equal to 0.1%. The target moisture content for this process was 15.5% ± 5%. Moisture content was then calculated using Equation 4.9.

$$w = \left(\frac{M_1 - M_2}{M_2 - M_C}\right) * 100 \qquad \text{(EQ. 4.8)}$$

where,

w = Water Content, (%)
M_1 = Mass of Container and Moist Specimen, (g)
M_2 = Mass of Container and Oven-Dried Specimen, (g)
M_c = Mass of Container, (g)

Once the moisture content had been calculated, the mass and volume of the drive cylinder were measured and recorded. Using this information, the in-situ wet density was calculated using Equation 4.10.

$$\rho_{wet} = \frac{(M_1 - M_2)}{V} \qquad \text{(EQ. 4.9)}$$

where,

ρ_{wet} = Wet Density, (g/cm^3)
M_1 = Mass of Cylinder and Wet Soil Sample, (g)
M_2 = Mass of Cylinder, (g)
V = Volume of Cylinder, (cm^3)

The values calculated from Equations 4.9 and 4.10 were then used to determine the in-place dry density of the soil by inserting those values into Equation 4.11.

$$\rho_d = \frac{\rho_{wet}}{\left(1 + (w/100)\right)} \quad \text{(EQ. 4.10)}$$

where,

ρ_d = Density (g/cm^3)
ρ_{wet} = Wet Density (g/cm^3)
w= Water Content, (%)

With the moisture content, wet density, and dry density calculated, the dry unit weight for the soil sample was determined. Once the dry unit weight was calculated, it was divided by the maximum dry unit weight, 108.1 lbs/ft^3 (17.0 kN/m^3) to determine the value for percent standard proctor density. The dry unit weight was calculated using Equation 4.12:

$$\gamma_d = 9.81 * \rho_d \quad \text{(EQ. 4.11)}$$

where,

γ_d = Dry Unit Weight, (kN/m^3)
ρ_d = Dry Density, (g/cm^3)

4.5.2 Rainfall Simulation for Control Testing

If the values were within the designated limits, a rainfall simulation was conducted on the bare slope for a duration of 60 minutes. The test was divided into six intervals of 10 minutes each. Over those six intervals, the rainfall intensities varied from 1.10 in./hr to 3.69 in./hr. The intensities were varied by activating or deactivating a series of solenoid valves that control flow to the sprinkler heads on each riser. During the test, grab samples were collected at the flume over the catchment basin in 3 minute intervals once runoff from the plot began and continued until runoff ceased.

4.5.3 Analysis of Samples for Suspended Sediment Concentration (SSC)

The samples were then taken to the lab to measure the SSC in each specimen to quantify the amount of erosion that occurred during a test. The test procedure for determining SSC follows ASTM D3977 protocol (ASTM 1997). First, once the sample had settled, the supernatant was vacuumed away by inserting a J-shaped tube to a depth near the bottom of the sample. The tube was then connected to a vacuum and the supernatant was removed without disturbing the sediment. The supernatant was retained for use in calculating the dissolved-solids correction factor. The remaining volume was measured by placing the bottle on a flat surface and marking the water level. Using water, the sediment and supernatant was then rinsed from the bottle into an evaporating dish. Once the bottle was empty, it was refilled with water from a graduated cylinder. The volume added to reach the water level mark was recorded as the volume for the sample. The evaporating dish containing the sample was then placed in an oven with the temperature set at 210°F (99°C). Once the water had evaporated, the temperature was raised to 221°F (105°C) for 2 hours. The dish was then transferred to a desiccator to cool to room temperature. After the dish had cooled, it was weighed to the nearest 0.0001 gram. The weight of the dish was also recorded. Pictures detailing this process are shown in Figure 4.12.

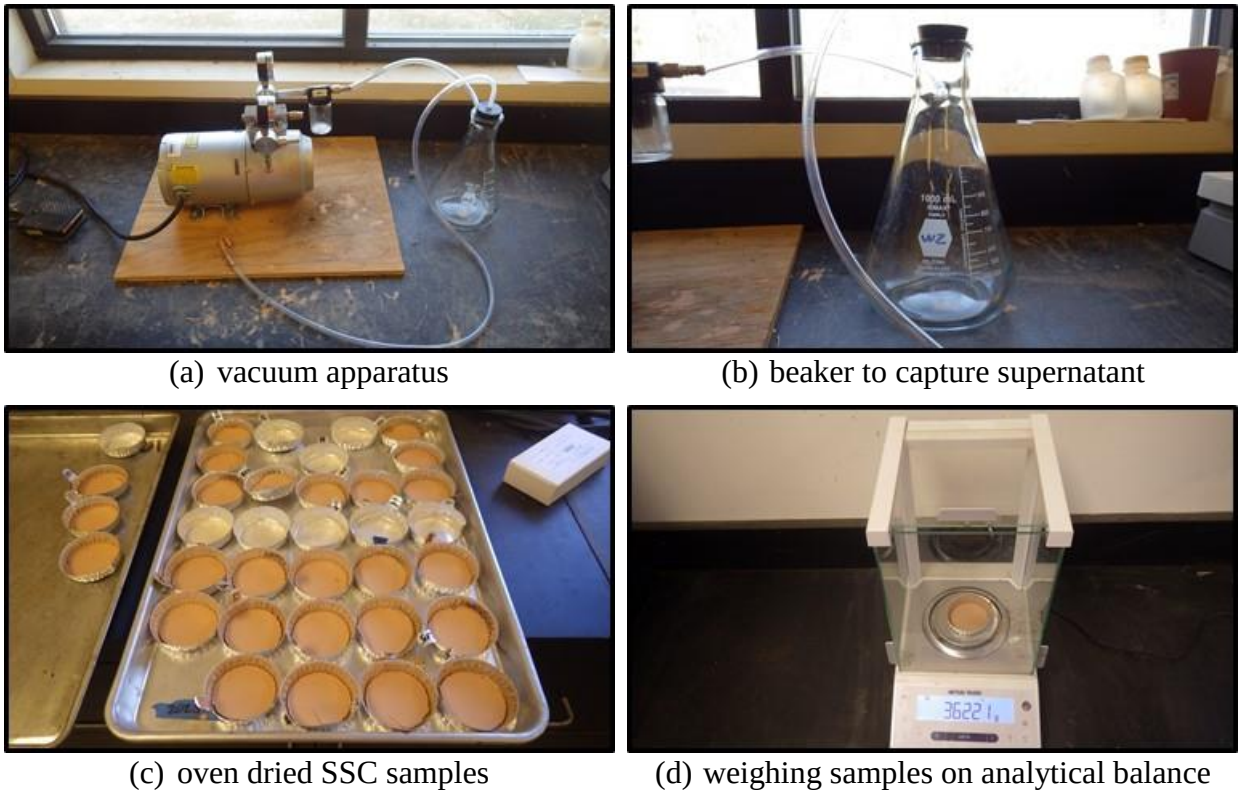

(a) vacuum apparatus (b) beaker to capture supernatant

(c) oven dried SSC samples (d) weighing samples on analytical balance

Figure 4.12 Lab Analysis of SSC Samples.

To determine the dissolved-solids correction factor, a measured volume from the supernatant was transferred to an evaporating dish using a volumetric pipet. The volume of the sample was recorded. The sample was then dried in an oven and cooled in a desiccator similarly to the SSC sample. The weight of the dish and sample was recorded to the nearest 0.0001 gram. The weight of the dish was also recorded separately. The dissolved-solids correction factor was then calculated using Equation 4.13.

$$DS_c = \left(\frac{DS}{V_a}\right) * V_s \qquad \text{(EQ. 4.12)}$$

where,

DS_c = Dissolved-Solids Correction, (g)
DS = Weight of Dissolved Solids, (g)
V_a = Sample Volume for Dissolved Solids, (mL)
V_s = Volume of Supernatant with Sediment, (mL)

The value for DS_c was then subtracted from the net weight of the sediment to calculate a corrected sediment weight. Finally, the corrected weight of the sediment was divided by the net weight of the sample and multiplied by 1,000,000 to convert the results into units of parts per million (ppm). According to ASTM D3977 (1997), it is more acceptable to report concentrations in terms of mg/L. Equation 4.14 was used to convert results from units of ppm to SSC.

$$C_1 = \frac{C}{1.0 - C * (622 * 10^{-9})} \quad \text{(EQ. 4.13)}$$

where,

C_1 = Sediment Concentration, (mg/L)
C = Sediment Concentration, (ppm)

4.6 STATISTICAL ANALYSES

The objectives of this study required that data collected during calibration be statistically analyzed to determine if there was a statistically significant difference between data sets (i.e. difference between theoretical and experimental intensities). Table 4.1 displays a summary of the hypotheses for the calibration process.

Table 4.1 Statistical Hypotheses for Calibration Testing.

Rainfall Intensity		
Test Interval 1/6	Null - H_0: $\mu = 0.98$ in./hr	Alternate – H_a: $\mu \neq 0.98$ in./hr
Test Interval 2/5	Null - H_0: $\mu = 1.70$ in./hr	Alternate – H_a: $\mu \neq 1.70$ in./hr
Test Interval 3/4	Null - H_0: $\mu = 3.45$ in./hr	Alternate – H_a: $\mu \neq 3.45$ in./hr
Uniformity of Rainfall Distribution		
Test Interval 1/6	Null - H_0: $\mu \geq 0.80$	Alternate – H_a: $\mu < 0.80$
Test Interval 2/5	Null - H_0: $\mu \geq 0.80$	Alternate – H_a: $\mu < 0.80$
Test Interval 3/4	Null - H_0: $\mu \geq 0.80$	Alternate – H_a: $\mu < 0.80$

The null hypotheses for rainfall intensity stated that the average rainfall intensity produced by the rainfall simulator equaled the theoretical targets from Figure 4.13.

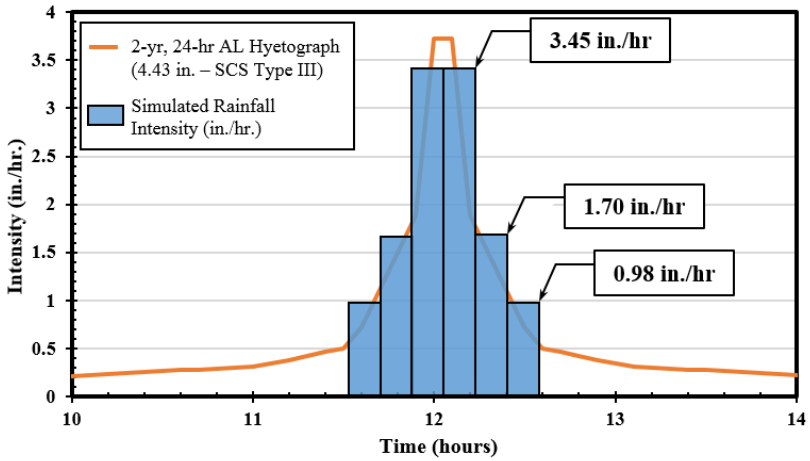

Figure 4.13 Theoretical Rainfall Intensity Targets.

The alternate hypotheses stated that the average intensities did not equal the theoretical targets. For uniformity of rainfall distribution, the null hypotheses for this study stated that the average value for the Christiansen coefficient of uniformity was greater than or equal to the minimum of 80%. The alternate hypotheses stated that the average uniformity was not greater than 80%. The data collected from the calibration process was used to calculate test statistics (z-scores) to determine if the null hypotheses would be accepted or rejected. A value for Type I error (α) of 0.05 was selected since a two-tailed test was being conducted. The variable α represents the probability of rejecting the null hypothesis when it is in fact, true (Ott and Longnecker 2010). In

a two-tailed test, if the value for the test statistic falls within the rejection range, the null hypothesis is rejected. The test statistic was computed using Equation 4.15. The minimum value for the rejection range is calculated using Equation 4.16.

$$z = \frac{\bar{x} - \mu_0}{\sigma/\sqrt{n}} \quad \text{(EQ. 4.14)}$$

where,

z = Z Score
$\bar{x}$ = Experimental Average
μ_0 = Theoretical Target
σ = Standard Deviation for Data Set
n = Sample Size

$$R.R. = \frac{\pm 1.96\sigma}{\sqrt{n}} \quad \text{(EQ. 4.15)}$$

where,

R.R. = Rejection Range
σ = Standard Deviation for Data Set
n = Sample Size

Once the test statistic and limits for the rejection range were calculated, the two values were compared. If the value for the test statistic was greater than the limit for the rejection range, the null hypothesis was rejected. If the value was within both limits the rejection range, the null hypothesis was accepted.

4.7 SUMMARY

The methods and procedures for this study were developed to ensure that: (1) the simulator was calibrated to accurately and repeatedly simulate a Type III 2-yr, 24-hr storm event in Auburn, Alabama, (2) the slope was prepared consistently between tests, and (3) validate the performance of the simulator through determining the repeatability of bare soil control tests. A summary of existing testing procedures from the literature review and the procedures developed for this study is provided in Table 4.2.

Table 4.2 Summary of Rainfall Simulation Test Methods

Test Protocol	Design Storm	Rainfall Intensities	Plot Area (Slope)	Number of Rain Gauges	Test Duration
ASTM D6459	10-yr, 6 hr	2, 4, 6 in./hr	320 ft^2 (3:1)	20	3, 20 min Intervals
AU-ESCTF	2-yr, 24 hr	1.10, 1.78, 3.76 in./hr	320 ft^2 (3:1)	29	6, 10 min Intervals

The test methods and procedures outlined in this section allowed the researchers to efficiently and consistently collect rainfall data from calibration testing as well as runoff data that was later analyzed to validate the performance of the rainfall simulator. The rainfall data was analyzed to determine if the simulated rainfall produced was similar to natural rainfall. Runoff collected during validation testing was analyzed to determine if the simulated rainfall eroded the test plot in a consistent, repeatable fashion.

CHAPTER FIVE:
RESULTS AND DISCUSSION

5.1 INTRODUCTION

Calibration experiments were conducted to provide a means to quantify the performance of the rainfall simulator and determine if the apparatus is capable of simulating rainfall with characteristics similar to natural rainfall on a consistent basis. Once calibration of the rainfall simulator was complete, the apparatus was validated by conducting field-scale tests on a bare soil plot. This chapter will present the findings generated from these experiments as well as the results from the statistical analyses performed on the data.

5.2 CALIBRATION RESULTS

The methods and procedures discussed in Section 4.4 produced a multitude of data in the form of rainfall depth measured from each of the 29 rain gauges after each calibration test. Raw data from the individual experiments is provided in Appendix C. The data from each test were analyzed to determine the average rainfall intensity and coefficient of uniformity. Finally, the values calculated from the calibration tests for each target rainfall intensity were averaged to provide a generalized report on the performance of the rainfall simulator in terms of experimental rainfall intensity and uniformity of rainfall distribution.

5.2.1 Experimental Rainfall Intensity and Uniformity

A total of fifty eight, 15 minute calibration tests were performed and rainfall was collected in a series of 29 rain gauges. Initially, 30 tests were going to be conducted for each target intensity.

However, after the first 30 tests, it was decided that if the standard deviation of the average rainfall intensity was less than or equal to 0.10 in./hr, testing could proceed to the next target intensity. At the end of each test, the depth in each rain gauge was measured and recorded to determine the experimental rainfall intensity for the calibration test. The results from the 30 calibration tests for test intervals 1 and 6 are tabulated in Table 5.1. The flow rate column represents the sum of the flow rates provided by the nozzles at a constant pressure of 10 psi (69 kPa).

Table 5.1 Calibration Testing Results for Test Intervals 1/6 (Target Intensity = 0.98 in./hr)

Flow Rate (gpm)	Experimental Intensity (in/hr)
9.48	1.1
9.48	1.1
9.48	1.0
9.48	1.1
9.48	1.1
9.48	1.1
9.48	1.0
9.48	1.0
9.48	1.1
9.48	1.0
9.48	1.2
9.48	1.1
9.48	1.1
9.48	1.1
9.48	1.1
9.48	1.1
9.48	1.1
9.48	1.1
9.48	1.2
9.48	1.2
9.48	1.2
9.48	1.1
9.48	1.1
9.48	1.1
9.48	1.1
9.48	1.1
9.48	1.1
9.48	1.1
9.48	1.1
9.48	1.1

The values for experimental rainfall intensity from each test were averaged and compared to the theoretical target intensity of 0.98 in./hr. The standard deviation between the values of experimental rainfall intensity for each test was also calculated to determine if the simulator was producing the same rainfall intensity consistently. These results are provided in Table 5.2.

Table 5.2 Calibration Summary for Test Intervals 1/6

Flow Rate (gpm)	Average Experimental Intensity (in./hr)	Sample Size	Standard Deviation (in./hr)	Theoretical Intensity (in./hr)	Percent Error (%)
9.5	1.10	30	0.05	0.98	12.2

After analyzing the values in Table 5.2, it was concluded that the rainfall simulator consistently produced rainfall intensities higher than theoretical target. In an attempt to reduce the experimental rainfall intensities, #11 nozzles were installed in the sprinkler heads. However, the combination of the small nozzles and low pressure resulted in poor, inconsistent performance between the sprinkler heads. Although the average rainfall intensities were higher than the theoretical target, the standard deviation between the 30 calibration tests was only 0.05 in./hr. This value provided confidence that at test intervals 1 and 6, the simulator was capable of producing repeatable results. After analyzing the results from the first 30 calibration tests, it was determined that conducting 30 calibration tests for each test intensity was not necessary if the standard deviations were small, 0.1 in/hr or less. In order to expedite the calibration process, it was decided that at least 10 calibration tests for each intensity should be conducted. The maximum standard deviation for the average rainfall intensity was set at 0.1 in./hr. If, after 10 tests, the standard deviation was less than or equal to this value, testing efforts would proceed to the next step.

Next, 18 calibration tests were conducted for test intervals 2 and 5. The process of collected rainfall in rain gauges to determine experimental rainfall intensity used for the initial calibration tests was repeated. The results from those tests are tabulated in Table 5.3.

Table 5.3 Calibration Testing Results for Test Intervals 2/5 (Target Intensity = 1.70 in./hr)

Flow Rate (gpm)	Experimental Intensity (in./hr)
15.0	1.6
15.0	1.6
15.0	1.7
15.0	1.7
15.0	1.8
15.0	1.8
15.0	1.8
15.0	1.9
15.0	1.7
15.0	1.8
15.0	1.8
15.0	1.9
15.0	1.9
15.0	1.8
15.0	1.8
15.0	1.9
15.0	1.8

The calculated experimental rainfall intensities for test intervals 2 and 5 were averaged and compared to the theoretical target of 1.70 in./hr. The standard deviation between the values of experimental rainfall intensity for each test was also calculated to determine if the simulator was producing the same rainfall intensity consistently. These results are provided in Table 5.4.

Table 5.4 Calibration Summary for Test Intervals 2/5

Flow Rate (gpm)	Average Experimental Intensity (in./hr)	Sample Size	Standard Deviation (in./hr)	Theoretical Intensity (in./hr)	Percent Error (%)
15.0	1.78	17	0.10	1.70	4.8

Once again, the average experimental rainfall intensity was higher than the theoretical target of 1.70 in./hr. However, the difference between the two values was slightly smaller than for test intervals 1 and 6. The standard deviation of the rainfall intensities was approximately double that of the standard deviation for test intervals 1 and 6. This is due in part to the average rainfall intensities ranging from 1.6 to 1.9 in./hr. One test resulted in an average rainfall intensity of 2.0 in./hr. Grubbs' test was used to analyze the data set and determine if the value of 2.0 in./hr was an outlier. In Grubbs' test, a test statistic is calculated and compared to a critical value. If the test

statistic is larger than the critical value, the value in question is labeled an outlier. The results of this analysis are presented in Table 5.5.

Table 5.5 Statistical Analysis Using Grubbs' Test

Test Statistic	Significance Level, α	Critical Value	Outlier
1.95	0.05	1.88	Yes

Finally, 10 calibration tests were conducted for test intervals 3 and 4. The data collection procedures for the first two iterations of the calibration process were replicated to obtain the data for this analysis. The results from those tests are provided in Table 5.6.

Table 5.6 Calibration Testing For Test Intervals 3/4 (Target Intensity = 3.45 in./hr)

Flow Rate (gpm)	Experimental Intensity (in./hr)
29.3	3.8
29.3	3.8
29.3	3.8
29.3	3.7
29.3	3.7
29.3	3.8
29.3	3.7
29.3	3.7
29.3	3.8
29.3	3.8

The results from these calibration tests were averaged and compared to the theoretical target intensity of 3.45 in./hr. The standard deviation between the values of experimental rainfall intensity for each test was also calculated to determine if the simulator was producing the same rainfall intensity consistently. These results are provided in Table 5.7.

Table 5.7 Calibration Summary for Test Intervals 3/4

Flow Rate (gpm)	Average Experimental Intensity (in./hr)	Sample Size	Standard Deviation (in./hr)	Theoretical Intensity (in./hr)	Percent Error (%)
29.3	3.76	10	0.05	3.45	8.9

The average experimental rainfall intensity followed the pattern set forth by the previous two calibration iterations, with the value being slightly higher than the theoretical intensity of 3.45 in./hr. On the other hand, the standard deviation between the experimental rainfall intensities was only 0.05 in./hr. This result ensured that the rainfall simulator was producing repeatable results in terms of rainfall intensity for test intervals 3 and 4. Figure 5.1 provides a comprehensive summary of the results compiled from calibration testing.

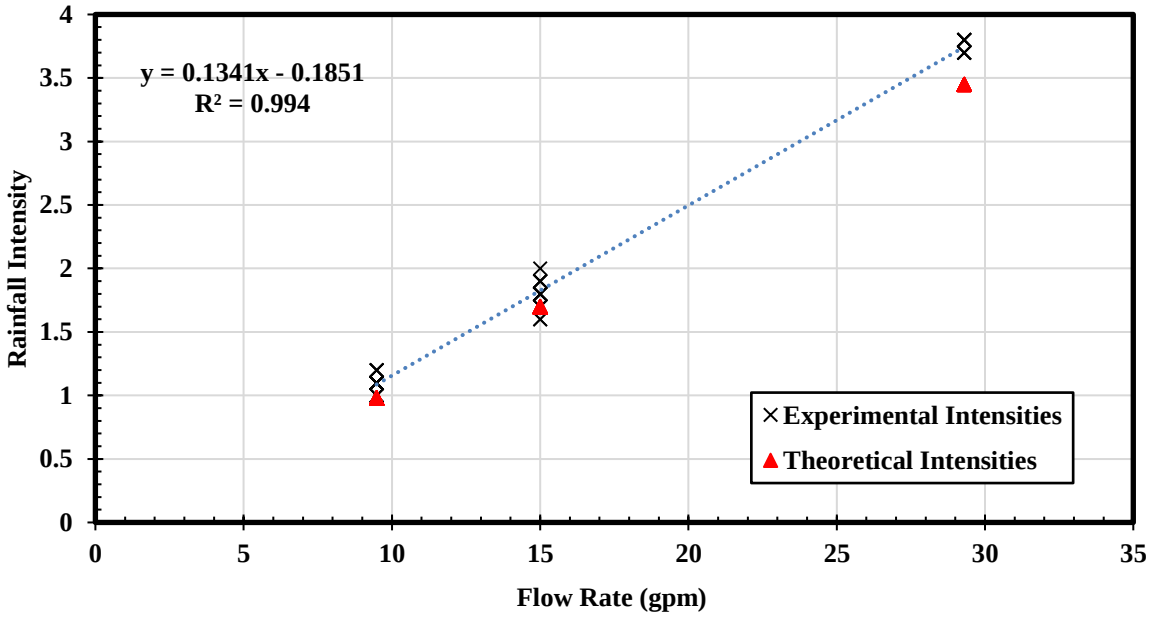

Figure 5.1 Experimental vs. Theoretical Rainfall Intensities.

Figure 5.1 graphically illustrates that the experimental rainfall intensities calculated during calibration were typically slightly higher than the theoretical targets. The intensity produced by the rainfall simulator follows a linear pattern based on the total flow rate in the sprinkler heads. The R^2 value quantifies how accurately the trendline fits the data. The closer the R^2 value is to 1,

the more accurate it is. With a R^2 value of 0.994, the linear trendline serves as a reliable means for estimating flow rates and corresponding nozzle sizes required to simulate specific rainfall intensities. The higher experimental rainfall intensities, in comparison to the theoretical values, produce slightly more surface runoff than should be expected for the design 2-yr, 24-hr storm event. An analysis was conducted on the collected rainfall data to quantify the increase in surface runoff. These results are tabulated in Table 5.8.

Table 5.8 Experimental vs. Theoretical Surface Runoff

Test Interval	1 & 6	2 & 5	3 & 4
Experimental Intensity (in./hr)	1.10	1.78	3.76
Theoretical Intensity (in./hr)	0.98	1.70	3.45
Experimental Volume (ft^3)	9.8	15.8	33.4
Theoretical Volume (ft^3)	8.7	15.1	30.7
Difference in Volume (ft^3)	1.1	0.7	2.8
Percent Difference (%)	11.5	4.6	8.6

All three experimental test intensities produce greater amounts of surface runoff over 20 minutes than should theoretically be expected. This increase in surface runoff increases the erosive energy of the rainfall on the 320 ft^2 (30 m^2) test plot during each test. This difference totals only 4.6 cubic feet (130.2 liters) over a 60 minute test. However, since the standard deviations for the experimental rainfall intensity ranged from 0.05 to 0.10 in./hr, it can be assumed that the simulator will produce similar amounts of surface runoff from test to test.

The average experimental rainfall intensities were used to calculate the erosion index (EI) and compared to the theoretical values. The EI quantifies the erosive potential of rainfall at various intensities. EI is also used in calculating the R-factor used in RUSLE calculations for expected erosion over a given area. The results from this analysis are presented in Table 5.9.

Table 5.9 Experimental vs. Theoretical EI Values

Experimental Intensity (in./hr)	Theoretical Intensity (in./hr)	Experimental Erosion Index	Theoretical Erosion Index	Percent Error (%)
1.10	0.98	993.62	853.65	16.40
1.78	1.70	1821.36	1713.01	6.33
3.76	3.45	4107.14	3757.41	9.31

The calculated values in Table 5.9 correspond with the results from Figure 5.1 and Table 5.8. The higher rainfall intensities produced by the rainfall simulator result in greater erosive potential on the test slope. The ensuing result is that higher rates of soil erosion are generated by the simulated rainfall versus what should be expected from an original 2-yr, 24-hr storm event. However, as the rainfall intensities increase, the relative error between the experimental and theoretical values decrease.

5.2.2 Statistical Analysis: Rainfall Intensities and Uniformities

To determine if there was a statistically significant difference between calculated values of experimental rainfall intensity versus theoretical rainfall intensities, z-scores were calculated for each test. If the z-score is within the rejection region, the null hypothesis stating that there was not a statistically significant difference between the values of experimental and theoretical rainfall intensities was rejected. These results are tabulated in Table 5.10.

Table 5.10 Statistical Analyses of Experimental Rainfall Intensities

Test Interval	Experimental Rainfall Intensity, $\bar{x}$ (in./hr)	Desired Rainfall Intensity, μ_0 (in./hr)	Z-Score	Rejection Limit	Significantly Different
1 & 6	1.10	0.98	12.51	0.02	Yes
2 & 5	1.78	1.70	3.79	0.05	Yes
3 & 4	3.76	3.45	18.98	0.03	Yes

For each grouping, there was a statistically significant difference between the values for experimental and theoretical rainfall intensities. The z-scores for test intervals 1/6 and 3/4 are much higher than the rejection limit since none of the values for experimental rainfall intensity were below the theoretical value. The z-score for test intervals 2/5 is much lower since two of the

values for experimental rainfall intensity were below the theoretical value. Although a statistically significant difference exists for each grouping, the practical difference between the values is small. For example, the difference between the experimental and theoretical values for test intervals 1/6 and 2/5 are 0.12 in./hr and 0.09 in./hr, respectively.

The experimental values for uniformity of rainfall distribution were quantified using Christiansen's coefficient of uniformity. These values were statistically analyzed similarly to the experimental intensities to determine if a statistically significant difference existed between the calculated values and the theoretical target of 80%. The values reported are the average values for uniformity over the 58 tests performed in the calibration process. Z-scores were calculated for each test. If the z-score was within the rejection region, the null hypothesis stating that the uniformity of rainfall distribution was consistently above the minimum was rejected. These results are tabulated in Table 5.11,

Table 5.11 Statistical Analyses of Experimental Uniformity of Rainfall

Test Interval	Experimental Uniformity (%)	Theoretical Minimum Uniformity (%)	Z-Score	Rejection Limit	Significantly Different
1 & 6	80.9	80.0	1.95	0.87	Yes
2 & 5	78.7	80.0	-2.94	-0.85	Yes
3 & 4	79.9	80.0	-0.24	-1.20	No

For the first two groupings, the null hypothesis that the average experimental uniformity of rainfall distribution is greater than 80% was rejected. In the case of test intervals 1/6, the experimental average is higher than the minimum target of 80%. However, the data set had a large standard deviation that resulted in the null hypothesis being rejected. For test intervals 3/4, the average value for experimental uniformity was below the minimum target of 80%. Nonetheless, the null hypothesis was rejected in this case due to the small standard deviation for this data set.

To aid in the visualization of the uniformity of rainfall distribution for each test interval, GIS raster surfaces showing rainfall depth and intensity were generated using ArcMap and overlaid on an aerial photo of the test plot. The raster surfaces are provided in Figure 5.2.

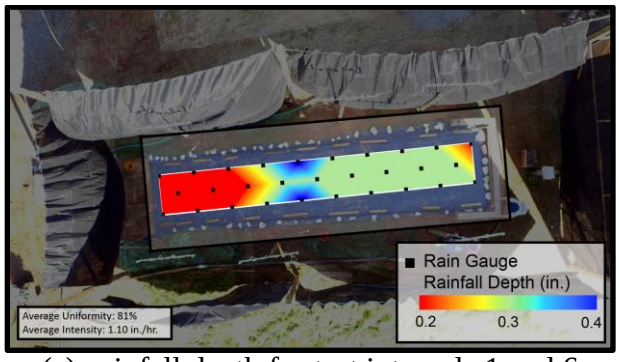

(a) rainfall depth for test intervals 1 and 6

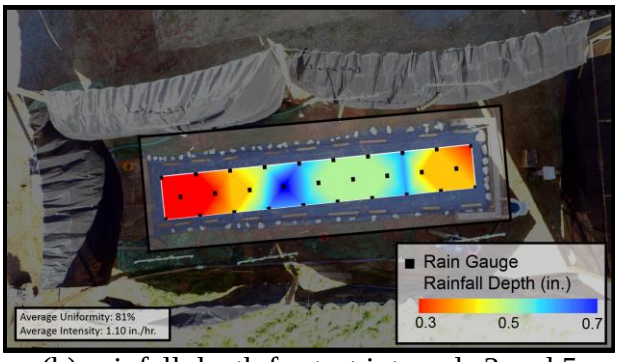

(b) rainfall depth for test intervals 2 and 5

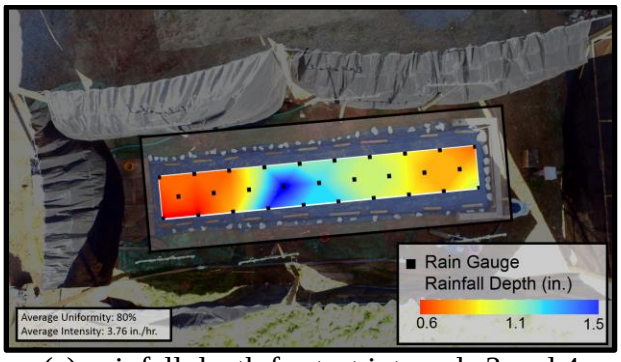

(c) rainfall depth for test intervals 3 and 4

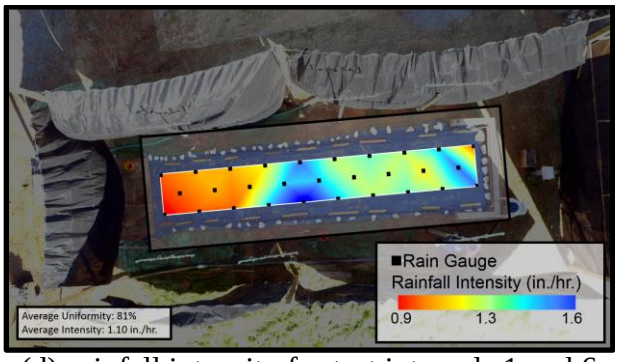

(d) rainfall intensity for test intervals 1 and 6

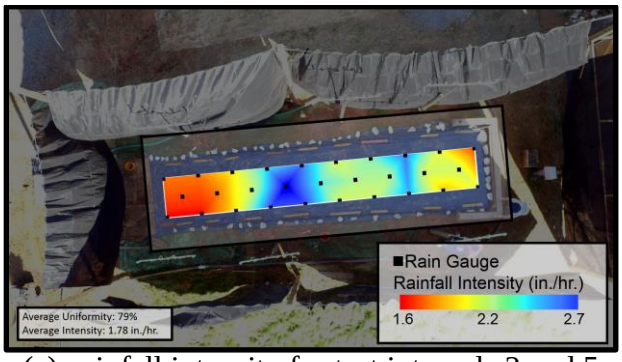

(e) rainfall intensity for test intervals 2 and 5

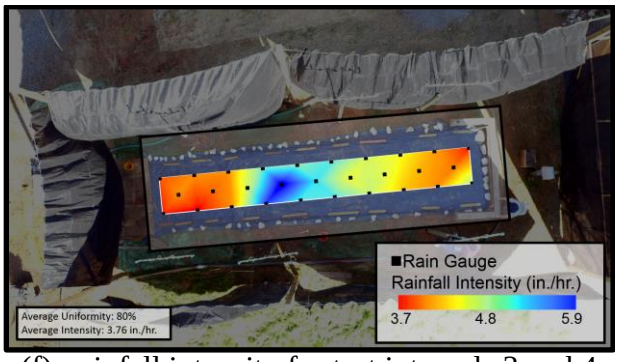

(f) rainfall intensity for test intervals 3 and 4

Figure 5.2 Raster Surfaces from Calibration Testing.

5.2.3 Drop Size Distribution

The drop diameters produced by the rainfall simulator were calculated using the flour pan method. For each intensity, three pans filled with sifted flour were set in the middle of the test plot at 10 ft (3 m), 20 ft (6 m), and 30 ft (9 m). Once the samples had been collected, the dried pellets were analyzed in the lab to calculate the drop diameters. The average drop diameter was then used to calculate the average mass of the rain drops. These results are tabulated in Table 5.12 and illustrated graphically in Figure 5.3.

Table 5.12 Drop Size Distribution Testing

Rainfall Intensity	1.10 in./hr	1.79 in./hr	3.76 in./hr
Average Drop Diameter (mm)	2.06	2.01	2.35
Theoretical Drop Diameter (mm)	2.22	2.46	2.79
Percent Error (%)	7.21	18.29	15.77
Average Drop Mass (mg)	4.58	4.25	6.80

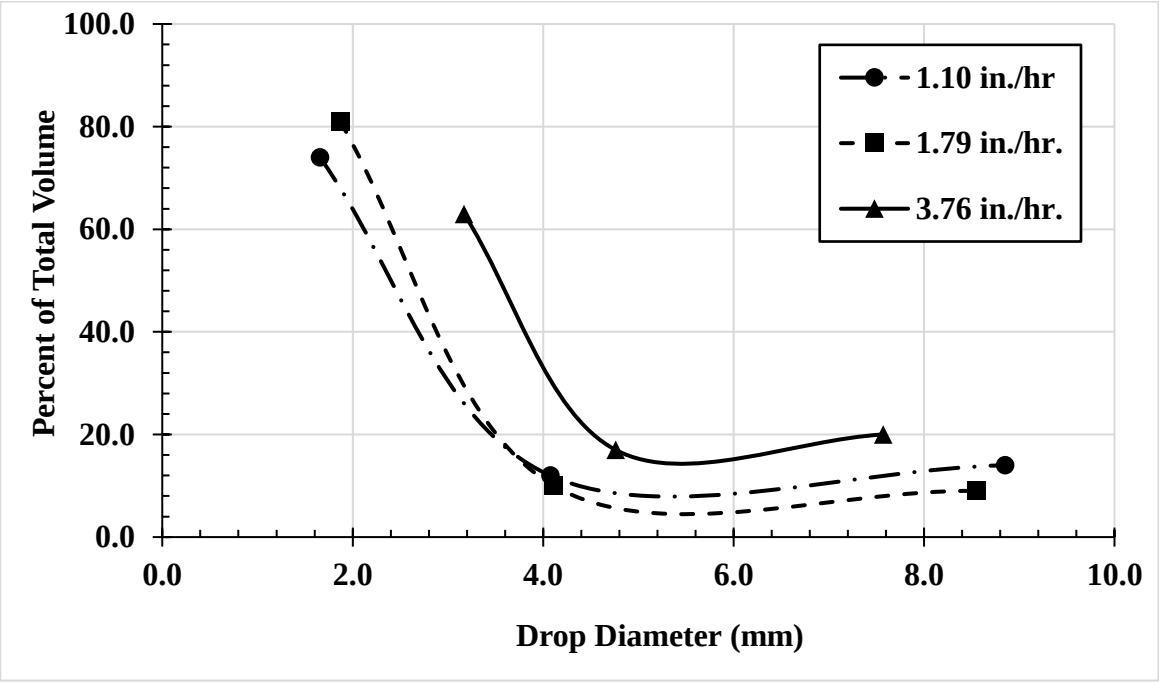

Figure 5.3 Drop Size Distribution.

At each intensity, the calculated drop diameter was smaller than the theoretical value. This is an issue common to pressurized rainfall simulators. Smaller raindrops are produced when pressurized flow is conveyed through small nozzle openings. In discussions with industry professionals, it was concluded that this issue could potentially be mitigated by increasing the nozzle size while simultaneously decreasing pressure. This would minimize the velocity of the flow in the sprinkler heads and possibly result in larger drop sizes. For the simulator designed for this research project, this could be accomplished by reducing the pressure regulators from 10 psi (69 kPa) to 5 psi (34.5 kPa) and increasing the nozzle sizes to compensate for the loss of pressure.

The values for average drop mass calculated previously were used to determine the experimental kinetic energy generated by the rainfall simulator. Values for rain drop velocity were estimated based on the diameter of the drop and the height from which the drops fell. In reality, the velocity of the drops is greater than estimated since the drops are projected from the sprinkler head with an initial outward and downward velocity. However, the actual velocity of the drops was not quantified in this study. The results of the kinetic energy analysis are presented in Table 5.13.

Table 5.13 Kinetic Energy of Rain Drops

Rainfall Intensity (in./hr)	Average Mass of Rain Drop (mg)	Velocity of Drop (m/s)	Kinetic Energy (J)
1.10	4.58	6.0	8.24E-05
1.79	4.25	6.0	7.65E-05
3.76	6.80	6.3	1.35E-04

For each rainfall intensity, the kinetic energy of a single raindrop is negligible. However, when combined with the energy of the thousands of other rain drops impacting the slope each second, the summation of this energy would be much more considerable.

5.3 VALIDATION RESULTS

A series of three, 60 minute bare soil control tests were performed to validate the rainfall simulator. This process was conducted to ensure that the rainfall simulator was capable of producing natural erosion patterns and repeatable results. During each test, grab samples were collected in 237 mL bottles once runoff began and continued in three minute intervals throughout the experiment. Furthermore, all runoff was detained to measure the bulk weight of eroded soil from the test plot after each test. During each test, photos were taken of the plot before rainfall commenced and in between each 10 minute test interval. A final photo was taken of the slope at the end of the test. This allowed researchers to view the progression of rill erosion on the slope over time. Slope conditions before the test as well as rainfall data is tabulated in Table 5.14. Pictures depicting slope erosion over the course of the first control test are provided in Figure 5.4.

Table 5.14 Slope Conditions and Rainfall Data for Control Test 1

Moisture Content (%)	Percent Compacted (%)	Average Rainfall Intensity (in./hr)	Coefficient of Uniformity (%)	Dry Weight of Eroded Soil (lb)
20.57	84.19	2.09	79.06	N/A[a]

[a] Data for weight of eroded soil was not collected in this test.

(a) slope erosion after interval 1

(b) slope erosion after interval 2

(c) slope erosion after interval 3

(d) slope erosion after interval 4

(e) slope erosion after interval 5

(f) slope erosion at end of test

Figure 5.4 Slope Erosion for Control Test 1.

The photos in Figure 5.4 show that significant erosion did not occur on the plot until the third test interval, where rainfall intensities average 3.76 in./hr. Overall, the erosion patterns for this test were similar to that of natural erosion. Starting with Figure 5.4(b), it can be seen that the rills began to form at the toe of the slope. As the test progressed, these rills slowly grew up the slope. The longest rills were found to be on the sides of the test plot. This served as an indication that the turf roller used to compact the soil in the plot did not adequately compact the soil along

the edges. In subsequent tests, a hand tamp was used to compact the soil around the edges to ensure that the soil reached a similar percent compaction to the rest of the soil on the plot.

Grab samples obtained during the test were analyzed for SSC. These calculations estimated the sediment load in the runoff from the slope. The results from this analysis are tabulated in Table 5.15 and presented graphically in Figure 5.5. Dash marks represent points where runoff had not yet begun.

Table 5.15 SSC from Control Test 1

Time (min)	SSC (mg/L)
0	--
3	--
6	--
9	42,251
12	55,149
15	34,739
18	29,317
21	31,655
24	22,691
27	23,192
30	24,194
33	22,348
36	17,846
39	32,584
42	26,511
45	31,372
48	33,435
51	20,345
54	28,968
57	27,463
60	20,314

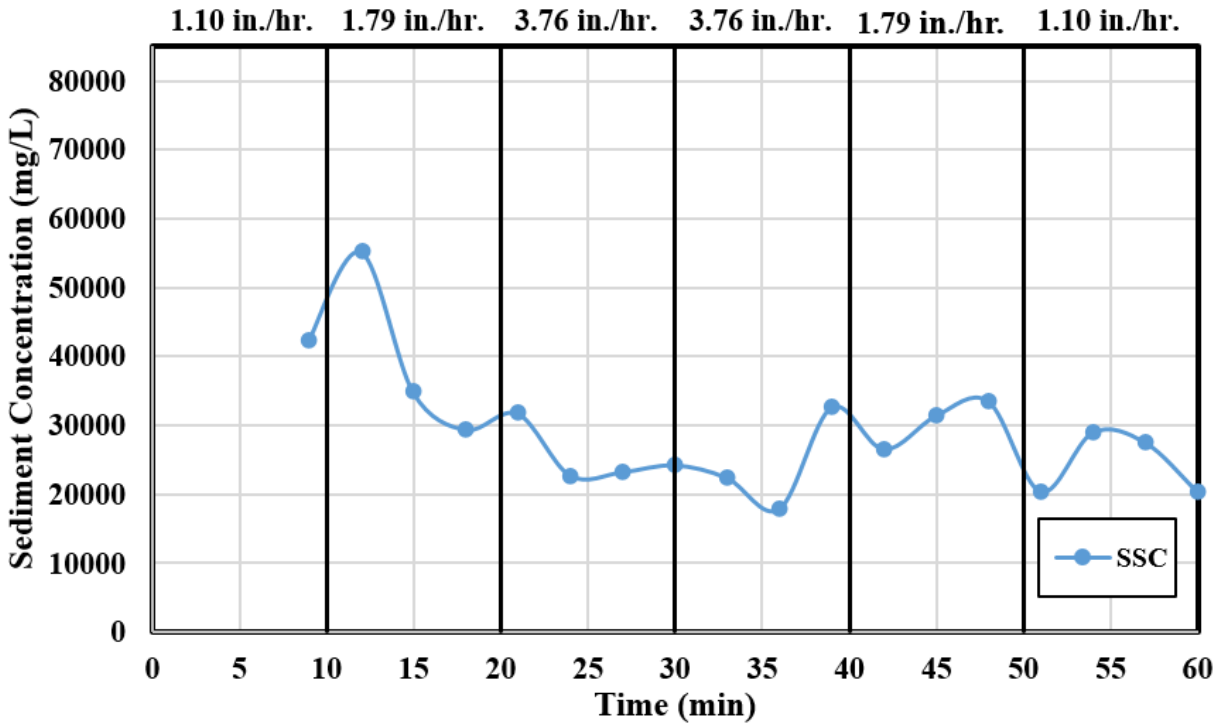

Figure 5.5 SSC vs. Time for Control Test 1.

From Figure 5.5, it can be seen that there was an initially high concentration of suspended particles. In subsequent tests, a concerted effort was made to ensure that the flume was clean of all soil particles before the start of a test. The flume is shown in Figure 5.6. If the results showed a decreased SSC value at the start of the test, it would be inferred that the greater concentrations at the start of Test 1 were caused by soil on the flume.

Figure 5.6 Flume for Channeling Runoff.

Between control tests 1 and 2, improvements were made to the flume so that runoff would not impound and run backwards on the flume. An 8 ft by 1 in. strip of plywood was inserted underneath the flume on the side nearest the plot border in order to slope the flume away from the test plot. Furthermore, a barrel was inserted in the catchment basin to detain all runoff from the flume. The sediment that settled on the flume and in the barrel was then weighed to determine the bulk mass of material eroded from the test plot during the test. The slope conditions and rainfall data for the second control test are presented in Table 5.16. Pictures depicting slope erosion over the course of the test are provided in Figure 5.7.

Table 5.16 Slope Conditions and Rainfall Data for Control Test 2

Moisture Content (%)	Percent Compacted (%)	Average Rainfall Intensity (in./hr)	Coefficient of Uniformity (%)	Dry Weight of Eroded Soil (lb)
22.05	83.35	2.21	80.14	88.2

(a) slope conditions before test

(b) slope erosion after interval 1

(c) slope erosion after interval 2

(d) slope erosion after interval 3

(e) slope erosion after interval 4

(f) slope erosion after interval 5

(g) slope erosion after interval 6

Figure 5.7 Slope Erosion for Control Test 2.

Once again, significant rill erosion did not begin to occur on the test plot until test interval 3. However, the higher moisture content in the soil caused runoff to occur much earlier, approximately 3 minutes into the test. Improvement was seen in the performance of the flume. Throughout the test, runoff consistently flowed over the flume towards the discharge point instead of impounding and flowing backwards. Hand tamping the soil along the edges of the test plot seemed to have minimal effect on the erosion in those areas. As in test 1, grab samples were collected in 3 minute intervals. These results of the SSC analysis conducted on those samples is tabulated in Table 5.17 and provided graphically in Figure 5.8.

Table 5.17 SSC from Control Test 2

Time (min)	SSC (mg/L)
0	--
3	27780
6	22983
9	19854
12	25028
15	23107
18	22243
21	37788
24	31470
27	30222
30	36449
33	57684
36	41334
39	41887
42	38846
45	37386
48	41869
51	27848
54	31306
57	34435
60	33072

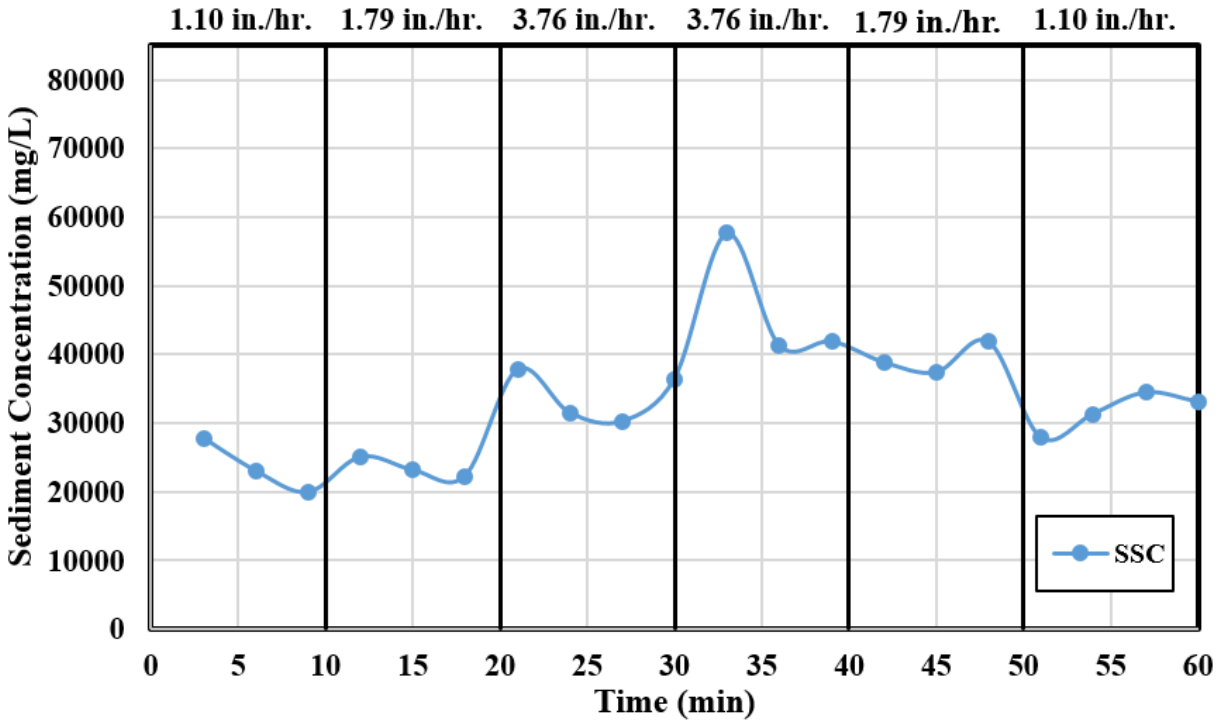

Figure 5.8 SSC vs. Time for Control Test 2.

From Figure 5.8, it can be seen that the initial concentration of sediment was much lower for this test. This provides evidence that soil on the flume at the beginning of the first test may have skewed the results for SSC. Furthermore, the greatest concentrations of SSC correspond with the intervals of greatest rainfall intensity. As stated earlier, significant rill erosion was not witnessed until test interval 3. The concentrations from test interval 3 onwards are higher than those at the beginning of the test, peaking at the 33 minute mark in interval 4 with 57,684 mg/L.

Between control tests 2 and 3, improvements were made to the flashing on the flume to prevent runoff from exiting through the sides of the flume. Small strips of flashing were attached to the lawn edging at the toe of the slope and connected to the flume to direct runoff exclusively onto the flume and into the detainment barrel. Once again, the sides of the test plot were hand tamped to provide better compaction where the turf roller did not have adequate surface contact. Information about the slope conditions and rainfall data for the test are presented in Table 5.18. Photos depicting erosion on the slope throughout the test are provided in Figure 5.9.

Table 5.18 Slope Conditions and Rainfall Data for Control Test 3

Moisture Content (%)	Percent Compacted (%)	Average Rainfall Intensity (in./hr)	Coefficient of Uniformity (%)	Dry Weight of Eroded Soil (lb)
19.38	83.94	2.43	80.58	121.4

(a) slope conditions before test

(b) slope erosion after interval 1

(c) slope erosion after interval 2

(d) slope erosion after interval 3

(e) slope erosion after interval 4

(f) slope erosion after interval 5

(g) slope erosion after interval 6

Figure 5.9 Slope Erosion for Control Test 3.

Once again, significant rill erosion did not begin to occur on the test plot until test interval 3. In this test, runoff did not begin until 10 minutes into the test. The additional flashing on the flume was effective in channeling runoff exclusively onto the flume and preventing runoff on the sides of the entrance. Hand tamping the soil along the edges of the test plot seemed to have minimal effect on the erosion in those areas. Overall, the formation of the rills through the test mimicked that of natural rill erosion. As in previous tests, grab samples were collected in 3 minute intervals. These results of the SSC analysis conducted on those samples is tabulated in Table 5.19 and provided graphically in Figure 5.10.

Table 5.19 SSC from Control Test 3

Time (min)	SSC (mg/L)
0	--
3	--
6	--
9	--
10	14116
12	44532
15	32470
18	24589
21	40134
24	46760
27	56070
30	55630
33	49948
36	71915
39	65459
42	82203
45	58289
48	55036
51	42793
54	48351
57	56261
60	48255

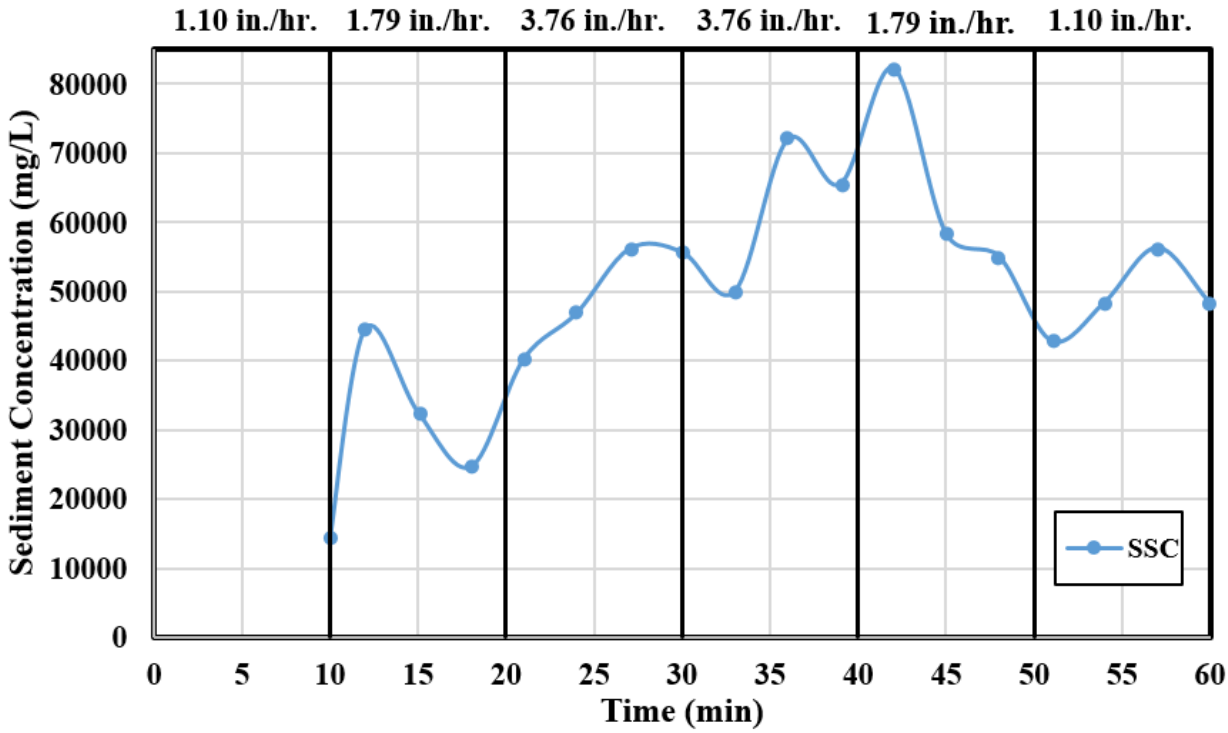

Figure 5.10 SSC vs. Time for Control Test 3.

From Figure 5.10, it can be seen that the concentration of sediment was much higher for this test. This provides evidence that the higher rainfall intensity resulted in greater erosion rates on the slope. The greatest concentrations of SSC correspond with the intervals of greatest rainfall intensity. As stated earlier, significant rill erosion was not witnessed until test interval 3. The concentrations from test interval 3 onwards are higher than those at the beginning of the test, peaking at the 42 minute mark in interval 4 with 82,203 mg/L.

5.4 SUMMARY

Data collected from calibration and validation testing was used to determine the optimal location for the sprinkler risers, which nozzles best replicated the target intensities from a 2-yr, 24 hr storm, and the erosive capabilities of the rainfall simulator. Data collected included: (1) rainfall depth, (2) flour pellet sizes, (3) SSC vs. time, and (4) total weight of eroded soil per test. T-tests were conducted on the values for average rainfall intensity and uniformity of rainfall distribution

to determine if there was a statistically significant difference between the experimental and theoretical values.

A total of fifty-eight, 15 minute calibration tests were performed to determine the experimental values for rainfall intensity and uniformity. The target intensities were 0.98, 1.70, and 3.45 in./hr. The corresponding experimental rainfall intensities were 1.10, 1.78, and 3.76 in./hr, respectively. After conducting a t-test analysis on each data set, it was determined that there was a statistically significant difference between each experimental rainfall intensity and its theoretical target.

Control testing was conducted to validate the performance of the rainfall simulator. Grab samples were collected at the flume in 3 minute intervals and analyzed for SSC. Eroded soil collected on the flume and in the catchment basin was weighed to calculate the total weight of eroded material for the test. Figure 5.11 provides a comparison of the SSC values versus time for each test.

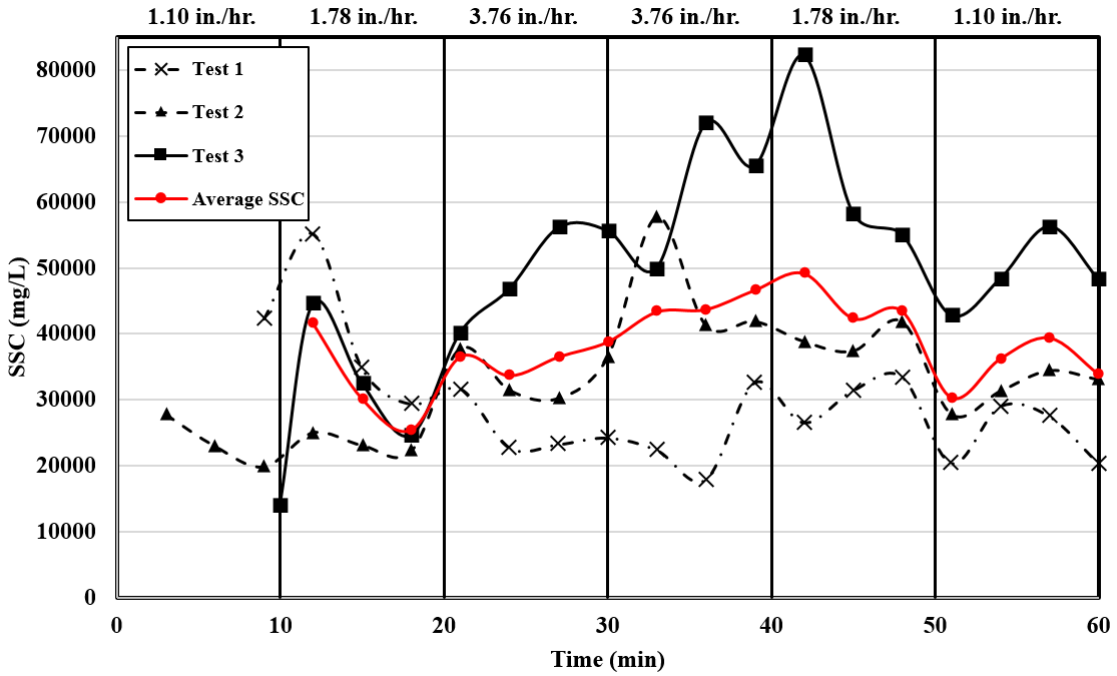

Figure 5.11 Summary of SSC vs. Time.

Overall, it was observed that the sediment concentrations from Figure 5.11 were not consistent. However, the sediment concentrations for the last two tests follow the same trend of increasing once significant erosion began in test interval 3. Increases in sediment concentration for tests 2 and 3 follow improvements to the flume preceding each test. For the three tests, the slope conditions (i.e. compaction and moisture content) were fairly consistent. On the other hand, each test saw an increase in average rainfall intensity. The average rainfall intensities for tests 1, 2, and 3 were 2.09, 2.21, and 2.43 in./hr, respectively. The increase in rainfall intensity corresponds to an increase in SSC over the duration of the test. Upon analyzing the results of the three control tests, further improvements should be made to flume and further testing should be done to improve the consistency of the SSC values.

CHAPTER SIX:
CONCLUSIONS

6.1 INTRODUCTION

The purpose of this research study was to design and construct a large-scale rainfall simulator capable of repeatedly simulating rainfall with characteristics similar to natural rainfall. Experiments followed procedures specified in ASTM D6459 (ASTM 2015) to calibrate the simulator to ensure that the apparatus was producing rainfall intensities and rainfall distribution similar to natural rainfall. The simulator apparatus was then validated through control tests performed on bare soil plots.

The first aspect of this research was to design and construct a test plot on a 3H:1V slope for conducting performance based testing of erosion control practices. This process included the construction of a retaining wall and catchment basin as well as backfilling the existing slope to increase the slope to 3:1. A rainfall simulator and electrical control system were then constructed around the test plot. Plot preparation protocols were developed to ensure consistent, repeatable conditions for preparing the test plot between test (i.e. plot preparation, soil type, compaction, moisture content). Finally, testing protocols were developed to calibrate and validate the rainfall simulator. Calibration testing was conducted to ensure that the system satisfied all criteria to produce uniform raindrop coverage that mimics natural rainfall. Validation testing was conducted to evaluate the performance and repeatability of the rainfall simulator through bare soil control tests. The repeatability of the system was quantified by collecting grab samples and detaining

runoff to calculate suspended sediment concentration (SSC) and bulk erosion from the test plot, respectively.

6.2 CONSTRUCTION OF LARGE-SCALE RAINFALL SIMULATOR

The rainfall simulator used in this study was constructed at the Auburn University Erosion and Sediment Control Test Facility (AU-ESCTF). Experiments were conducted on a 40 ft (12 m) long, 8 ft (2.4 m) wide test plot on a 3:1 slope, as specified by ASTM D6459. Sandy soil from a stockpile on site was used to initially fill the slope. Additional soil was added to the plot as needed between tests.

Rainfall was generated using a newly constructed large-scale rainfall simulator. The design for the rainfall simulator was largely based on existing designs in ASTM D6459. However, several changes were made due to the lack of specified products available for purchase and a desire to improve upon the existing design. Changes include: (1) substituting the VeeJet nozzles for Nelson Irrigation PC-S3000 sprinkler heads, (2) increasing the height of the sprinkler risers from 10 ft (3 m) to 14 ft (4.3 m), and (3) substituting ball valves for solenoid valves. VeeJet nozzles have historically been used for rainfall simulators following the ASTM D6459 design. However, these nozzles are no longer in production. In this study, research was done to identify a suitable replacement. In this case, Nelson Irrigation PC-SC3000 sprinkler heads were selected for several reasons: (1) pressure regulators can be installed underneath each sprinkler head to maintain constant pressure, (2) interchangeable nozzles allow the researchers to select which flow rates, and thereby which intensities should be produced, (3) deflector pieces in the sprinkler head channel the rainfall into a 190° arc instead of a 360° circle, and (4) spinner plates that break apart the flow in the sprinkler head to generate rain like drops. The height of the risers was increased to compensate for the substitution of VeeJet nozzles for Nelson Irrigation sprinkler heads. The

nozzles spray 4 ft (1.2 m) into the air whereas the sprinkler heads spray directly out and downwards. It is for this reason that the height of the risers was increased to 14 ft (4.3 m) to satisfy ASTM D6459 specifications. Ball valves in the original design were substituted for solenoid valves to allow for instantaneous changes in rainfall intensity. This addition required the installation of electrical wiring and conduit surrounding the test plot. The electrical wires were routed to a control box at the top of the slope which connected the multitude of wires to a series of four switches which allowed for individual operation of the solenoid valves. The electrical system was powered by two, 12V batteries wired in parallel and connected to the control box using alligator clips.

6.3 CALIBRATION AND VALIDATION PROCEDURES

Theoretical target rainfall intensities for this study were selected to estimate the peak 60 minutes of a 2-yr, 24 hr storm event in Auburn, AL. Fifty-eight, 15-minute calibration experiments were conducted to determine the average experimental rainfall intensities and uniformities, drop size distribution, and erosive energy produced by the rainfall simulator. The experimental values were then compared with their corresponding theoretical targets to determine if the apparatus was adequately simulating natural rainfall. The theoretical target rainfall intensities for this study were 0.98, 1.70, and 3.45 in./hr. The average experimental rainfall intensities produced by the rainfall simulator were found to be 1.10, 1.79, and 3.76 in./hr, respectively. The uniformity of the rainfall distribution, quantified using Christiansen's coefficient of uniformity, was calculated to be 79 to 81%. The average drop size for the intensities of 1.10, 1.79, and 3.76 in./hr where calculated to be 2.06, 2.01, and 2.35 mm, respectively.

Bare soil control testing was conducted to validate the performance of the rainfall simulator. A flume was installed over the catchment basin to allow researchers to collect grab

samples for SSC analysis during testing. Furthermore, eroded soil was collected and weighed at the end of each test to determine the weight of the soil. Overall, the results of the SSC analysis conducted for each test showed no consistency from test to test. However, the results from tests 2 and 3 followed the same trend, where concentrations increased once significant erosion began during test interval 3. Increases in SSC corresponded to increases in average rainfall intensity for each test. Due to the inconsistency of the SSC values for the first three tests, further control testing should be conducted and further improvements should be made to the flume.

6.4 RECOMMENDED FUTURE RESEARCH

Results presented in this study show that the rainfall simulator constructed for this research is capable of consistently simulating rainfall with characteristics similar to that of natural rainfall. However, the construction and installation of additional sprinkler risers may provide significant benefits to the performance of the apparatus. The addition of two sprinkler risers would decrease the spacing of the existing risers and provide eight more sprinkler heads. This could result in an increase in the uniformity of rainfall distribution on the test plot. Furthermore, if additional risers are installed, calibration testing should be reinitiated to determine if nozzle configurations capable of more accurately reaching the theoretical target intensities and increasing the uniformity of rainfall distribution exist.

Further research should be conducted to determine if it would be beneficial to switch from 10 psi (69 kPa) pressure regulators to 5 psi (34.5 kPa) and install larger nozzle sizes to compensate for the loss in pressure. The combination of larger nozzle openings and lower pressures could result in the creation of larger rain drops that more closely match the sizes of natural raindrops. Calibration experiments should be conducted to determine which nozzle sizes most accurately simulate rainfall intensities of 2, 4, and 6 in./hr. These rainfall intensities correspond with the

values specified by ASTM D6459. Installation of these nozzles would allow testing to be conducted at the AU-ESCTF that is comparable to other National Transportation Product Evaluation Program (NTPEP) certified laboratories around the country.

Finally, upon analysis of the data for SSC collected during the validation process, it is recommended that further testing be conducted to determine if greater consistency can be achieved in the experimental results from test to test before moving to testing of erosion control practices. Additional improvements to the flume may aid in this endeavor. Currently, large amounts of sediment are deposited on the flat, plywood surface of the flume in the middle of the test where rainfall intensities reach 3.76 in./hr. It is possible that some of this sediment is re-suspended by runoff on the flume and artificially increasing the SSC values at later points during testing. Increasing the amount of flashing on the flume as well as the slope of the flume may aid in preventing soil from depositing on the flume during testing and help provide more consistency in experimental results from test to test.

REFERENCES

ASTM (1997). "Standard Test Methods for Determining Sediment Concentration in Water Samples."West Conshohocken, PA, 1-7.

ASTM (2008). "Standard Test Method for Determination of Water (Moisture) Content of Soil by Microwave Oven Heating."West Conshohocken, PA, 1-7.

ASTM (2010). "Standard Test Method for Density of Soil in Place by the Drive-Cylinder Method."West Conshohocken, PA, 1-7.

ASTM (2015). "Standard Test Method for Determination of Rolled Erosion Control Product (RECP) Performance in Protecting Hillslopes from Rainfall-Induced Erosion."West Conshohocken, PA, 1-10.

Barnett, A. P., and Dooley, A. E. (1972). "Erosion Potential of Natural and Simulated Rainfall Compared." *Transactions of the ASABE*, 15(6), 1112-1114.

Benik, S. R., Wilson, B. N., Biesboer, D. D., Hansen, B., and Stenlund, D. (2003). "Performance of Erosion Control Prodcuts on a Highway Embankment." *Transactions of the ASABE*, 46(4), 1113-1119.

Birt, L. N., Persyn, R. A., and Smith, P. K. (2007). "Technical Note: Evaluation of an Indoor Nozzle-Type Rainfall Simulator." *Applied Engineering in Agriculture*, 23(3), 283-287.

Blanquies, J., Scharff, M., and Hallock, B. (2003). "The Design and Consruction of a Rainfall Simulator."

Brady, N. C., and Weil, R. R. (1999). *The Nature and Properties of Soils*, Prentice Hall, Upper Saddle River, New Jersey.

Bubenzer, G. D., and Jones Jr., B. A. (1971). "Drop Size and Impact Velocity Effects on the Detachment of Soils Under Simulated Rainfall." *Transactions of the ASABE*, 14(4), 625-628.

Bubenzer, G. D., and Meyer, L. D. (1965). "Simulation of Rainfall and Soils for Laboratory Research." *Transactions of the ASABE*, 8(1), 73.

Bubenzer, G. D., Myron, M., and McCool, D. K. (1985). "Low Intensity Rainfall with a Rotating Disk Simulator." *Transactions of the ASABE*, 28(4), 1230-1232.

Cabalka, D. A., Clopper, P. E., Johnson, A. G., and Vielleux, M. T. (1998). "Research, Development, and Implementation of Test Protocols for Rainfall Erosion Facilities (REFS)."

Christiansen, J. P. (1942). "Irrigation by Sprinkling " *University of California Agricultural Experiment Station, Bulletin No. 670*, 124.

Clark, S. E., and Pitt, R. (1999). "Stormwater Treatment at Critical Areas - Evaluation of Filtration Media." EPA/600/R-00/010, Birmingham, AL.

Congress, U. S. (2015). "H.R.2353 Highway and Transportation Funding Act of 2015."Washington D.C.

Crowe, C. T. D., F. E.; Roberson, J. A. (2005). *Engineering Fluid Mechanics*, John Wiley and Sons, Inc., Hoboken, NJ.

Cullum, R. F. (1997). "Electronic Controls for Rainfall Simulators." *Transactions of the ASAE*, 40(3), 643-648.

ECTC (2014). "Rolled Erosion Control Products (RECPs) General Usage and Installation Guidelines for Slope." <http://www.ectc.org/assets/docs/ectc_march2014_recp%20slope%20usage%20install%20guidelines%20final.pdf>. (July 21, 2016).

Eigel, J. D., and Moore, I. D. (1983). "A Simplified Technique for Measuring Raindrop Size and Distribution." *Transactions of the ASABE*, 26(4), 1079-1084.

Ekern, P. C. (1950). "Raindrop Impact as the Force Initiating Soil Erosion." University of Wisconsin.

Elbasit, M. A. M. A., C. S. P. Ojha, M. A., Yasuda, Z. A. H., Salmi, A., and Ahmed, F. (2015). "Rain Microstructure and Erosivity Relationships under Pressurized Rainfall Simulator." *Journal of Hydrologic Engineering*, 20(6), C6015001: 6015001-6015006.

Engineering, V. (2012). "Head Loss Coefficients." <https://vanoengineering.wordpress.com/2012/12/30/head-loss-coefficients/>. (November 4, 2016).

Epstein, E., and Grant, W. J. (1966). "Design, Construction, and Calibration of a Laboratory Rainfall Simulator." *Maine Agricultural Experiment Station Technical Bulletin 22*.

Foltz, R. B., and Dooley, J. H. (2003). "Comparison of Erosion Reduction Between Wood Strands and Agricultural Straw." *Transactions of the ASABE*, 46(5), 1389-1396.

Foster, G. R., Neibling, W. H., and Nattermann, R. A. (1982). "A Programmable Rainfall Simulator." *ASAE Winter Meeting*St. Joseph, Michigan.

Guo, Q. (2006). "Correlation of Total Suspended Solids (TSS) and Suspended Sediment Concentration (SSC) Test Methods." Rutgers, New Brunswick, NJ, 1-52.

Hall, M. J. (1970). "Use of the Stain Method in Determining the Drop-Size Distributions of Coarse Liquid Sprays." *Transactions of the ASABE*, 13(1), 33-37.

Hall, N. (2015). "Terminal Velocity." <https://www.grc.nasa.gov/www/k-12/airplane/termv.html>. (August 3, 2015).

Hershfield, D. M. (1961). "Technical Paper No. 40: Rainfall Frequency Atlas of the United States for Durations from 30 Minutes to 24 Hours and Return Periods from 1 to 100 Years.", USDA, Washington D.C., 1-65.

Hirschi, M. C., Mitchell, J. K., Feezor, D. R., and Lesikar, B. J. (1990). "Microcomputer-Controlled Laboratory Rainfall Simulator." 33(6).

Hudson, N. W. (1993). *Field Measurement of Soil Erosion and Runoff*, Food and Agriculture Organization of the United Nations, Rome, Italy.

Humphry, J. B., Daniel, T. C., Edwards, D. R., and Sharpley, A. N. (2002). "A Portable Rainfall Simulator for Plot–Scale Runoff Studies." *Applied Engineering in Agriculture*, 18(2), 199-204.

Kim, K. S., Choi, J. D., and Kweon, K. S. (2001). "Effect of PAM Application on Soil Erosion of a Sloping Field with a Chinese Cabbage Crop." *2001 ASAE Annual Meeting*, ASABE, St. Joseph, Mich.

King, B. A., and Bjorneberg, D. L. (2011). "Evaluation of Potential Runoff and Erosion of Four Center Pivot Irrigation Sprinklers." *Applied Engineering in Agriculture*, 27(1), 75-85.

Kinkade-Levario, H. (2006). "Rainwater Harvesting, Low Impact Development Strategies, and Meeting the National Pollution Discharge Elimination System (NPDES) Stormwater Discharge Standards." *World Environmental and Water Resource Congress 2006*, 1-8.

Laws, J. O. (1941). "Measurements of the Fall-Velocity of Waterdrops and Raindrops." *Transactions of the American Geophysical Union*, 22, 709-721.

Laws, J. O., and Parsons, D. A. (1943). "The Relation of Raindrop-Size to Intensity." *Transactions of the American Geophysical Union*, 24, 452-460.

McCool, D. K. (1982). "Personal Communication." USDA-ARS, ed., Agricultural Engineering Department, Washington State University, Pullman.

McLaughlin, R. A., and Brown, T. T. (2006). "Evaluation of Erosion Control Products With and Without Added Polyacrylamide." *Journal of the American Water Resources Association*, 42(3), 675-684.

McLaughlin, R. A., Rajbhandari, N., Hunt, W. F., Line, D. E., Sheffield, R. E., and M., W. N. (2001). "The Sediment and Erosion Control Research and Education Facility at North Carolina State University." *Soil Erosion Research for the 21st Century, Proc. Int. Symp.*Honolulu, HI.

Meyer, L. D. (1965). "Simulation of Rainfall for Soil Erosion Research." *Transactions of the ASABE*, 8(1), 63-65.

Miller, W. P. (1987). "A Solenoid-Operated, Variable Intensity Rainfall Simulator." *Soil Science Society of America Journal*, 51(3), 832-834.

Ming-Han, L., Harlow, C. L., and Jett, M. (2003). "Comparison of Field and Laboratory Experiment Test Results for Erosion Control Products." *ASAE Annual International Meeting*, ASABE, St. Joseph, Mich.

Moore, I. D., Hirschi, M. C., and Barfield, B. J. (1983). "Kentucky Rainfall Simulator." *Transactions of the ASABE*, 26(4), 1085-1089.

Mutchler, C. K., and Hermsmeier, L. F. (1965). "A Review of Rainfall Simulators." *Transactions of the ASABE*, 8(1), 67-68.

NOAA (2014). "NOAA Atlas 14 Point Precipitation Frequency Estimates: AL." <http://hdsc.nws.noaa.gov/hdsc/pfds/pfds_map_cont.html?bkmrk=al>. (July 31, 2015).

Novotny, V. (2003). *Water Quality: Diffuse Pollution and Watershed Management*, J. Wiley, Hoboken, New Jersey.

NRCS (1986). "Technical Release 55 - Urban Hydrology for Small Watersheds." United States Department of Agriculture.

Ott, R. L., and Longnecker, M. (2010). *An Introduction to Statistical Methods and Data Analysis*, Brooks/Cole, Belmont, CA.

Paige, G. B., Stone, J. J., Smith, J. R., and Kennedy, J. R. (2003). "The Walnut Gulch Rainfall Simulator: A Computer-Controlled Variable Intensity Rainfall Simulator." *Transactions of the ASAE*, 20(1).

Perez, M. A. (2014). "Evaluation of Inlet Protection Practices (IPPs) Using Large-Scale Testing Techniques." Master of Science, Auburn University.

Perez, M. A., Zech, W. C., Donald, W. N., and Fang, X. (2015). "Design Methodology for the Selection of Temporary Erosion and Sediment Control Practices based on Regional Hydrological Conditions." Auburn University.

Regmi, T. P., and Thompson, A. L. (2000). "Rainfall Simulator for Laboratory Studies." *Applied Engineering in Agriculture*, 16(6), 641-647.

Riverkeeper, B. W. (2013). "Sedimentation from development in Birmingham makes its way into Bayview Lake of Village Creek of the Black Warrior." <http://blackwarriorriver.org/siltation-sedimentation/>. (December, 15, 2015).

Robeson, M. D. (2014). "Unification of Large-Scale Laboratory Rainfall Erosion Testing." Doctor of Philosophy, Colorado State University, Fort Collins.

Sharpley, A. N., and Kleinman, P. (2003). "Effect of Rainfall Simulator and Plot Scale on Overland Flow and Phosphorus Transport." *Journal of Environmental Quality*, 32, 2172-2179.

Shelton, C. H., Bernuth, R. D. v., and Rajbhandari, S. P. (1985). "A Continuous-Application Rainfall Simulator." *Transactions of the ASABE*, 28(4).

Shoemaker, A. L. (2009). "Evaluation of Anionic Polyacrylamide as an Erosion Control Measure Using Intermediate-Scale Experimental Procedures." Master of Science, Auburn University, Auburn, AL.

Shoemaker, A. L., Zech, W. C., and Clement, T. P. (2012). "Laboratory-Scale Evaluation of Anionic Polyacrylamide as an Erosion and Sediment Control Measure on Steep-Sloped Construction Sites." *Transactions of the ASABE*, 55(3), 809-820.

Swanson, N. P. (1965). "Rotating-Boom Rainfall Simulator." *Transactions of the ASABE*, 8(1), 71-72.

Thomas, N. P., and El Swaify, S. A. (1989). "Construction and Calibration of a Rainfall Simulator." *Journal of Agriculture and Engineering Research*, 43(1), 1-9.

USEPA (2005). "Stormwater Phase II Final Rule." United States Environmental Protection Agency.

USEPA (2012). "National Pollutant Discharge Elimination System General Permit for Discharges from Construction Activities." Office of Water, Washington, D.C.

USEPA (2014). "Water: Permitting (NPDES)." <http://water.epa.gov/polwaste/npdes/>. (July 20, 2015).

Wischmeier, W. H., and Smith, D. D. (1958). "Rainfall Energy and its Relationship to Soil Loss." *Transactions of the American Geophysical Union*, 39(2), 285-291.

Xiao, M., Reddi, L. N., and Howard, J. (2010). "Erosion Control on Roadside Embankment Using Compost." *Applied Engineering in Agriculture*, 26(1), 97-106.

APPENDICES

Appendix A: Manufacturer's Specifications for Rainfall Simulator Components

Appendix B: SSC Processing Procedures

Appendix C: Experimental Data

Appendix D: Rolled Erosion Control Product Installation Procedures

APPENDIX A

MANUFACTURER'S SPECIFICATIONS FOR RAINFALL SIMULATOR COMPONENTS

PART CIRCLE SPRINKLERS

FULL LINE FOR INTEGRATION INTO ALL SPRINKLER PACKAGE TYPES UTILIZING THE 3TN "ONE" NOZZLE SYSTEM

Part Circle Rotator

Black #10843-001
(#40-#50 3TN Nozzle)
Tan #10843-003
(#24-#39 3TN Nozzle)
White # 10843-002
(#14-#23 3TN Nozzle)

Important: Mount only on a straight rigid drop or a Hose Boom utilizing a Torque Clip and Sideforce Control Fitting such as the IACO HB.

Part Circle Spinner #9926-001

Part Circle Sprayhead #9894-001

Note: Part numbers do not include 3TN Nozzle and Square Thread Adapter.

NELSON
SAVE WATER, SAVE ENERGY AND DO A BETTER JOB OF IRRIGATING

PART CIRCLE SPRINKLERS FOR MECHANIZED IRRIGATION

PART CIRCLE FOR DRY WHEEL PACKAGES

The PC-R3000 with rotating streams provides the widest throw available and better overlap! **Part Circle Rotators can now be used on "boombacks" with IACO's Hose Boom!**

PART CIRCLE FOR END OF SYSTEM COVERAGE

Gain added end of system acreage at low pressure.

Complement traditional end gun packages to fill the pattern going in and out of corners.

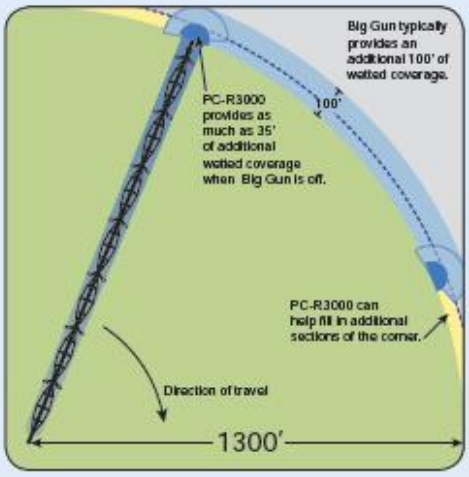

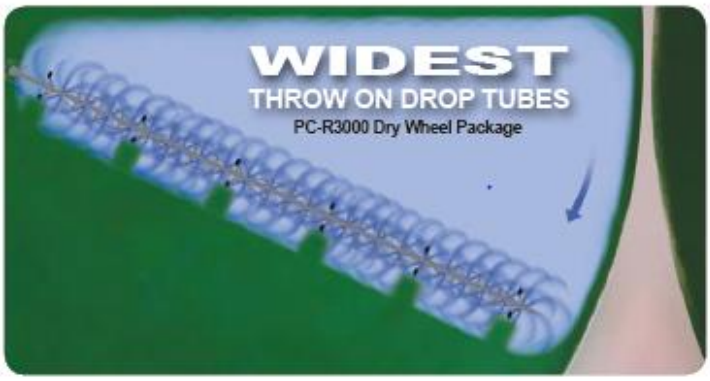

DISTINCT ADVANTAGES OF A ROTATOR PACKAGE

Engineered Speed Control – The Right Balance of Rotating Streams. Designed specifically for providing the very best water application on center pivots, the controlled rotation of engineered streams provides superior throw, superior uniformity and the best available conditions for getting the water into the ground.

Greatest Throw on Drops. The Rotator® applies water further ahead of the machine than any other pivot sprinkler and wets the field with intermittent applications of target droplets for optimal soil infiltration conditions.

Years of Field Results & Scientific Research Show the Pivot Rotator Gets Water Into the Ground. The wide throw delivers the lowest Average Application Rates on drop tubes — and testing shows that the Pivot Rotator is the best in class at minimizing runoff and soil erosion.

PC-R3000 — PART CIRCLE ROTATOR®

The PC-R3000 is available with 3 different plate options - choose based on nozzle size (see chart on lower right). The Part Circle Rotator distributes water to one side in an approximate semicircle. It can be used to minimize application on pivot towers or other structures. The Part Circle Rotator utilizes the 3TN nozzle of the conventional R3000 Rotator.

PERFORMANCE:

- 180° Arc (varies slightly with flowrate)
- Wide Throw
- High Uniformity
- Wind Fighting Pattern

OPERATING SPECS:

- 15-30 PSI (1-2 BAR)
- #14-#50 3TN Nozzle
- Mount on a rigid drop assembly or IACO Hose Boom Assembly

Go to www.boombacks.com.

PERFORMANCE INFORMATION:

3TN Nozzle Size	Plate	Pressure Min - Max	Spacing Limit	Stream Height
#14 - #23	white	15 - 25 psi	11'	20-39"
#24 - #39	tan	15 - 25 psi	11'	10-18"
#40 - #50	black	15 - 30 psi	11'	29-41"

PC-S3000 — PART CIRCLE SPINNER

The Part Circle Spinner distributes water to one side in an approximate semicircle. It can be used to minimize application on pivot towers or other structures. The Part Circle Spinner utilizes the 3TN nozzle of the conventional S3000 Spinner. The directional control is provided by a 'stream deflector' which is inserted between the nozzle and the spinner body.

OPERATING SPECS:

- 10-20 PSI (.7-1.4 BAR)
- #14-#40 3TN Nozzle
- Mount on a rigid drop assembly

PERFORMANCE:

- 190° Arc (varies slightly with flowrate)
- Gentle, Rain-like Droplets
- High Uniformity
- Low Instantaneous Rates

THROW RADIUS:

(At midpoint of arc, throw to the sides may be less.)

- 15 PSI (1.0 BAR)
- #36 3TN Nozzle
- Stream Height = 13 in. (330 mm)

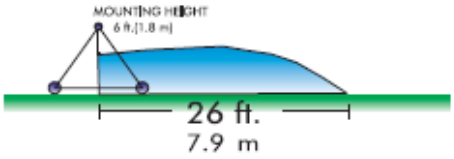

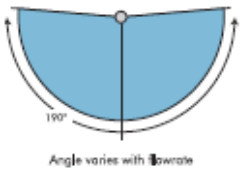

PC-D3000 — PART CIRCLE SPRAYHEAD

The Part Circle Sprayhead has a 170° arc setting to provide part-circle operation for applications at the span towers or offset drops or boombacks. The PC-D3000 spray plate provides stream definition similar to the spray plate geometry of the #9493 Blue spray plate. The medium grooves and concave trajectory provide wind-penetration and wide throw distance.

OPERATING SPECS:

- 10-20 PSI (.7-1.4 BAR)
- #9-#50 3TN Nozzle
- Mount on a rigid drop assembly

PERFORMANCE:

- 170° Arc (varies slightly with flowrate)
- Low Trajectory
- Concave Medium Groove Blue Spray Plate

THROW RADIUS:

(At midpoint of arc, throw to the sides may be less.)

- 10 PSI (.7 BAR)
- #36 3TN Nozzle
- Stream Height = 5 in. (127 mm)

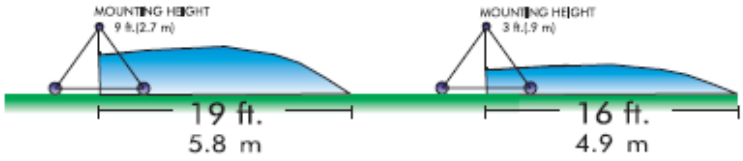

> DESIGNING WITH PART CIRCLE SPRINKLERS

STEP 1: Plan the system with conventional full circle sprinklers.
For Linears/Laterals select sprinkler spacing and determine the nozzle size to deliver your desired application rate. For pivot systems, planning should include a Sprinkler Package Chart. Nelson part circle devices will fit best in packages with sprinkler spacing of 11 feet (3.3 m) or less. If the part circle devices are to be mounted on boombacks, maintain uniform spacing between all sprinklers. The IACO 15' Hose Boom is the only "boomback" style configuration recommended for the Part Circle Rotator (PC-R3000). If the devices will be mounted on conventional drops, a distance of 1 to 3 feet (.3 to 1m) between the wheel and the closest sprinkler on each side is optimal.

STEP 2: Determine which outlets need modified sprinklers.
Use the preliminary design to compare the distance to the tower with the radius for each sprinkler. If you are working from a Sprinkler Package Chart, adjust the listed Tower location for the wheel offset. An offset of 2 feet (.6m) is common. Coverage diameter information on other 3000 Series Sprinklers is available at www.nelsonproducts.info or by contacting Nelson Irrigation.

STEP 3: Plan the orientation angles for the Part Circle Sprinklers.
The semicircular pattern of the Part Circle Sprinklers adjacent to the towers should be oriented as close to perpendicular to the main pipe as possible. On boombacks, they should face directly away from the main pipe as shown in the diagram. On straight drops, they should be adjusted so the edge of the semicircle falls immediately behind the rear tower wheel. If possible, orient adjacent part circles at opposite directions from the pipe. This reduces the application rate.

Part Circle Sprinklers can be installed in a variety of configurations

BOOMBACKS

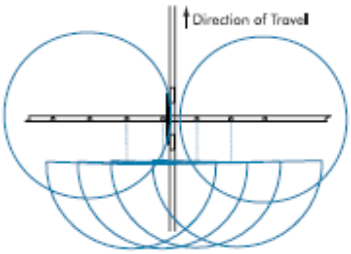

Installations on boombacks minimize the compromise in uniformity that occurs when part circle devices are utilized.

STRAIGHT DROPS

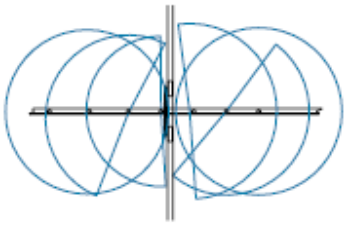

Installations on straight drops require careful adjustment of the orientation.

ADDITIONAL CAUTIONS:

It is important to mount Part Circle Sprinklers on rigid drops or Hose Booms. Side thrust will cause extreme movement of flexible drops. Part Circle Sprinklers cannot provide the whole solution to traction, rutting, or runoff problems. If you are trying to utilize mechanized irrigation systems on steep slopes or heavy soils you should carefully consider all aspects of system design and management that can contribute to reduced soil loading and application rate minimization. The distribution profile of the Part Circle Sprinklers provides good overlaps with conventional sprinklers in most configurations. However, it is likely that a system intended to minimize application at the tower will not achieve the high uniformity possible with a well designed conventional system. For best results keep the spacing within the limits described above. Part Circle Sprinklers can be used to minimize, but they will not totally eliminate, application on the towers or wheel tracks.

NELSON
Nelson Irrigation Corporation
848 Airport Rd., Walla Walla, WA 99362 USA
Tel: 509.525.7660 Fax: 509.525.7907 info@nelsonirrigation.com
Nelson Irrigation Corporation of Australia Pty. Ltd.
35 Sudbury Street, Darra QLD 4074 info@nelsonirrigation.com.au
Tel: +61 7 3715 8555 Fax: +61 7 3715 8666
WWW.NELSONIRRIGATION.COM

NELSON

3000 & 3030 Series Pivot Products

3TN & 3NV NOZZLE CHART

14 | 15 | 16 | 17 | 18 | 19

The nozzle sizing system is based on 128th inch increments, e.g. 3TN/3NV Nozzle #26 has an orifice diameter of 26/128th inches while 3TN/3NV Nozzle #27 has an orifice diameter of 27/128th inches. For 3TN Nozzles, the odd-numbered nozzles have a color box around the number marking. This color box denotes the color of the next larger nozzle size. The odd-numbered 3NV Nozzles have a scalloped edge rather than secondary coloring.

3TN COLOR-CODED SYSTEM.
Odd numbers have color box around #.

3NV COLOR-CODED SYSTEM.
Odd numbers have scalloped edge.

NOZZLE #		#9		#10		#11		#12		#13		#14		#15		#16		#17		#18		#19	
Color		Light Blue		Beige		Beige		Gold		Gold		Lime		Lime		Lavender		Lavender		Gray		Gray	
Stripe		Beige				Gold				Lime				Lavender				Gray				Turquoise	
PSI	BAR	GPM	LPM	GPM	LPM	GPM	LPM	GPM	LPM	GPM	LPM	GPM	LPM	GPM	LPM	GPM	LPM	GPM	LPM	GPM	LPM	GPM	LPM
5	0.4	0.34	1.28	0.42	1.59	0.50	1.89	0.61	2.30	0.71	2.68	0.82	3.10	0.95	3.59	1.08	4.08	1.22	4.61	1.36	5.14	1.53	5.79
10	0.7	0.44	1.66	0.54	2.04	0.65	2.46	0.79	2.99	0.92	3.48	1.06	4.01	1.23	4.65	1.40	5.29	1.58	5.98	1.75	6.62	1.97	7.45
15	1.0	0.53	2.00	0.66	2.50	0.79	2.99	0.96	3.63	1.13	4.27	1.29	4.88	1.51	5.71	1.71	6.47	1.93	7.30	2.14	8.09	2.41	9.12
20	1.4	0.62	2.34	0.76	2.87	0.92	3.48	1.11	4.20	1.30	4.92	1.49	5.63	1.74	6.58	1.96	7.40	2.23	8.44	2.46	9.30	2.79	10.56
25	1.7	0.69	2.61	0.85	3.22	1.02	3.86	1.24	4.69	1.46	5.52	1.67	6.32	1.95	7.38	2.21	8.36	2.50	9.46	2.77	10.48	3.12	11.81
30	2.1	0.76	2.87	0.93	3.52	1.12	4.23	1.36	5.14	1.59	6.01	1.83	6.92	2.14	8.09	2.42	9.15	2.74	10.37	3.03	11.46	3.41	12.90
40	2.8	0.87	3.29	1.07	4.05	1.29	4.88	1.57	5.94	1.84	6.96	2.11	7.98	2.47	9.34	2.80	10.59	3.16	11.96	3.50	13.24	3.94	14.91
50	3.4	0.97	3.67	1.20	4.54	1.45	5.48	1.76	6.66	2.06	7.79	2.36	8.93	2.76	10.44	3.13	11.84	3.53	13.32	3.91	14.79	4.41	16.69

NOZZLE #		#20		#21		#22		#23		#24		#25		#26		#27		#28		#29		#30	
Color		Turquoise		Turquoise		Yellow		Yellow		Red		Red		White		White		Blue		Blue		Dark Brown	
Stripe				Yellow				Red				White				Blue				Dark Brown			
PSI	BAR	GPM	LPM	GPM	LPM	GPM	LPM	GPM	LPM	GPM	LPM	GPM	LPM	GPM	LPM	GPM	LPM	GPM	LPM	GPM	LPM	GPM	LPM
5	0.4	1.70	6.43	1.84	6.96	2.04	7.72	2.22	8.40	2.44	9.23	2.64	9.99	2.87	10.86	3.07	11.61	3.35	12.68	3.58	13.55	3.83	14.49
10	0.7	2.19	8.28	2.38	9.00	2.64	9.99	2.85	10.82	3.16	11.96	3.41	12.90	3.70	14.00	3.97	15.00	4.32	16.35	4.62	17.48	4.94	18.69
15	1.0	2.69	10.18	2.91	11.01	3.23	12.22	3.50	13.24	3.86	14.61	4.17	15.78	4.53	17.14	4.86	18.39	5.29	20.02	5.66	21.42	6.06	22.93
20	1.4	3.10	11.73	3.36	12.71	3.73	14.11	4.05	15.32	4.46	16.88	4.82	18.24	5.23	19.79	5.61	21.23	6.11	23.12	6.53	24.71	6.99	26.45
25	1.7	3.47	13.13	3.76	14.23	4.17	15.78	4.52	17.10	4.99	18.88	5.38	20.36	5.85	22.14	6.27	23.73	6.83	25.85	7.30	27.63	7.82	29.59
30	2.1	3.80	14.38	4.12	15.59	4.56	17.25	4.95	18.77	5.47	20.70	5.90	22.33	6.41	24.26	6.87	26.00	7.48	28.31	8.00	30.28	8.56	32.39
40	2.8	4.39	16.61	4.76	18.01	5.27	19.94	5.72	21.65	6.31	23.88	6.81	25.77	7.40	28.00	7.94	30.05	8.64	32.70	9.24	34.97	9.89	37.43
50	3.4	4.90	18.54	5.32	20.13	5.89	22.29	6.40	24.22	7.06	26.72	7.61	28.80	8.28	31.33	8.87	33.57	9.66	36.56	10.33	39.13	11.06	41.86

NOZZLE #		#31		#32		#33		#34		#35		#36		#37		#38		#39		#40		#30	
Color		Dark Brown		Orange		Orange		Dark Green		Dark Green		Purple		Purple		Black		Black		Dark		Dk. Turquoise	
Stripe		Orange				Dark Green				Purple				Black				Dk. Turquoise		Turquoise		Mustard	
PSI	BAR	GPM	LPM	GPM	LPM	GPM	LPM	GPM	LPM	GPM	LPM	GPM	LPM	GPM	LPM	GPM	LPM	GPM	LPM	GPM	LPM	GPM	LPM
5	0.4	4.06	15.36	4.36	16.50	4.65	17.60	4.94	18.69	5.20	19.68	5.47	20.67	5.84	22.10	6.18	23.39	6.52	24.68	6.85	25.92	7.26	27.48
10	0.7	5.24	19.83	5.63	21.50	6.00	22.71	6.37	24.11	6.72	25.43	7.06	26.72	7.54	28.54	7.97	30.16	8.42	31.87	8.85	33.49	9.37	35.47
15	1.0	6.41	24.26	6.89	26.07	7.35	29.71	7.81	29.56	8.23	31.15	8.65	32.74	9.24	34.97	9.77	36.98	10.31	39.02	10.84	41.02	11.48	43.45
20	1.4	7.40	28.00	7.96	30.12	8.49	32.13	9.01	34.10	9.50	35.95	9.98	37.77	10.67	40.38	11.28	42.69	11.91	45.08	12.51	47.35	13.26	50.19
25	1.7	8.28	31.34	8.90	33.68	9.49	35.91	10.08	38.15	10.62	40.19	11.16	42.24	11.92	45.11	12.61	47.72	13.31	50.38	13.99	52.95	14.82	56.09
30	2.1	9.07	34.32	9.75	36.90	10.39	39.32	11.04	41.78	11.64	44.05	12.23	46.29	13.06	49.43	13.81	52.27	14.58	55.19	15.33	58.02	16.23	61.43
40	2.8	10.47	39.62	11.26	42.62	12.00	45.42	12.75	48.25	13.44	50.87	14.12	53.44	15.08	57.07	15.95	60.37	16.84	63.74	17.70	66.99	18.75	70.97
50	3.4	11.71	44.32	12.59	47.65	13.42	50.79	14.25	53.93	15.02	56.85	15.79	59.76	16.86	63.81	17.83	67.48	18.81	71.20	19.79	74.90	20.96	79.33

NOZZLE #		#42		#43		#44		#45		#46		#47		#48		#49		#50	
Color		Mustard		Mustard		Maroon		Maroon		Cream		Cream		Dark Blue		Dark Blue		Copper	
Stripe				Maroon				Cream				Dark Blue				Copper			
PSI	BAR	GPM	LPM	GPM	LPM	GPM	LPM	GPM	LPM	GPM	LPM	GPM	LPM	GPM	LPM	GPM	LPM	GPM	LPM
5	0.4	7.60	28.76	7.96	30.13	8.33	31.52	8.73	33.04	9.12	34.51	9.58	36.25	9.96	37.69	10.31	39.02	10.77	40.76
10	0.7	9.81	37.13	10.28	38.91	10.75	40.68	11.27	42.66	11.77	44.54	12.36	46.78	12.86	48.67	13.31	50.38	13.91	52.64
15	1.0	12.01	45.45	12.59	47.65	13.17	49.84	13.80	52.23	14.41	54.54	15.14	57.30	15.75	59.61	16.30	61.70	17.03	64.45
20	1.4	13.87	52.49	14.54	55.03	15.20	57.53	15.93	60.30	16.64	62.98	17.49	66.20	18.19	68.84	18.82	71.23	19.67	74.45
25	1.7	15.51	58.70	16.25	61.51	17.00	64.34	17.81	67.41	18.61	70.43	19.55	74.00	20.33	76.94	21.05	79.67	21.99	83.23
30	2.1	16.99	64.30	17.80	67.37	18.62	70.47	19.51	73.85	20.38	77.13	21.42	81.07	22.28	84.32	23.05	87.24	24.09	91.18
40	2.8	19.61	74.22	20.55	77.82	21.50	81.37	22.53	85.28	23.54	89.09	24.73	93.60	25.72	97.35	26.62	100.76	27.82	105.29
50	3.4	21.93	83.00	22.98	86.96	24.04	90.99	25.19	95.34	26.31	99.58	27.65	104.66	28.76	108.85	29.76	112.64	31.10	117.71

This flow data was obtained under ideal test conditions and may be adversely affected by poor hydraulic entrance conditions, turbulence or other factors. Nelson Irrigation makes no representation regarding sprinkler flow rate accuracy under various plumbing and drop pipe conditions.

Tel: +1 509.525.7660 / Fax: +1 509.525.7907 / nelsonirrigation.com / info@nelsonirrigation.com

PRESREG-E 4/08

PRESSURE REGULATION

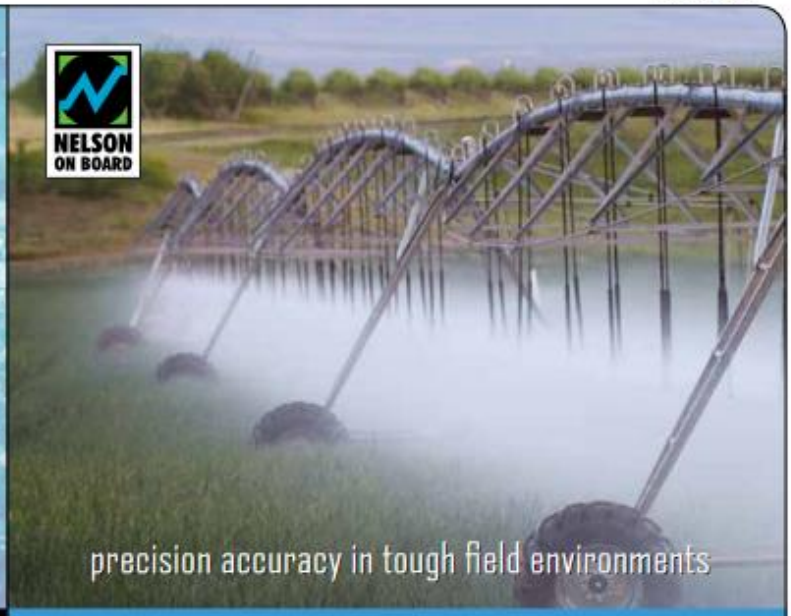

Cut-away of Pressure Regulator

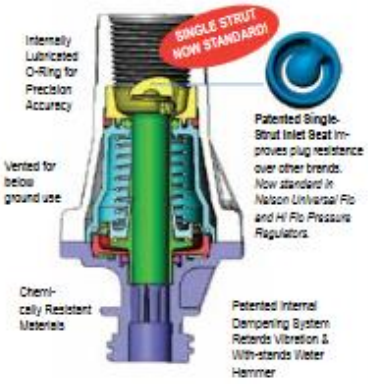

TECHNICAL TIPS FOR REGULATING SYSTEMS

IMPORTANT: Allow approximately 5 PSI (.35 BAR) extra pressure in order for the regulator to function properly. For example, the minimum design pressure for a 20 PSI (1.4 BAR) pressure regulator is 25 PSI (1.7 BAR).

IMPORTANT: If your system is designed with Nelson sprinklers, use Nelson Pressure Regulators. Individual manufacturers' pressure regulator performance varies. Interchanging could result in inaccurate nozzle selection.

NELSON

SAVE WATER, SAVE ENERGY AND DO A BETTER JOB OF IRRIGATING

NELSON'S UNIVERSAL FLO AND HI FLO REGULATORS

The function of a pressure regulator is to fix a varying inlet pressure to a set outlet pressure, regardless of changes in the system pressure due to hydraulic conditions, elevation changes, pumping scenarios, etc. The benefits include a uniform depth of water application, controlled sprinkler performance (droplet size and throw distance), and flexibility in system operation.

FEATURES & BENEFITS:

SINGLE STRUT SEAT DESIGN STANDARD WITH UNIVERSAL FLO. The new "single-strut" technology in the Universal Flo regulator minimizes "hair-pinning" of debris around the inlet seat, providing more plug resistance for systems operating in dirty water condtions.

PATENTED DAMPENING SYSTEM. The patented o-ring dampening system of all Nelson pressure regulators handles severe pressure surges to withstand water hammer.

WIDE FLOW RANGE. The Nelson Universal Pressure Regulator has a flow up to 12 GPM (2.7 M^3/H) at 15 PSI (1.0 BAR) and above.

EXTENDED PERFORMANCE AND PRECISION ACCURACY. Precision components coupled with an internally lubricated o-ring minimize frictional drag and hysteresis.

PRECISION MANUFACTURED. Made of the toughest chemically resistant materials. 100% tested for accuracy.

UNIVERSAL 3000 SERIES CONNECTION OPTION. Integral adapter connects directly into all Nelson 3000 Series Pivot Sprinklers and creates an easy to assemble, economical pivot sprinkler package.

> UNIVERSAL FLO and HIGH FLO – CONNECTIONS & PERFORMANCE

PIPE THREAD CONNECTION

INLET
3/4" FNPT

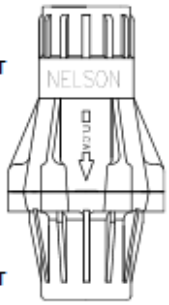

OUTLET
3/4" FNPT

3000 SERIES PIVOT CONNECTION

(Integral adapter for 3000 Series Pivot Products)

INLET
3/4" FNPT

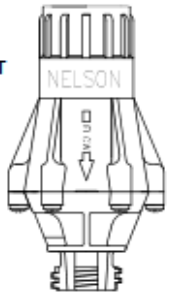

OUTLET
3000 ST

HOSE THREAD CONNECTION

(Connections for Micro/Drip)

INLET
3/4" FHT

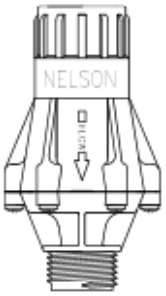

OUTLET
3/4" MHT

ORDERING SPECIFICATIONS: When ordering Nelson Pressure Regulators specify Pressure, Flow (Universal Flo or Hi Flo) & Connection (Inlet x Outlet). (Example: 10 PSI Hi Flo 3/4"FNPT x 3/4"FNPT.) **More connection options available — please contact Nelson factory for more information.**

UNIVERSAL FLO REGULATOR

PSI	BAR	GPM	M³/HR	CONNECTIONS AVAILABLE ■ 3/4" FNPT 3/4" FNPT	3/4" FNPT 3/4" ST	3/4" FHT 3/4" MHT
6	0.41	0.5-8	0.11-1.82	■	■	■
10	0.70	0.5-10	0.11-2.27	■	■	■
15	1.0	0.5-12	0.11-2.72	■	■	■
20	1.4	0.5-12	0.11-2.72	■	■	■
25	1.7	0.5-12	0.11-2.72	■	■	■
30	2.0	0.5-12	0.11-2.72	■	■	■
40	2.8	0.5-12	0.11-2.72	■	■	■
50	3.4	0.5-12	0.11-2.72	■	■	■

HI-FLO REGULATOR

PSI	BAR	GPM	M³/HR	CONNECTIONS AVAILABLE ■ 3/4" FNPT 3/4" FNPT	3/4" FNPT 3/4" ST
6	0.41	4-16	.91-3.63	■	■
10	0.70	4-16	.91-3.63	■	■
15	1.0	2-20	.45-4.54	■	■
20	1.4	2-20	.45-4.54	■	■
25	1.7	2-20	.45-4.54	■	■
30	2.0	2-20	.45-4.54	■	■
40	2.8	2-20	.45-4.54	■	■
50	3.4	2-20	.45-4.54	■	■

APPLICATION NOTES

Nelson Pressure Regulators can be used in a variety of applications (e.g. Center Pivot, Solid Set, Tree & Vine). Choose the proper pressure rating for your application.

Performance Tables. Contact the Nelson factory for detailed performance information.

Design Considerations. Maintain a 5 PSI (0.35 BAR) threshold above the nominal spring rated pressure.

CAUTION! Pressure regulators should be installed downstream from all shut-off valves.

NELSON
Nelson Irrigation Corporation
848 Airport Rd., Walla Walla, WA 99362 USA
Tel: 509.525.7660 Fax: 509.525.7907 info@nelsonirrigation.com
Nelson Irrigation Corporation of Australia Pty. Ltd.
35 Sudbury Street, Darra QLD 4074 info@nelsonirrigation.com.au
Tel: +61 7 3715 8555 Fax: +61 7 3715 8666

WWW.NELSONIRRIGATION.COM

Specification Overview		
Temperature Range	15 to 265° F	-10 to 130°C
Pressure Range	0 - 115 PSI (No Minimum Pressure)	
Flow Rate	Cv 7.6 (Appx 58 GPM @ 60 PSI)	
Power Requirments	18 Watts	1.50 Amps
Response Time	Fast Acting (Less than one second)	
Duty Cycle	100% but not indefinitely	
*Suitable Media	Water – Air - Fuel - *Etc	

*Consult a chemical compatibility expert for correct seal and valve body material c

Valve Details	
Function	Normally Closed
Port Size	3/4" Female NPT
Valve Body	Brass
Seal Material	Viton® Diaphragm
Components	Stainless Steel
Operation Type	Semi-Direct Lift Valve
Coil Connection	Lead Wires
Orifice Size	20mm
Weight	1 lb 10 oz
Height	4.25"
Length	2.65" port to port
Width	2.00"

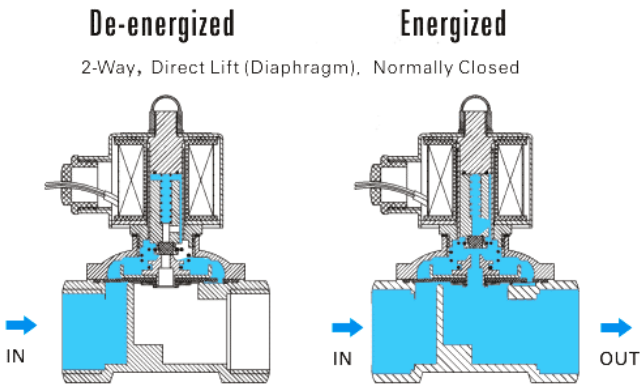
De-energized
Energized
2-Way, Direct Lift (Diaphragm), Normally Closed
IN
IN
OUT

APPENDIX B

SSC PROCESSING PROCEDURES

SSC PROCESSING PROCEDURES

Storage Note: *Refrigerate water samples for a minimum of 24 hrs before processing.*

1. The following process should be repeated for each sample bottle.
2. Weigh each evaporating dish and crinkle dish. Record the weight to the nearest 0.0001 g. Both the evaporating and crinkle dishes are labeled with a number corresponding to the sample bottles.
3. Vacuum away the supernatant by inserting the J-tube into the bottle. Attach the tube to a vacuum to remove the excess water without disturbing the sediment. The excess water will be retained in the flask attached to the pump.

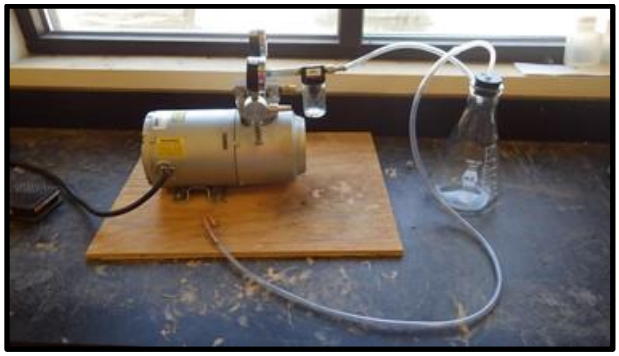

4. Retain the supernatant for future calculation of the dissolved solids correction factor.
5. Measure the remaining volume in the original sample by placing the bottle on a level surface and marking the water level.
6. Use water to wash the sediment and supernatant from the bottle into an evaporating dish.

7. Refill the bottle to the mark made in step 4 using a graduated cylinder and record the volume added in mL.
8. Place the evaporating dishes containing the samples into an oven set at 210 ^{o}F (99 ^{o}C). Bake for 3 hours.
9. Once the water has evaporated, raise the temperature in the oven to 221 ^{o}F (105 ^{o}C) for 2 hours.
10. Once the dishes have baked for 2 hours, remove the dishes containing the sample and weigh it to the nearest 0.0001 gram. Discard the sediment.

11. To calculate the dissolved solids correction factor, transfer a measured volume from the excess supernatant collected in steps 29-30 using a volumetric pipet. Record the volume.
12. Dry the sample similarly to steps 7-8.
13. Record the weight of the dish and sample to the nearest 0.0001 gram. Discard the sediment.
14. Calculate the dissolved solids correction factor using Equation 5:
15. Subtract the value of DS_c from the net weight recorded in step 12. Record this value in the second heading labeled weight of sediment-net.

16. Divide the net weight of sediment (second value) by the net weight of the sample. Multiply the quotient by 1,000,000. The result is the sediment concentration in parts per million (ppm). Record this value on the data collection sheet.
17. Repeat this process for each sample taken during the test.

APPENDIX C

EXPERIMENTAL DATA

CALIBRATION DATA

Interval 1		Test Number																													
		1	2	3	4	5	6	7	8	9	10	11	12	13	14	15	16	17	18	19	20	21	22	23	24	25	26	27	28	29	30
x (ft)	y (ft)	Rainfall Depth (cm)																													
2	2	0.6	0.7	0.8	0.8	0.8	0.9	0.9	0.8	0.7	0.8	1.0	0.9	1.0	1.0	1.0	0.8	1.0	0.9	0.9	0.9	0.9	0.9	1.0	0.9	0.9	1.0	0.9	0.9	0.8	0.9
6	2	0.2	0.3	0.3	0.4	0.4	0.6	0.6	0.4	0.5	0.5	0.4	0.5	0.6	0.6	0.6	0.5	0.6	0.5	0.4	0.5	0.5	0.5	0.5	0.6	0.6	0.7	0.6	0.6	0.7	0.6
4	4	0.8	0.7	0.9	0.8	0.8	0.8	0.6	0.7	0.7	0.9	1.0	0.9	0.7	1.2	0.9	1.2	0.8	0.9	0.9	0.9	1.0	0.8	0.8	0.9	0.8	1.1	0.8	0.8	0.8	0.9
2	6	0.8	0.7	0.6	0.6	0.6	0.7	0.7	0.6	0.7	0.6	0.7	0.8	0.8	0.8	0.6	0.7	0.6	0.7	0.8	0.7	0.8	0.8	0.8	0.8	0.8	0.7	0.6	0.8	0.7	0.6
6	6	0.8	0.7	0.7	0.7	0.7	0.7	0.6	0.7	0.7	0.6	1.2	0.9	0.9	0.7	0.9	0.7	0.9	1.1	1.0	0.9	0.8	0.8	0.7	0.7	0.7	0.8	1.0	0.8	1.0	1.2
4	8	0.5	0.6	0.6	0.6	0.6	0.7	0.6	0.6	0.5	0.6	0.7	0.7	0.6	0.6	0.7	0.7	0.6	0.6	0.7	0.7	0.7	0.6	0.6	0.6	0.6	0.7	0.7	0.7	0.7	0.7
2	10	0.6	0.5	0.6	0.5	0.7	0.7	0.7	0.8	0.9	0.7	0.8	0.8	0.9	0.8	0.8	0.7	0.8	0.8	0.8	0.8	0.8	0.8	0.8	0.8	0.8	0.7	0.8	0.8	0.8	0.7
6	10	0.5	0.5	0.6	0.6	0.6	0.6	0.8	0.6	0.7	0.6	0.7	0.8	0.7	0.8	0.6	0.8	0.7	0.7	0.7	0.8	0.7	0.7	0.7	0.7	0.7	0.7	0.8	0.7	0.7	0.7
4	12	0.7	0.6	0.6	0.7	0.6	0.6	0.6	0.7	0.8	0.6	0.7	0.7	0.8	0.8	0.7	0.7	0.6	0.8	0.7	0.8	0.8	0.8	0.8	0.8	0.8	0.8	0.7	0.7	0.7	0.7
2	14	0.6	0.6	0.5	0.7	0.6	0.7	0.7	0.6	0.7	0.7	0.7	0.8	0.9	0.8	0.7	0.8	0.7	0.7	0.8	0.8	0.7	0.7	0.8	0.7	0.7	0.8	0.8	0.8	0.8	0.7
6	14	0.6	0.6	0.7	0.8	0.8	0.8	0.7	0.6	0.7	0.8	1.0	0.8	0.9	0.8	0.7	0.8	0.7	0.8	0.8	0.9	0.8	0.7	0.7	0.8	0.8	0.6	0.7	0.8	0.8	0.8
4	16	0.6	0.6	0.7	0.8	0.8	0.7	0.7	0.6	0.7	0.6	0.8	0.7	0.7	0.7	0.6	0.7	0.6	0.7	0.8	0.8	0.8	0.6	0.7	0.7	0.6	0.8	0.6	0.8	0.7	0.7
2	18	0.8	0.7	0.8	0.8	0.6	0.9	0.7	0.7	0.7	0.8	1.0	0.9	1.0	0.7	0.8	0.8	0.9	0.9	0.8	1.1	1.0	0.9	0.8	0.8	0.8	0.8	0.9	0.9	0.8	0.8
6	18	0.7	0.7	0.6	0.6	0.7	0.7	0.7	0.6	0.8	0.7	0.8	0.8	0.8	0.8	0.6	0.8	0.6	0.7	0.7	0.8	0.7	0.7	0.7	0.7	0.7	0.7	0.8	0.7	0.7	0.7
4	20	1.0	1.0	0.9	0.9	0.6	0.8	0.8	0.8	0.8	0.6	0.9	0.7	0.7	0.8	0.7	0.7	0.7	0.9	0.8	0.9	0.8	0.8	0.9	0.9	0.7	0.8	0.7	0.8	0.8	0.8
2	22	1.2	1.2	1.2	1.1	1.0	1.1	1.1	1.1	1.1	0.8	0.9	1.0	0.9	1.0	0.9	1.1	0.9	1.0	1.1	1.0	1.2	1.0	1.0	0.9	1.0	1.0	0.9	0.9	0.9	1.0
6	22	0.8	1.0	0.9	0.9	0.9	0.9	0.8	0.9	0.9	0.9	1.1	0.8	0.9	0.9	1.0	1.0	0.7	0.8	1.0	1.0	1.0	0.8	0.9	0.8	0.9	0.8	0.8	0.9	0.9	0.9
4	24	1.1	1.1	0.8	0.8	0.9	0.8	0.7	0.8	0.9	0.6	0.8	0.8	0.8	0.8	0.8	1.0	0.8	0.9	1.0	0.9	0.9	0.8	0.8	0.8	0.8	0.9	0.8	0.8	0.8	0.8
2	26	1.2	1.1	0.7	0.8	0.9	0.7	0.7	0.6	0.7	0.8	1.0	0.8	0.8	0.8	0.7	0.8	0.8	0.8	0.9	0.7	0.8	0.7	0.8	0.9	0.8	0.9	0.7	0.8	0.8	0.8
6	26	0.8	0.9	0.6	0.6	0.9	0.7	0.7	0.5	0.6	0.6	0.7	0.6	0.6	0.6	0.7	0.7	0.6	0.6	0.7	0.6	0.7	0.7	0.6	0.7	0.6	0.6	0.6	0.7	0.6	0.6
4	28	0.6	0.7	0.4	0.5	0.5	0.5	0.5	0.6	0.6	0.5	0.6	0.6	0.6	0.6	0.6	0.7	0.6	0.6	0.7	0.6	0.6	0.6	0.6	0.6	0.6	0.6	0.5	0.5	0.6	0.6
2	30	0.6	0.5	0.5	0.5	0.4	0.5	0.5	0.5	0.4	0.6	0.6	0.5	0.6	0.5	0.6	0.5	0.5	0.6	0.5	0.6	0.5	0.5	0.5	0.5	0.5	0.6	0.5	0.6	0.5	0.5
6	30	0.5	0.5	0.6	0.6	0.5	0.6	0.6	0.5	0.5	0.6	0.5	0.6	0.6	0.6	0.6	0.6	0.6	0.6	0.4	0.6	0.5	0.5	0.5	0.5	0.6	0.6	0.5	0.6	0.6	0.6
4	32	0.5	0.5	0.6	0.6	0.6	0.6	0.6	0.6	0.6	0.4	0.5	0.6	0.5	0.5	0.6	0.5	0.6	0.6	0.6	0.5	0.6	0.5	0.6	0.6	0.6	0.6	0.5	0.5	0.5	0.6
2	34	0.5	0.6	0.5	0.5	0.6	0.6	0.5	0.5	0.5	0.5	0.6	0.5	0.5	0.4	0.5	0.4	0.5	0.5	0.6	0.5	0.6	0.5	0.5	0.7	0.5	0.5	0.5	0.5	0.5	0.4
6	34	0.5	0.5	0.7	0.6	0.7	0.6	0.6	0.5	0.6	0.6	0.6	0.5	0.6	0.5	0.5	0.6	0.6	0.6	0.5	0.5	0.5	0.4	0.4	0.4	0.5	0.5	0.5	0.6	0.4	0.6
4	36	0.5	0.4	0.6	0.6	0.6	0.6	0.6	0.6	0.4	0.5	0.6	0.6	0.5	0.5	0.4	0.4	0.5	0.6	0.6	0.5	0.6	0.5	0.6	0.5	0.5	0.5	0.5	0.4	0.5	0.5
2	38	0.6	0.6	0.6	0.5	0.5	0.5	0.5	0.6	0.5	0.4	0.5	0.5	0.4	0.3	0.3	0.4	0.4	0.5	0.5	0.4	0.6	0.5	0.5	0.5	0.4	0.4	0.4	0.5	0.4	0.5
6	38	0.6	0.6	0.5	0.6	0.6	0.6	0.5	0.5	0.5	0.5	0.5	0.5	0.6	0.4	0.4	0.4	0.5	0.6	0.6	0.5	0.6	0.6	0.5	0.5	0.6	0.4	0.5	0.5	0.5	0.5

Interval 2		Test Number																	
		1	2	3	4	5	6	7	8	9	10	11	12	13	14	15	16	17	18
x (ft)	y (ft)	Rainfall Depth (cm)																	
2	2	1.0	1.0	1.0	1.1	1.0	1.0	0.8	0.7	1.2	1.2	1.3	1.0	1.1	1.0	1.1	1.2	1.1	1.1
6	2	0.6	0.7	0.6	0.6	0.6	0.7	0.7	0.8	0.7	0.7	0.7	0.9	0.9	0.9	1.1	0.7	0.8	0.7
4	4	1.2	1.2	1.2	1.2	1.0	1.1	1.2	1.1	1.1	1.1	1.2	1.2	1.0	1.1	1.1	1.1	1.2	1.2
2	6	1.0	1.0	1.0	0.9	1.0	1.0	1.1	0.8	1.0	1.0	1.1	0.8	0.9	0.8	0.8	0.8	1.0	1.0
6	6	1.0	1.2	1.1	1.1	1.0	1.1	1.0	1.3	1.1	1.1	1.3	1.5	0.9	0.9	1.0	0.9	1.0	1.0
4	8	1.2	1.2	1.2	1.3	1.0	1.2	0.9	1.0	1.2	1.2	1.4	1.2	1.1	1.0	1.0	1.0	1.1	1.1
2	10	1.5	1.6	1.6	1.5	1.6	1.5	1.1	1.4	1.6	1.4	1.5	1.2	1.5	1.5	1.3	1.3	1.4	1.4
6	10	1.6	1.6	1.4	1.8	1.5	1.5	1.2	1.6	1.6	1.5	1.5	1.7	1.6	1.4	1.5	1.4	1.4	1.4
4	12	1.2	1.2	1.3	1.3	1.3	1.2	1.2	1.1	1.2	1.3	1.3	1.2	1.1	1.1	1.1	1.2	1.2	1.2
2	14	1.2	1.2	1.3	1.2	1.2	1.2	1.2	1.2	1.2	1.3	1.3	1.2	1.0	1.0	0.9	1.0	1.1	1.1
6	14	1.4	1.4	1.4	1.4	1.2	1.3	1.4	1.3	1.4	1.4	1.4	1.0	1.1	1.3	1.2	1.3	1.2	1.3
4	16	1.2	1.2	1.2	1.2	1.3	1.3	1.2	1.2	1.2	1.3	1.4	1.4	1.0	0.9	1.0	1.1	1.1	1.1
2	18	1.2	1.2	1.2	1.2	1.3	1.3	1.2	1.2	1.2	1.2	1.3	1.2	1.0	0.9	0.9	1.0	1.1	1.1
6	18	1.2	1.0	1.0	1.2	1.3	1.3	1.4	1.2	1.1	1.2	1.2	1.2	0.9	1.0	1.0	1.2	1.1	1.2
4	20	1.4	1.3	1.2	1.4	1.6	1.4	1.6	1.4	1.4	1.5	1.5	1.4	1.1	1.2	1.3	1.1	1.3	1.4
2	22	1.7	1.7	1.7	1.7	1.7	1.6	1.6	1.6	1.6	1.6	1.8	1.7	1.2	1.4	1.5	1.5	1.5	1.5
6	22	1.6	1.4	1.5	1.4	1.6	1.4	1.5	1.5	1.5	1.5	1.6	1.4	1.4	1.4	1.6	1.6	1.6	1.6
4	24	1.6	1.6	1.5	1.6	1.8	1.8	1.6	1.8	1.7	1.8	2.0	1.8	1.7	1.6	1.6	1.8	1.6	1.6
2	26	1.6	1.6	1.5	1.5	1.8	1.6	1.8	1.5	1.6	1.7	1.9	1.6	1.4	1.4	1.5	1.6	1.6	1.8
6	26	1.4	1.4	1.4	1.4	1.6	1.5	1.6	1.3	1.4	1.4	1.5	1.4	1.2	1.2	1.2	1.4	1.3	1.3
4	28	1.1	1.1	1.1	1.0	1.2	1.2	1.5	1.2	1.3	1.3	1.2	1.2	1.0	1.0	1.0	1.0	1.0	1.0
2	30	1.0	1.0	1.0	1.0	1.0	1.0	1.0	1.0	1.1	1.1	1.1	1.1	0.8	0.8	1.0	1.0	1.0	1.0
6	30	1.0	1.0	1.0	1.0	1.0	1.0	1.0	1.0	1.1	1.1	1.1	1.0	0.9	1.0	1.1	1.0	1.0	1.0
4	32	0.9	0.8	0.9	0.9	1.0	0.9	0.9	0.7	0.8	0.9	0.9	0.8	0.7	0.7	0.7	0.8	0.7	0.7
2	34	0.8	0.8	0.8	0.9	0.7	0.6	0.8	0.5	0.7	0.6	0.7	0.5	0.7	0.7	0.6	0.8	0.8	0.6
6	34	0.9	0.9	0.9	0.9	0.8	0.9	0.9	0.8	1.0	1.0	0.9	0.6	0.7	0.8	0.7	0.8	0.9	0.8
4	36	0.9	0.9	0.9	0.8	0.8	0.8	0.8	0.6	0.8	0.8	0.8	0.6	0.7	0.7	0.7	0.8	0.8	0.6
2	38	0.7	0.7	0.8	0.8	0.8	0.8	0.7	0.6	0.8	0.8	0.8	0.6	0.6	0.6	0.6	0.7	0.7	0.6
6	38	0.8	0.8	0.8	0.9	0.8	0.8	0.8	0.7	0.8	0.8	0.8	0.8	0.7	0.7	0.8	0.8	0.8	0.9

Interval 3		Test Number									
		1	2	3	4	5	6	7	8	9	10
x (ft)	y (ft)	Rainfall Depth (cm)									
2	2	2.8	2.8	2.4	2.6	2.6	2.8	2.5	2.8	2.7	2.6
6	2	1.6	1.6	1.7	1.6	1.7	1.6	1.6	1.6	1.7	1.9
4	4	2.0	2.0	1.9	2.0	1.9	1.8	1.9	2.0	1.8	2.0
2	6	2.0	2.0	1.9	1.9	1.9	2.0	1.9	2.0	1.9	2.0
6	6	2.0	2.0	1.9	1.9	2.0	2.0	2.0	1.9	2.1	2.5
4	8	2.2	2.2	2.1	2.1	1.9	2.1	2.0	2.0	2.2	2.1
2	10	2.1	2.1	2.4	2.1	2.2	2.2	2.1	2.3	2.2	2.1
6	10	2.3	2.3	2.5	2.4	2.4	2.4	2.6	2.4	2.3	2.2
4	12	2.5	2.5	2.6	2.4	2.4	2.5	2.4	2.5	2.5	2.3
2	14	2.7	2.7	2.6	2.5	2.6	2.6	2.6	2.6	2.6	2.6
6	14	2.5	2.5	2.6	2.6	2.6	2.6	2.6	2.5	2.6	2.5
4	16	2.5	2.5	2.5	2.4	2.4	2.4	2.4	2.5	2.4	2.4
2	18	3.0	3.0	2.8	3.2	2.9	2.9	3.0	3.0	3.0	2.9
6	18	3.0	3.0	3.0	3.1	3.0	3.0	3.1	3.1	2.8	2.8
4	20	3.1	3.1	3.0	3.2	2.9	3.1	3.1	3.2	3.0	2.7
2	22	3.0	3.0	3.0	3.0	3.1	3.0	3.1	3.0	2.8	2.7
6	22	2.8	2.8	3.0	2.9	2.8	2.8	2.9	2.9	2.8	2.7
4	24	4.0	4.0	3.6	4.0	3.8	3.8	3.9	3.8	3.7	3.6
2	26	3.6	3.6	3.6	3.6	3.3	3.6	3.5	3.5	3.6	3.6
6	26	3.0	3.0	2.6	3.0	2.8	2.8	2.9	3.0	3.0	3.0
4	28	2.6	2.6	2.5	2.6	2.5	2.6	2.5	2.5	2.4	2.5
2	30	2.0	2.0	1.8	2.0	1.9	2.0	2.0	2.0	2.0	2.3
6	30	2.0	2.0	1.7	2.0	2.0	1.8	2.0	1.8	2.0	2.2
4	32	1.8	1.8	1.9	1.9	1.7	1.8	1.8	1.7	1.8	2.2
2	34	1.6	1.6	1.6	1.5	1.4	1.6	1.4	1.7	1.8	1.8
6	34	2.0	2.0	1.9	1.9	1.8	1.8	2.0	1.9	2.0	2.2
4	36	1.9	1.9	1.9	2.0	1.8	1.9	1.8	2.0	2.0	2.2
2	38	1.6	1.6	1.7	1.7	1.5	1.6	1.6	1.7	1.7	1.8
6	38	1.9	1.9	1.8	1.7	1.7	1.8	1.8	1.8	1.8	1.7

0.98 in./hr						With 30	Without 30	Average Total Weight (mg)		% Error	
Sieve #	Mass of Dish (g)	Mass Total (g)	Mass of Pellets (g)	Number of Pellets	Average Weight (mg)	% of Pellets	% of Pellets	With 30	Without 30	With 30	Without 30
4	0	0	0	0	0	0	0	3.3	4.6	17.19	7.18
8	14.4398	14.8285	0.3887	28	13.9	0.08	0.14	Average Drop Size (mm)			
10	14.4400	14.6012	0.1612	25	6.4	0.07	0.12	With 30	Without 30		
16	14.4387	14.8258	0.3871	151	2.6	0.41	0.74	1.84	2.06		
30	14.4388	14.6986	0.2598	163	1.6	0.44	0.00	Theoretical Drop Size (mm)	2.22		
1.70 in./hr						With 30	Without 30	Average Total Weight (mg)		% Error	
Sieve #	Mass of Dish (g)	Mass Total (g)	Mass of Pellets (g)	Number of Pellets	Average Weight (mg)	% of Pellets	% of Pellets	With 30	Without 30	With 30	Without 30
4	0	0	0	0	0	0.00	0.00	3.0	4.3	27.30	18.08
8	14.4378	14.9747	0.5369	40	13.4	0.05	0.09	Average Drop Size (mm)			
10	14.4374	14.7022	0.2648	41	6.5	0.05	0.10	With 30	Without 30		
16	14.4379	15.4446	1.0067	343	2.9	0.43	0.81	1.79	2.01		
30	14.4361	14.9887	0.5526	368	1.5	0.46	0.00	Theoretical Drop Size (mm)	2.46		
3.45 in./hr						With 30	Without 30	Average Total Weight (mg)		% Error	
Sieve #	Mass of Dish (g)	Mass Total (g)	Mass of Pellets (g)	Number of Pellets	Average Weight (mg)	% of Pellets	% of Pellets	With 30	Without 30	With 30	Without 30
4	0	0	0	0	0	0.00	0.00	3.3	6.8	33.89	15.96
8	14.4352	15.5886	1.1534	97	11.9	0.08	0.20	Average Drop Size (mm)			
10	14.4356	15.0413	0.6057	81	7.5	0.06	0.17	With 30	Without 30		
16	14.4352	15.9633	1.5281	307	5.0	0.24	0.63	1.85	2.35		
30	14.4342	15.3851	0.9509	800	1.2	0.62	0.00	Theoretical Drop Size (mm)	2.79		

CONTROL TEST DATA

Date: 03/09/17	Control Test #: 1		
Sample Location	29	3	52
Container #	1	2	3
Container Mass, g	283.5	283.5	283.5
Container + Moist Specimen Mass, g	700.7	692.3	713.0
Time in Oven	10:38	10:56	11:10
Initial Container + Oven Dry Specimen, g	655.0	644.7	644.5
Time out of Oven	10:42	11:00	11:14
Secondary Container + Oven Dry Specimen, g	628.4	628.4	639.6
Time out of Oven	10:45	11:03	11:17
Third Container + Oven Dry Specimen, g	626.4	628.0	638.3
Time out of Oven	10:46	11:04	11:18
Final Container + Oven Dry Specimen, g	625.9	627.8	638.1
Time out of Oven	10:47	11:05	11:19
Water Content, %	21.85	18.73	21.12

Date: 03/09/17	Control Test #: 1		
Sample Location	29	3	52
Container Number	1	2	3
Volume of Drive Cylinder (DC), ft^3	0.033	0.033	0.033
Wet Wt. of Soil + DC, g	2217	2199	2227
Wt. of DC, g	575	569	572
Wet Wt. of Soil, g	1642	1630	1655
Wet Wt. of Soil, lb	3.6	3.6	3.6
Moisture Content, %	21.85	18.73	21.12
Wet Density, lb/ft^3	109.7	108.9	110.6
Dry Density, lb/ft^3	90.0	91.7	91.3
Maximum Dry Density, lb/ft^3	108.1	108.1	108.1
Percent Compacted, %	83.3	84.8	84.4

Rain Gauge		
x (ft)	**y (ft)**	**Depth (cm)**
2	5	4.9
6	5	5.2
2	15	6.0
6	15	5.9
2	25	7.3
6	25	6.5
2	35	3.2
6	35	3.5

Date: 03/09/17				Control Test #: 1			
	Weight of Sample						
Sample Time:	Weight of Bottle, g	Weight of Bottle and Sample, g	Weight of Total Sample, g	Weight of Dish, g	Volume of Sample, mL	Weight of Sample and Dish, g	Net Weight of Sample, g
0							
3							
6							
9	16.1	224.8	208.7	6.5243	48	15.1467	8.6224
12	16.3	235.6	219.3	6.5216	58	18.2342	11.7126
15	16.3	226.5	210.2	6.5051	56	13.6736	7.1685
18	16.5	233.8	217.3	6.4372	46	12.7146	6.2774
21	15.9	274.4	258.5	6.4125	42	14.4595	8.0470
24	16.5	237.7	221.2	6.4717	40	11.4499	4.9782
27	16.5	268.5	252.0	6.4633	42	12.2472	5.7839
30	16.6	270.9	254.3	6.5632	44	12.6646	6.1014
33	16.0	236.5	220.5	6.4887	44	11.373	4.8843
36	16.3	240.9	224.6	6.4706	40	10.7672	4.2966
39	16.2	217.3	201.1	6.552	50	12.9953	6.4433
42	15.4	246.3	230.9	6.537	50	12.5727	6.0357
45	16.0	248.2	232.2	6.4596	58	13.6313	7.1717
48	16.7	239.9	223.2	6.4798	52	13.8048	7.3250
51	15.5	235.6	220.1	6.5059	46	10.95	4.4441
54	16.0	231.8	215.8	6.4765	48	12.6373	6.1608
57	15.8	210.2	194.4	6.5519	58	11.8153	5.2634
60	16.7	265.5	248.8	6.4937	64	11.5016	5.0079

Dissolved Solids						Results		
Weight of Dish, g	Volume of Supernate, mL	Volume of Supernate Sample, mL	Weight of Supernate and Dish, g	Weight of Dissolved Solids, g	DS_c, g	Net Weight of Sample, g	Concentration (ppm)	Concentration (mg/L)
1.2834	152	13	1.286	0.0026	0.03040	8.5920	41169	42251
1.2962	134	13	1.2981	0.0019	0.01958	11.6930	53320	55149
1.2855	150	13	1.2873	0.0018	0.02077	7.1477	34004	34739
1.2953	170	13	1.2969	0.0016	0.02092	6.2565	28792	29317
1.2792	170	13	1.2809	0.0017	0.02223	8.0248	31044	31655
1.2961	178	13	1.2982	0.0021	0.02875	4.9494	22375	22691
1.2874	196	13	1.2889	0.0015	0.02262	5.7613	22862	23192
1.2858	208	13	1.2883	0.0025	0.04000	6.0614	23836	24194
1.2926	174	13	1.2944	0.0018	0.02409	4.8602	22042	22348
1.264	180	13	1.2880	0.024	0.33231	3.9643	17650	17846
1.2816	142	13	1.2835	0.0019	0.02075	6.4225	31937	32584
1.2545	178	13	1.2555	0.001	0.01369	6.0220	26081	26511
1.3011	182	13	1.3030	0.0019	0.02660	7.1451	30771	31372
1.2925	156	13	1.2937	0.0012	0.01440	7.3106	32754	33435
1.2814	170	13	1.2831	0.0017	0.02223	4.4219	20090	20345
1.2765	164	13	1.2781	0.0016	0.02018	6.1406	28455	28968
1.2845	132	13	1.2859	0.0014	0.01422	5.2492	27002	27463
1.2831	182	13	1.2843	0.0012	0.01680	4.9911	20061	20314

Date: 03/16/17	Control Test #: 2		
Sample Location	19	32	46
Container #	1	2	3
Container Mass, g	117.3	98.2	115.7
Container + Moist Specimen Mass, g	310.4	258	291.4
Time in Oven	9:54	10:07	10:18
Initial Container + Oven Dry Specimen, g	275.5	230	260.7
Time out of Oven	9:58	10:11	10:22
Secondary Container + Oven Dry Specimen, g	274.9	229.7	260.1
Time out of Oven	10:03	10:13	10:25
Third Container + Oven Dry Specimen, g	274.7	229.6	259.9
Time out of Oven	10:05	10:17	10:27
Final Container + Oven Dry Specimen, g	274.7	229.6	259.9
Water Content, %	22.68	21.61	21.84

Date: 03/16/17	Control Test #: 2		
Sample Location	19	32	46
Container Number	1	2	3
Volume of Drive Cylinder (DC), ft^3	0.033	0.033	0.033
Wet Wt. of Soil + DC, g	2337	2130	2189
Wt. of DC, g	576	569	572
Wet Wt. of Soil, g	1761	1561	1617
Wet Wt. of Soil, lb	3.9	3.4	3.6
Moisture Content, %	22.68	21.61	21.84
Wet Density, lb/ft^3	117.6	104.3	108.0
Dry Density, lb/ft^3	95.9	85.8	88.7
Maximum Dry Density, lb/ft^3	108.1	108.1	108.1
Percent Compacted, %	88.7	79.3	82.0

Rain Gauge		
x (ft)	**y (ft)**	**Depth (cm)**
2	5	5.4
6	5	4.6
2	15	6.2
6	15	6
2	25	8.02
6	25	6.7
2	35	4
6	35	4

Date: 03/16/17				Control Test #: 2			
	Weight of Sample						
Sample Time:	Weight of Bottle, g	Weight of Bottle and Sample, g	Weight of Total Sample, g	Weight of Dish, g	Volume of Sample, mL	Weight of Sample and Dish, g	Net Weight of Sample, g
0							
3	16.1	251.1	235.0	6.5345	52	13.0229	6.4884
6	16.3	236.4	220.1	6.4850	52	11.4398	4.9548
9	16.1	223.4	207.3	6.4872	58	10.5117	4.0245
12	16.3	270.6	254.3	6.4881	44	12.7298	6.2417
15	16.3	233.9	217.6	6.4765	72	11.4333	4.9568
18	16.5	239.5	223.0	6.4704	66	11.3826	4.9122
21	15.9	279.8	263.9	6.4050	38	16.1793	9.7743
24	16.5	242.1	225.6	6.4830	66	13.4403	6.9573
27	16.5	257.7	241.2	6.5177	74	13.6976	7.1799
30	16.6	217.4	200.8	6.4680	66	13.6438	7.1758
33	16.0	230.7	214.7	6.5500	70	18.5037	11.9537
36	16.3	249.1	232.8	6.5182	74	15.6781	9.1599
39	16.2	279.1	262.9	6.5283	52	17.2962	10.7679
42	15.4	219.1	203.7	6.4710	58	14.1781	7.7071
45	16.0	225.1	209.1	6.5997	48	14.2347	7.6350
48	16.7	227.1	210.4	6.5290	46	14.7845	8.2555
51	15.5	216.4	200.9	6.5492	58	11.8302	5.2810
54	16.0	262.9	246.9	6.4919	44	14.1117	7.6198
57	15.8	275.9	260.1	6.5641	50	15.3716	8.8075
60	16.7	261.7	245.0	6.4873	52	14.4520	7.9647

Dissolved Solids						Results		
Weight of Dish, g	Volume of Supernate, mL	Volume of Supernate Sample, mL	Weight of Supernate and Dish, g	Weight of Dissolved Solids, g	DS_c, g	Net Weight of Sample, g	Concentration (ppm)	Concentration (mg/L)
1.2839	174	13	1.2892	0.0053	0.07094	6.4175	27308	27780
1.3025	156	13	1.2998	-0.0027	-0.03240	4.9872	22659	22983
1.2916	148	13	1.288	-0.0036	-0.04098	4.0655	19612	19854
1.3012	194	13	1.2995	-0.0017	-0.02537	6.2671	24644	25028
1.2822	132	13	1.2822	0	0.00000	4.9568	22779	23107
1.2954	150	13	1.2971	0.0017	0.01962	4.8926	21940	22243
1.2883	192	13	1.2904	0.0021	0.03102	9.7433	36920	37788
1.2875	156	13	1.2870	-0.0005	-0.00600	6.9633	30866	31470
1.3088	162	13	1.3108	0.002	0.02492	7.1550	29664	30222
1.2898	124	13	1.2918	0.002	0.01908	7.1567	35641	36449
1.2845	136	13	1.2843	-0.0002	-0.00209	11.9558	55686	57684
1.2746	154	13	1.2559	-0.0187	-0.22152	9.3814	40298	41334
1.3012	200	13	1.3035	0.0023	0.03538	10.7325	40824	41887
1.2968	146	13	1.2951	-0.0017	-0.01909	7.7262	37929	38846
1.2843	156	13	1.2839	-0.0004	-0.00480	7.6398	36537	37386
1.306	162	13	1.2795	-0.0265	-0.33023	8.5857	40807	41869
1.3081	142	13	1.2881	-0.02	-0.21846	5.4995	27374	27848
1.2833	198	13	1.2858	0.0025	0.03808	7.5817	30708	31306
1.2888	210	13	1.2912	0.0024	0.03877	8.7687	33713	34435
1.2822	194	13	1.2839	0.0017	0.02537	7.9393	32405	33072

Date: 03/22/17	Control Test #: 3		
Sample Location	13	32	43
Container #	1	2	3
Container Mass, g	115.7	117.2	98.3
Container + Moist Specimen Mass, g	255.4	253.9	235.9
Time in Oven	9:29	9:38	9:48
Initial Container + Oven Dry Specimen, g	231.9	231.7	214.9
Time out of Oven	9:33	9:42	9:52
Secondary Container + Oven Dry Specimen, g	231.8	231.3	214.9
Time out of Oven	9:36	9:45	9:54
Final Container + Oven Dry Specimen, g	231.8	231.3	214.9
Water Content, %	20.33	19.81	18.01

Date: 03/22/17	Control Test #: 3		
Sample Location	13	32	43
Container Number	1	2	3
Volume of Drive Cylinder (DC), ft^3	0.033	0.033	0.033
Wet Wt. of Soil + DC, g	2206	2152	2192
Wt. of DC, g	564	558	564
Wet Wt. of Soil, g	1642	1594	1628
Wet Wt. of Soil, lb	3.6	3.5	3.6
Moisture Content, %	20.33	19.81	18.01
Wet Density, lb/ft^3	109.7	106.5	108.8
Dry Density, lb/ft^3	91.2	88.9	92.2
Maximum Dry Density, lb/ft^3	108.1	108.1	108.1
Percent Compacted, %	84.3	82.2	85.3

Rain Gauge		
x (ft)	y (ft)	Depth (cm)
2	5	6.5
6	5	5.2
2	15	6.4
6	15	6.4
2	25	8.9
6	25	7.4
2	35	4.2
6	35	4.3

Date: 03/22/17				Control Test #: 4			
	Weight of Sample						
Sample Time:	Weight of Bottle, g	Weight of Bottle and Sample, g	Weight of Total Sample, g	Weight of Dish, g	Volume of Sample, mL	Weight of Sample and Dish, g	Net Weight of Sample, g
0							
3							
6							
9							
10	16.3	247.5	231.2	6.5326	50	9.8303	3.2977
12	16.1	267.9	251.8	6.4836	50	17.4185	10.9349
15	16.3	245.1	228.8	6.4933	70	13.7885	7.2952
18	16.3	258.5	242.2	6.4961	40	12.3906	5.8945
21	16.5	232.2	215.7	6.5362	42	15.0229	8.4867
24	15.9	258.7	242.8	6.5059	48	17.5662	11.0603
27	16.5	243.1	226.6	6.4457	48	18.7553	12.3096
30	16.5	259.0	242.5	6.4857	46	19.5526	13.0669
33	16.6	249.4	232.8	6.5187	50	17.8273	11.3086
36	16.0	259.7	243.7	6.4716	54	23.2893	16.8177
39	16.3	252.8	236.5	6.5544	46	21.4695	14.9151
42	16.2	261.9	245.7	6.5221	48	25.7727	19.2506
45	15.4	251.4	236.0	6.5274	52	19.8433	13.3159
48	16.0	281.5	265.5	6.5016	56	20.6748	14.1732
51	16.7	247.1	230.4	6.6012	44	16.2375	9.6363
54	15.5	262.3	246.8	6.5176	54	18.1302	11.6126
57	16.0	244.7	228.7	6.5576	52	19.0166	12.4590
60	15.8	247.6	231.8	6.5033	50	17.4031	10.8998

Dissolved Solids						Results		
Weight of Dish, g	Volume of Supernate, mL	Volume of Supernate Sample, mL	Weight of Supernate and Dish, g	Weight of Dissolved Solids, g	DS_c, g	Net Weight of Sample, g	Concentration (ppm)	Concentration (mg/L)
1.284	170	13	1.2866	0.0026	0.03400	3.2637	14116	14241
1.2968	194	13	1.2984	0.0016	0.02388	10.9110	43332	44532
1.2877	154	13	1.2888	0.0011	0.01303	7.2822	31828	32470
1.2965	196	13	1.2984	0.0019	0.02865	5.8659	24219	24589
1.2801	170	13	1.2832	0.0031	0.04054	8.4462	39157	40134
1.2956	190	13	1.2975	0.0019	0.02777	11.0325	45439	46760
1.2883	168	13	1.2908	0.0025	0.03231	12.2773	54180	56070
1.2869	190	13	1.2888	0.0019	0.02777	13.0391	53770	55630
1.3095	176	13	1.3118	0.0023	0.03114	11.2775	48443	49948
1.2897	184	13	1.2927	0.003	0.04246	16.7752	68836	71915
1.2833	178	13	1.2862	0.0029	0.03971	14.8754	62898	65459
1.2541	186	13	1.2566	0.0025	0.03577	19.2148	78204	82203
1.3011	178	13	1.3041	0.003	0.04108	13.2748	56249	58289
1.2932	194	13	1.2962	0.003	0.04477	14.1284	53214	55036
1.2823	176	13	1.2847	0.0024	0.03249	9.6038	41683	42793
1.2777	182	13	1.2797	0.002	0.02800	11.5846	46939	48351
1.286	168	13	1.2881	0.0021	0.02714	12.4319	54359	56261
1.2834	174	13	1.2864	0.003	0.04015	10.8596	46849	48255

APPENDIX D

ROLLED EROSION CONTROL PRODUCT

INSTALLATION PROCEDURES

The ECTC provides a standardized method for installing RECPs, which can be used in conjunction with the plot preparation techniques provided in ASTM D6459-15. Adopting the installation procedures specified by the ECTC in our testing of RECPs will ensure that our products are installed in a standardized manner similar to how these products are installed in the field. The installation procedures for RECPs as specified by the ECTC are described below.

Site Preparation

To begin, the slope should be graded into a smooth profile. Foreign objects on the slope (i.e., roots, rocks, and weeds) should be removed and all voids should be filled (ECTC 2014).

Seeding

A seed mixture should be selected based on the site's geographical location as well as the time of year (i.e. winter, summer, etc.). If, before the RECP is installed, the seed bed is damaged or eroded, the affected area should be repaired and reseeded (ECTC 2014).

Prepare Anchor Trench

At the top of the slope, a trench 6 in. deep by 6 in. wide (15 cm by 15 cm) should be excavated. The RECP will then be secured to the anchor trench using staples spaced at 1 ft (30 cm) on center. If the terrain allows it, the anchor trench should be installed at least 3 ft (1 m) from the crest of the slope, thereby preventing water from undercutting the RECP and causing soil erosion (ECTC 2014). Figure D.1 provides an example of how the trench should be prepared.

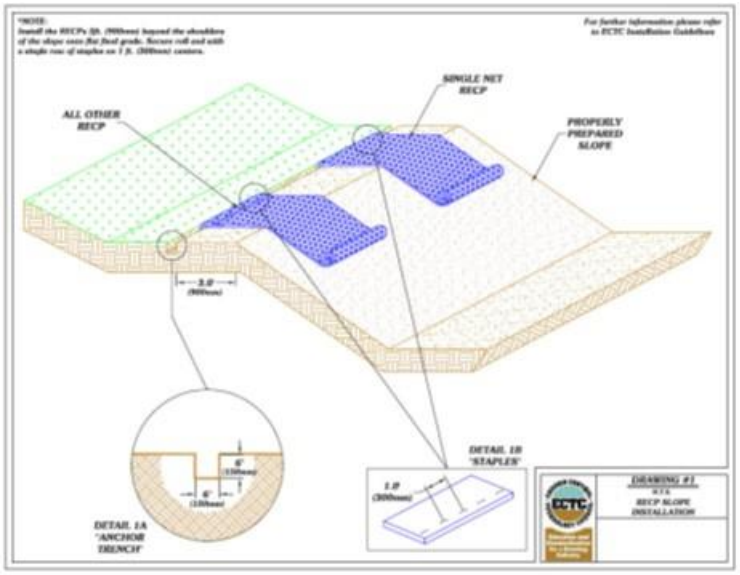

Figure D.1 Detail for Anchor Trench Preparation (ECTC 2014).

Secure RECP in Anchor Trench

The RECP should be extended 30 in. (76 cm) past the anchor trench. As stated above, the RECP is then secured to the anchor trench using staples spaced 12 in. (30 cm) spaced on center for the width of the RECP. Once the RECP is secured, the trench should then be filled and compacted. The soil can then be seeded and the remaining 12 in. (30 cm) of the terminal end of the RECP should be folded over the trench and secured with staples placed 12 in. (30 cm) on center (ECTC 2014). Drawings depicting this process for both single net and all other RECPs are shown in Figure D.2.

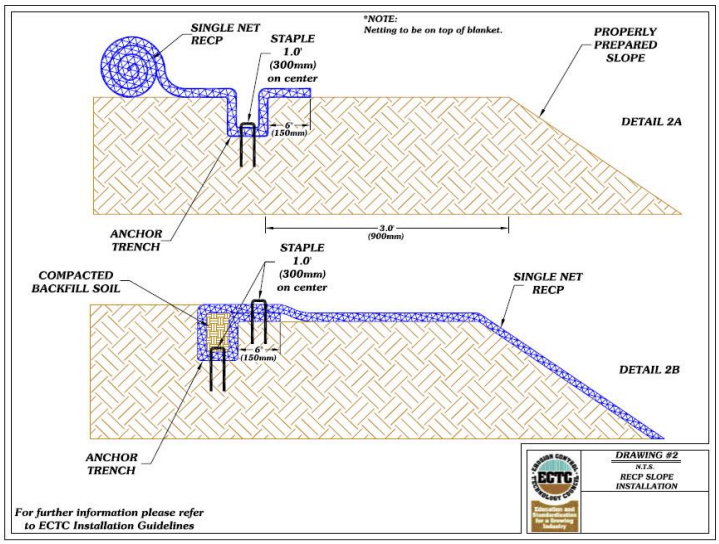

single net RECP

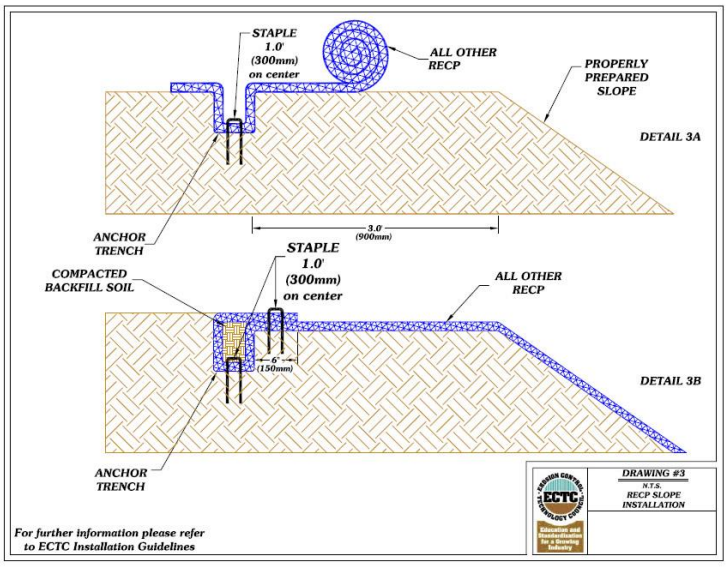

all other RECPs

Figure D.2 Detail for RECP Installation in Trench (ECTC 2014).

RECP Deployment

The RECP should then be deployed by walking the roll downhill with each backward step. The roll should be tightened to remove slack at intervals of 20 to 25 ft (6 to 7.5 m). Adjacent rolls should be overlapped 2 to 4 in. (5 to 10 cm) (ECTC 2014).

Staple or Stake the RECP

Staples should be placed at intervals of 3 to 5 ft (1 to 1.5 m) along the vertical length of the RECP to secure the edges or overlap of the RECP. To secure the width of the RECP, staples should be placed horizontally every 18 to 24 in. (45 to 60 cm). If the RECP must be spliced on the slope, the top roll should overlap the lower roll by 2 to 6 in. (5 to 15 cm) and secured by staples spaced 4 in. (10 cm) on center. A second row of staples can be installed, spaced 4 in. (10 cm) on center, staggered from the first row (ECTC 2014). Drawings depicting this process for both single net and double net/netless RECPs are shown in Figure D.3.

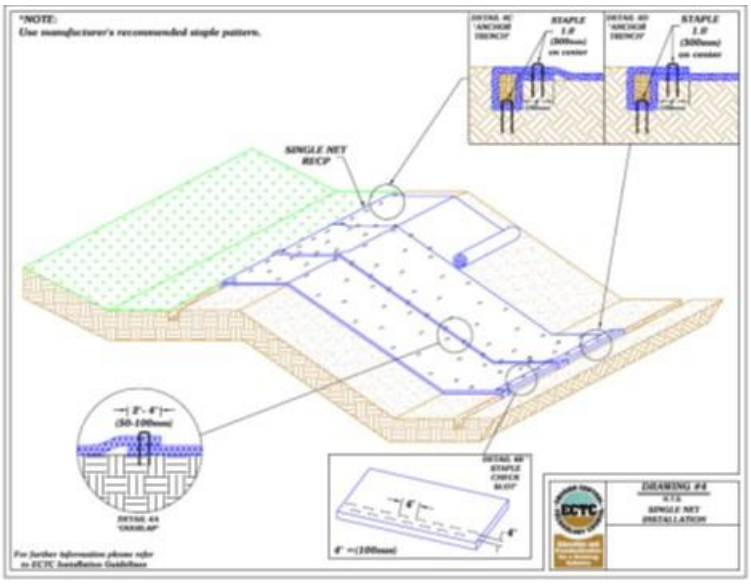

(a) single net RECP

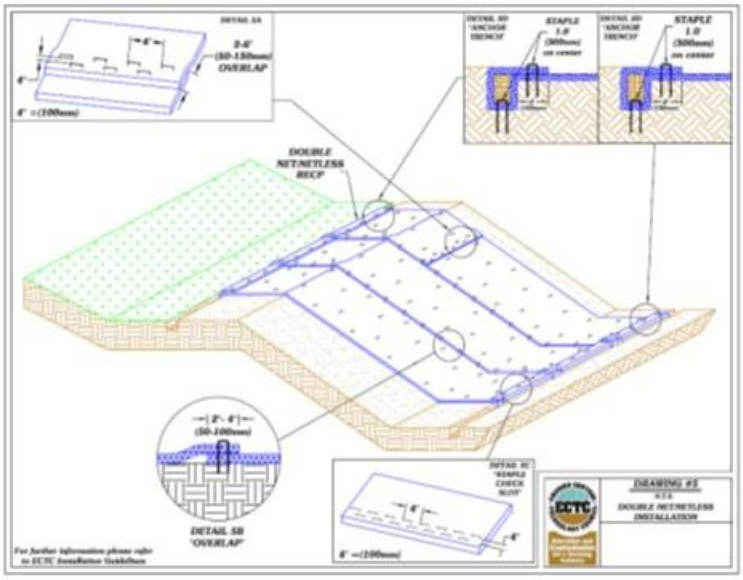

(b) double net/netless RECP

Figure D.3 Detail for Securing a RECP using Staples (ECTC 2014).

Securing the RECP at the Slope Toe

The RECP should be brought 2 ft (60 cm) past the toe of the slope and secured with staples placed 1 ft (30 cm) on center (ECTC 2014).